Fractional Brownian Motions in Financial Models, Simulation and Pricing

Chun Ming Tam[1]

[1]Graduate School of Social Sciences, Tokyo Metropolitan University
Email: tam-chunmingjeffy@ed.tmu.ac.jp

Contents

Abstract

Fractional Brownian motion (fBM) was first introduced within a Hilbert space framework by Kolmogorov [Kol40], while studying spiral curves in Hilbert space; the process was further studied and was coined the name 'fractional Brownian motion' in the 1968 paper by Mandelbrot and Van Ness [MVN68]. It has been widely used in various scientific fields, most notability in hydrology as first suggested in [Man65]. It also plays an important role in communication technology by enriching the queuing theory in terms of simulating real network traffic.

In recent years, it has been steadily gaining traction in finance. This is due to the fact that, traditional stochastic volatility model driven by ordinary Brownian motion implies exponential decay of the implied volatility smile, where empirical studies shows the decay is of power order. This can be explained by the long-memoryness found in autocovariance of the time-series, and this long-memory feature in instantaneous volatility process is called the **volatility persistence**. Even though this phenomenon is commonly observed on market implied volatility surface, it has been largely ignored because of the difficulty to capture it within the ordinary stochastic volatility framework. Within the framework of time-series analysis, the volatility persistence is concluded as the long-range dependence displaying in the instantaneous volatility time-series, or depicted by prominent components at low frequency under spectral density of the autocovariance function. This phenomenon is so commonly found, that Granger [Gra66] considered such phenomenon as the "typical spectral shape of an economic variable". The presence of the long-memory phenomenon has important implication in financial economics and financial engineering, especially in the area of the portfolio optimization: the choice of optimal consumption/saving because now the optimal decision might become very sensitive to the investment horizon instead of an asymptotically time-homogeneous problem if the asset return now is long-range dependent, also in the area of derivative pricing. The introduction of long-memory process is inconsistent with the pre-existing continuous-time process framework commonly utilized in derivative pricing (see, [Mah90b], [Mah90a]), and in [Mer87], [LeR89], Merton and Leroy respectively discussed the relationship of the efficient market hypothesis argument and the presence of the long-memory phenomenon. For detail discussion about the statistical test for the existence of long-range memory, see [Lo91] (the author has also proposed a robust extension of the R/S statistics for the purpose of robust statistical inference). Abudant empirical studies have been done with real data, most exmplemary the study done by Greene and Fielitz [GF77]. The studies was done on securities listed on the New York Stock Exchange, and many were found displaying long-range dependence in their daily returns. Several modeling approaches have been suggested capturing this persistence in conditional variance either via a unit-root or long memory process. In order to keep the pricing-framework largely intact, it is more interesting to study the long memory process, and fBM offers a simplistic extension particular for this purpose, owning to its similarity to the ordinary Brownian motion and its Gaussian properties, on the familiar process.

In this paper, several approaches to simulate fractional Brownian motion with $H > 1/2$ are outlined, including the exact methods and approximate methods, where the Hurst Index H is a parameter used in literature to generalize Brownian motion into fractional Brownian motion, first made popular by Benoit Mandelbrot. Brief introduction of the truncated fractional Brownian motion (long-memory model in continuous time) is also included, as proposed in [CR96], [CR98], which is shown to be inadequate to replicate the fractional Brownian motion. Through the full Monte-Carlo simulation scheme, the implied volatility surface is constructed. One of the main result in the research is that, imposing correlation between the fractional Brownian motion driven stochastic volatility and the ordinary Brownian motion driven asset process does not translates into skewness of the implied volatility surface, this is further

supported by E.Alos's paper [ALV07] on the observation of the close-to-maturity implied volatility surface. Unfortunately, since explicit pricing of the European option under the fractionally-driven stochastic volatility is not available in closed-form due to the non-Markovian nature of the fractional Brownian Motion driven stochastic volatility, and market participants have to rely on computational intensive method such as Monte-Carlo simulation, such dilemma serves as our motivation to explore for an robust approximation. The simulation is built on top of the work of Funahashi [Fun12], which provides a closed-form approximation of European option under the stochastic local-volatility model, this serves as a starting point of our robust simulation approach, reducing the brute-force simulation dimension from three to just one, rendering it a computationally inexpensive pricing scheme. As mentioned before, the skewness cannot be modeled by simply imposing correlation between the fractional Brownian motion and ordinary Brownian motion. To have a significant skewness under our proposed framework, it is necessary to add an ordinary Brownian motion driver in the stochastic volatility as well, in order to establish a correlation between the asset process and the stochastic volatility, thus the correlation. Our approximation-based-simulation scheme is also capable of pricing European option under this rather complicated stochastic environment, which captures the skewness, smile and persistence of the implied volatility surface.

The paper is structured as following: In chapter 1 the motivation is provided in financial context, and a brief description of different common approaches pertaining to the particular problem at hand. In chapter 2, the background information and technical definition of the fractional Brownian motion are outlined. Chapter 3 depicts various financial modeling involves fractional Brownian motion, such as the asset process model, various stochastic volatility models, as well as discussion of presence of arbitrage in the presence of fractional Brownian motion. Chapter 4 outlines various approach to simulate the exact fractional Brownian motion, which we also provide the Fast-Fourier-Transform (FFT) based simulation in detail, as it is our choice of simulation tool. We also go into detail of some approximate simulation approach in chapter 5 for the sake of completion, and comparison, providing the reader choices to of simulation scheme, for example, the spectral method is a great substitution for FFT-based simulation, and the correlated random walk draws an analogy with construction of ordinary Brownian motion by independent random walks. Chapter 6 gives a numerical example of the Comte, Renault approach and point out the inadequacy of this widely adapted approach. Chapter 7 gives us the full simulation scheme for the asset process with fractionally driven stochastic volatility, while exploration the effect of various factors such as the correlation, fractional Brownian motion, and the vol-of-vol for both ordinary Brownian motion and fractional Brownian motion, arguing the necessity for a fully extended hybrid fBM model which has both the correlated ordinary Brownian motion (with the asset return), and uncorrelated fractional Brownian motion to fully captures the stylized phenomenon observed on the market. Chapter 8 depicts the Funahashi approximation scheme and its derivation. Chapter 9 outlines the extension of the Funahashi approximation scheme for our robust simulation scheme which is capable of pricing the fully extended mixture fBM model, and various results depicting the stylized features we aim to capture. In chapter 10, calibration scheme against the market data utilizing the previous pricing scheme is provided, as well as exploring the relationship between parameters. Chapter 11 concludes the finding in this research.

1 Financial Motivation and Backgrounds

In this chapter, the motivation of utilizing the fractional Brownian motion in the context of financial engineering or econometric is outlined, as well as the basic technical background behind the fractional Brownian motion. In the following chapter, it can be seen that the fractional Brownian motion is a generalized centered Gaussian process with a more complicated autocovariance structure than the ordinary Brownian motion. Owning to this simple extension, fractional Brownian motion offers an attractive, tractable alternative to generalize the ordinary Brownian motion to be able to capture the aforementioned volatility persistence. Also, as the chapter proceed, it can be seen that the fractional Brownian motion can be defined in various ways, based on different original mathematical intention.

1.1 Financial Motivation

It's a well-known fact that, in options markets, the implied volatility, is known as the input of the volatility in the Black-Scholes formula that reproduce the market price. And when plotted against the strikes (or Moneyness), the curvature and slope shown on the plots are known as the volatility smiles and skewness; the smile effect, which is well known to practitioners, is generally described as the "U Shape" found on the implied volatility surface. In Hull and White [HW87] and Scott [Sco87], they have proposed this feature of volatility to be captured by stochastic regime, known as the stochastic volatility model:

$$\begin{cases} \frac{dS(t)}{S(t)} = \mu(t, S_t)dt + \sigma(t)dB^1(t) \\ d(\ln \sigma(t)) = k(\theta - \ln(\sigma(t))dt + \nu dB^2(t) \end{cases} \tag{1.1}$$

Here, $S(t)$ is the asset price and $\sigma(t)$ is the instantaneous volatility at time t, and $\{B^1(t), B^2(t)\}$ are ordinary standard Brownian motions. The logarithm of the volatility is assumed to follow an Ornstein-Uhlenbeck process, so the instantaneous volatility process is stationary, making it a natural choice of extension of the constant volatility Black-Scholes model. Hull and White [HW87] have shown that, the price of European option at time t of exercise date T under this statistical choice of instantaneous volatility is the conditional expectation of the Black Scholes option pricing formula where the constant volatility σ from the original formula is replaced by the quadratic average over the period $[t, T]$:

$$\sigma^2_{t,T} = \frac{1}{T-t}\int_t^T \sigma^2(u)d(u) \tag{1.2}$$

In another word, according to Hull-White's volatility formula, the square of implied volatility $\sigma^{imp}_{t,T}$ can be considered as the risk-neutral market expectation of the temporal aggregation $\sigma^2_{t,T}$ of the instantaneous volatility $\sigma\,(u)$. Implied volatility can be expressed as the function of time to maturity T and strike K, and the models proposed by Hull-White/Scott are successful at capturing the symmetric smile and skewness of the implied volatility by imposing relations between the driving Brownian motions $\{B^1(t), B^2(t)\}$ in (1.1), and the symmetric smile is explained by independence between $\{B^1(t), B^2(t)\}$, while skewness can be explained by linear correlation.

Due to the temporal aggregation effect evident in [MVN68], however, the smile effect deteriorates along with time-to-maturity since the temporal aggregation gradually erases the conditional heteroskedasticity by taking average over the period $[t, T]$; in the standard stochastic volatility setup, this particular decay is much faster than what is observed in market data, while the parametric stochastic volatility suggests the volatility smile decays in the order of exponential, it is observed that on the market the decay is much slower: Chou [Cho88] studied the NYSE stock index return, and estimate the return with GARCH(1,1)

model, to which the maximum-likelihood estimation gives rise to parameters set (α, β) ,where $\alpha+\beta \approx 1$, this means the data display unit-root behavior in variance reaction to shock, the meaning of unity is that the current shock persists forever (with very little to no decay), and the unconditional variance is not determined by the model, Engle and Bollerslev [EB86] proposed IGARCH for this type of process, but Baillie et al. [BBM96] has deemed this model to be unattractive for asset pricing purpose since "the occurrence of a shock to the IGARCH volatility process will persist for an infinite prediction horizon". This slow decaying volatility smile is known as the volatility persistence (long-memoryness found in instantaneous volatility process). This phenomenon is particularly poignant for high frequency data, for which the conditional variance process also displays near unit-root behavior.

Furthermore, emphasizing the existence of such phenomenon collaborated by large quantities of researches, pointing out that the conditional volatility of asset returns also displays long range dependence: [DGE93], [CdL94], [BBM96], [BM96] have discussed extensively the evidence of such phenomenon in empirical data. Bayesian estimation in [JPR94] of stochastic volatility models shows similar patterns of persistence. There also were studied done on the long-range dependence on various asset classes' daily return instead, such as, Booth and Kaen on the gold prices [BK79], Booth, Kaen and Koveos on Foreign Exchange rates [BKK82], Helms, Kaen and Rosenman on future contracts [HKR84], these, along with Mandelbrot and Wallis [MW69] with R/S statistics. As a side-note, volatility persistence is similar to volatility clustering, but the latter only refers to the case where the long-memoryness is found only in absolute value of the volatility time-series but not the original time-series, where in the case of volatility persistence, the long-memoryness is founded in both.

Both unit-root and long-memory process are suitable candidate to capture the volatility persistence, but the latter was deemed more appropriate enrichment extension to the continuous-time Hull-White setting. Hence, fractional Brownian motion is a prime candidate among all long-memory process given its tractability and similarity with the ordinary Brownian motion: both the fractional Brownian motion and ordinary Brownian motion are self-similar with similar Gaussian structure. For discussions of estimation and evidence of the long-range dependence in conditional variance of asset returns, the reader is referred to [CdL94] and section 3.1 of [BCdL98]. And [CR98] for discussion between the choice of time-series model such as FIARCH, FSV and its continuous-time counterparts.

As mentioned before, the idea of adapting fractional Brownian motion is it offers an simplistic extension to the well-established Stochastic Volatility Comte, Renault [CR98] to capture the slow-decaying volatility smile on the implied volatility surface. It is a good idea to review other models that's in the similar vein to understand the ending goal of the model: deterministic volatility produces a flat volatility surface that is inconsistent with what is observed on the market place; local volatility provides the state variable dependency on S_t, which can be calibrated to the implied volatility surface [Dup94], the shortcoming of this approach is it would take a continuum of option prices to calibrate, as well as the sensitivity of the instantaneous volatility is of opposite direction from the reality, for detail, refer to [Dup94]. The natural next step is to extend to the Stochastic Volatility, in order to gurantee non-negativity of the instantaneous volatility, one can model the instantaneous volatility as Cox-Ingersoll-Ross (CIR) process as it was suggested in the Heston model [Hes93], or exponential functional of an Ornstein-Uhlenbeck process, for example in [CR98] or Schobel-Zhu model [SZ99], the reason of OU or CIR process is instantaneous volatility in general is mean-reverting, and CIR, under the Feller condition, is guranteeded to be non-negative. In this paper we pick the latter approach because the OU process is more tractable than the CIR process, and the exponential functional guarantees the non-negativity as well. One last extension is adding jump to the stochastic volatility, as it is simple in the case of the ordinary stochastic volatility, we see quickly that the non-Markovian nature of the fractional Brownian motion complicates the inversion of the characteristic function (as proposed by Carr and Madan [CM99], Lewis [Lew00]), making it difficult to adapt the original option pricing approach. As we are interested in the long term nature

of the implied volatility surface, jump phenonmenons are mostly responsible of short-term behavior, we omit the general jump-diffusion in our process, though as it can be seen later on, the extension should be possible as the option prices of underlying governs by stochastic volatility with ordinary Brownian motion with jumps can be calculated readily. Other approach such as the econometric approach such as FIGARCH or FSV pointed out earlier, are also capable of capturing this long-memory behavior, but considering it deviates too far from the continuous-time model option pricing literature, we will omit them here, interested readers please refer to the related papers cited.

2 Background definition

Dormal definition of fractional Brownian motion (fBM) is provided here, the definition as given in [BHOZ08].

Definition 2.1. Let $H \in (0,1)$ be a constant, the "Hurst Index". A fractional Brownian motion $\left\{B^H(t)\right\}_{t\geq 0}$ with Hurst index H is a continuous and centered Gaussian process with covariance function

$$\mathbf{E}[\mathbf{B}^H(t)\mathbf{B}^H(s)] = \frac{1}{2}(t^{2H} + s^{2H} - |t-s|^{2H}) \tag{2.1}$$

In particular, for $H = 1/2$, it reduces to the ordinary Brownian motion with $\mathbf{E}[B^H(t)B^H(s)] = \min(\mathbf{t}, \mathbf{s})$. From equation (2.1) we have the following properties:

- $B^H(0) = 0$ and $E[B^H(t)] = 0, \forall t \geq 0$.
- $B^H(\cdot)$ has stationary increment: $B^H(t+s) - B^H(s)$ has the same distribution as $B^H(t)$ for any $s, t \geq 0$.
- $B^H(\cdot)$ displays self-similarity, which is defined as: $B^H(Tt) \stackrel{d}{=} (T)^H B^H(t)$.
- $B^H(\cdot)$ is a Gaussian process with the variance $\mathbf{E}[B^H(t)^2] = t^{2H}, \forall t \geq 0$.
- $B^H(\cdot)$ has continuous trajectories.

Fractional Brownian motions are divided into three very different categories: $H < 1/2, H = 1/2, H > 1/2$ .This is of particular importance because there is a deterministic difference between the case of $H < 1/2$ and $H > 1/2$, as we introduce the mathematical notion of long-range dependence.

It bears mentioning that for the case that $H \neq 1/2$, that $B^H(t)$ is not a semi-martingale. Recalling the definition of semi-martingale is that the p-variation of the process has to be equal to 2 for it to be a semi-martingale. For the case $H > 1/2,\ p < 2$ and $H < 1/2, p > 2$ respectively.

Definition 2.2. (Long-range Dependence)
The stationary sequence $\{X_n\}_{(n\in N)}$ is said to exhibit long-range dependence (or long-memory or strong dependence), given non-negative integers n, k, such that the autocovariance function $\gamma(n) \equiv cov(X_k, X_{(k+n)})$ satisfies

$$\lim_{n\to\infty} \frac{\gamma(n)}{cn^{-\alpha}} = 1$$

for some constants c and $\alpha \in (0,1)$. This can be written as $\gamma(n) \sim |n|^{-\alpha}$.

Under long-range dependence, the covariance between X_k and X_{k+n} decays so slowly that for $n \to \infty$

$$\sum_{n=1}^{\infty} \gamma(n) = \infty$$

Remark: The equation above governs just the decay of the autocovariance, it is possible to have relatively small lag-correlations, but a significant cumulative effect. Also, it is entirely possible to have particularly large specific lag $\gamma(n)$, making it difficult to detect any long-range dependence. Actually with only finite sample, it is impossible to conclude with certainty the presence of long-range dependence.
If we set $X_k = B^H(k) - B^H(k-1)$and $X_{k+n} = B^H(k+n) - B^H(k+n-1)$and apply equation (2.1), we have

$$\begin{aligned} \gamma_H(n) &\equiv \mathbf{E}(X_k X_{k+n}) \\ &= cov\left(B^H(k) - B^H(k-1), B^H(k+n) - B^H(k+n-1)\right) \\ &= \frac{1}{2}[(n+1)^{2H} + (n-1)^{2H} - 2n^{2H}] \end{aligned} \tag{2.2}$$

In particular,

$$\lim_{n\to\infty} \frac{\gamma_H(n)}{H(2H-1)n^{2H-2}} = 1$$

Therefore:

$$\begin{cases} \sum\limits_{n=1}^{\infty} \gamma_H(n) = \infty & \text{for } H > \frac{1}{2} \\ \sum\limits_{n=1}^{\infty} |\gamma_H(n)| < \infty & \text{for } H < \frac{1}{2} \end{cases}$$

Hence, only in the case of $H > 1/2$, fractional Brownian motions display long-memory dependence.

As pointed out in [Con07], large lags difference between $\gamma(\cdot)$ may be difficult to estimate in practice, so that models with long-range dependence are often formulated in terms of self-similarity. Self-similarity allows us to extrapolate across time scales and deduce long time behavior from short time behavior, which is more readily observed.
Because we are interested in capturing the long-memory phenomenon observed in financial markets, the rest of this paper will only concern with the case of $H > 1/2$.

2.1 Stochastic Integral Representation

In the original paper [MVN68], Mandelbrot and van Ness provided a time-averaging represention of the fBM in stochastic integral with respect to the ordinary Brownian motion:

$$B^H(t) = \frac{1}{\Gamma(H+\frac{1}{2})}\left(\int_{-\infty}^{0}\left[(t-s)^{H-\frac{1}{2}}-(-s)^{H-\frac{1}{2}}\right]dB(s)+\int_0^t(t-s)^{H-\frac{1}{2}}dB(s)\right) \quad (2.3)$$

$$= \frac{1}{\Gamma(H+\frac{1}{2})}\left(\int_{-\infty}^{+\infty}\left\{(t-s)_+^{H-1/2}-(-s)_+^{H-1/2}\right\}dB(s)\right) \quad (2.4)$$

where $\Gamma(\cdot)$ is the gamma function, $\Gamma(\alpha)\equiv\int_0^\infty x^{\alpha-1}\exp(-x)\,dx$.
The above integral (2.3) can be written in terms of iterative integral, following the Cauchy formula of repeated integration:

$$\frac{1}{(n-1)!}\int_0^t(t-s)^{n-1}g(s)\,ds=\int_0^t dt_{n-1}\int_0^{t_{n-1}}dt_{n-2}\cdots\int_0^{t_2}dt_1\int_0^{t_1}g(s)\,ds$$

Where the iterative integral is defined in the hyper-cube $0\le t_1\le t_2\le\cdots\le t_{n-2}\le t_{n-1}\le t$

It is common to rename $n=H+1/2$, as it is the approach adopted by Comte, Renault in their papers [CR96], [CR98], [CCR12].

To see the equivalence of the stochastic integral representation equal to the fBM defined in the previous section. Samorodnitsky, Taqqu [ST94] has given the following result:

Proposition 2.1. Suppressing the constant $\Gamma\left(H+\frac{1}{2}\right)$ for the sake of simplicity, given that $B^H(t)$ is a centered Gaussian process, also the integrand are $\mathcal{F}_t$-adapted, it is easy to see $E\left[B^H(t)\right]=0$

So we need only to compute the covariance function, we provide the following as the sketch of the proof. Substituting $u=\frac{s}{t}$:

$$\begin{aligned}E\left[B^H(t)\right]^2 &= \int_{-\infty}^{+\infty}\left((t-s)_+^{H-1/2}-(-s)_+^{H-1/2}\right)^2ds\\ &= t^{2H}\int_{-\infty}^{+\infty}\left((1-u)_+^{H-1/2}-(-u)_+^{H-1/2}\right)^2du\\ &= C(H)\,t^{2H}\end{aligned}$$

Also we can see that for the increment, substituting $u=s+u'$ in the 2nd step, applying the first part of the proposition:

$$\begin{aligned}E\left[\left|B^H(t)-B^H(s)\right|\right]^2 &= \int_{-\infty}^{+\infty}\left((t-u)_+^{H-1/2}-(s-u)_+^{H-1/2}\right)^2du\\ &= \int_{-\infty}^{+\infty}\left(((t-s)-u')_+^{H-1/2}-(-u')_+^{H-1/2}\right)^2du'\\ &= C(H)\,|t-s|^{2H}\end{aligned}$$

Here the $C(H)$ is the normalizing constant.

So it is easy to see we have the following relationship reconciling with the discrete-time counterpart:

$$\begin{aligned} E\left[B^H(t)\,B^H(s)\right] &= -\frac{1}{2}\left\{E\left[\left|B^H(t)-B^H(s)\right|^2\right]-E\left[B^H(t)^2\right]-E\left[B^H(s)^2\right]\right\} \\ &= \frac{1}{2}\left(t^{2H}+s^{2H}-|t-s|^{2H}\right) \end{aligned}$$

They have also included an alternative representation of the fBM which is the basis of the model in [CR96], [CR98]:

$$\widehat{B^H(t)} = \int_0^t \frac{(t-s)^{H-1/2}}{\Gamma(H+1/2)} dB(s) \tag{2.5}$$

This version of fBM is 'truncated' in the sense that the integration from negative infinity to zero in equation (2.3) is truncated. The model (2.5) is referred as the 'truncated fractional Brownian motion' in the rest of this paper. As pointed out in [MVN68], the representation (2.5) was first proposed by Paul Lévy to define the fBM by the Riemann-Liouville fractional integral, while the original integral in equation (2.3) is the Weyl fractional integral.
The definition (2.5) of fBM is in general not asymptotically covariance-stationary, even though it retains self-similarity.We refer to [CR96], for the construction of this process.

Here we adapt the notation from the original paper [CR96]

Definition 2.3. All stationary regular processes, can be expressed in linear representations, i.e. moving average representations of possibly infinite order. This is shown by the continuous time Wold theorem of representation (from Rozanov [Roz67], p. 116-119), in which that, any linearly regular stationary process Y can be written as

$$Y(t) = m + \int_{-\infty}^{t} A(t-s)\, d\zeta(s)$$

Where $d\zeta$ is an uncorrelated random measure and A is a square matricial function, which:

$$\int_0^{\infty} A(x)^T A(x)\, dx < +\infty$$

In the original paper of Comte, Renault [CR96], they study the case where $d\zeta = dW(t)$, for some uncorrelated ordinary Brownian motion $W(t)$.
Define $X(t)$ only for $t \geq 0$,

$$X(t) = \int_0^t A(t-s)\, dW(s)$$

Then the Wold's theorem representation dictates that the stationary process $Y(t)$ is asymptotically equivalent to the process $m + X$, in the following sense:

$$\lim_{t\to\infty} E\left[Y(t)-(m+X)\right]^T\left[Y(t)-(m+X)\right] = 0$$

So look back at (2.3), we see that (2.5) is the asymptotically equivalence of the stationary stochastic integral representation of the fBM.
Given the differences, most of the analytically tools (such as Malliavin Calculus) developed for fBMs might not be directly applicable to the truncated fBMs. This truncated version of fBM is convenient to work in terms of simulation; yet, in chapter 6, it is shown that the asymptotic convergence is not robust enough for pricing purpose. Indeed, one can see from equation (2.5), because of truncating the stochastic integral before $t = 0$, the time-averaging effect is severely weakened. These two types of fBMs and their theoretical differences are covered in detail in [MR99].

3 Fractional Brownian Motions in Financial Models

First, let's look at several examples that utilize the fractional Brownian motions in the realm of financial modeling.

3.1 Asset Price Model

In the previous section, it was mentioned that the motivation of fBM in finance models is to capture the long-range dependence in the volatility process. However, it is worth discussing the possibility of applying it to the risky asset process S_1 itself. Some of the candidate asset price model for $H > 1/2$ along with the fractional SDEs solved by fractional Ito-lemma are included:

$$\begin{cases} dS_1(t) = \mu S_1(t)\,dt + \sigma S_1(t) \diamond dB^H(t) \\ S_1(t) = S_1(0)\exp\left[\mu t + \sigma B^H(t) - \frac{1}{2}\sigma^2 t^{2H}\right] \end{cases}$$

Here the $\diamond$ is the Wick product. As well as the plain multiplicative case:

$$\begin{cases} dS_1(t) = \mu S_1(t)\,dt + \sigma S_1(t)\,dB^H(t) \\ S_1(t) = S_1(0)\exp\left[\mu t + \sigma B^H(t)\right] \end{cases}$$

Also, for the mixture setup, for which $\left(B, B^H\right)$ are assumed to be independent:

$$\begin{cases} dS_1(t) = \left(\mu - \frac{1}{2}a^2\right) S_1(t)\,dt + aS_1(t)\,dB(t) + \sigma S_1(t)\,dB^H(t) \\ S_1(t) = S_1(0)\exp\left[\mu t + aB(t) + \sigma B^H(t)\right] \end{cases}$$

These are all candidates of asset process with fractionally driven random factor. And construct the self-financing portfolio under any of these asset process with the riskless asset $S_0(t)$, defined by the money-market account.

$$\begin{cases} V^\theta(t) = \alpha(t) S_1(t) + \beta(t) S_0(t) \\ dV^\theta(t) = \alpha(t)\,dS_1(t) + \beta(t)\,dS_0(t) \end{cases}$$

Unfortunately, the self-financing portfolio with any of these process in general does not guarantee no-arbitrage opportunities in the market, as discussed in [Ell06]. i.e.:

$$V^\theta(0) \neq E\left[e^{-rT} V^\theta(T)\right]$$

But under mild assumption, Bender, etc. [BSV06] has shown that the mixture model above involving both $\left(B, B^H\right)$ permits arbitrage-free regular portfolios for pricing and hedging purposes, so mixture seems like a more sensible choice if one inclines to introduce fractional Brownian motion in the asset price process, for detail please refer to the paper cited.

In practice, it is considered that an asset process driven by fBM will result in arbitrage. The idea is that, since for $H \neq 1/2, B^H(t)$ is not a semi-martingale in continuous time, the asset process described by $B^H(t)$ violates the NFLVR (no free lunch with vanishing risk), a weaker version of arbitrage, and thus doesn't admit an equivalent martingale measure according to Theorem 7.2 of [DS94]. Such findings and construction of arbitrage can be found in Rogers [Rog97], also Rogers has contrusted a similar Gaussian process with long-memory property but also retain the semi-martingale property.

Proposition 3.1. Defining $X(t)$:

$$X(t) = \int_{-\infty}^{t} \varphi(t-s)\, dB_s - \int_{-\infty}^{0} \varphi(-s)\, dB_s$$

For $\varphi \in C^2(\mathbb{R})$ and $\varphi(0) = 1, \varphi'(0) = 0$ and if $\lim_{t\to\infty} \varphi''(t)\, t^{5/2-H}$ exist in $(0,\infty)$, then $X(t)$ is a Gaussian process that has the same long-range dependence as fractional Brownian motion but still retains semi-martingale property, as shown by integration-by-parts:

$$\begin{aligned} X(t) &= B_t + \int_{-\infty}^{t} \varphi'(t-s)\, B_s ds - \int_{-\infty}^{0} \varphi'(-s)\, B_s ds \\ &= B_t + \int_{0}^{t} \left(\int_{-\infty}^{s} \varphi''(s-v)\, B_v dv \right) ds \end{aligned}$$

For which the integrand is $\mathcal{F}_s$-adapted, thus showing $X(t)$ is semi-martingale.

Rogers proved that within small time-scales, if the asset process follows fBM, arbitrage arises with non-zero probability. But with Proposition 3.1, one of the choice for φ is $\varphi(t) = (\epsilon + t^2)^{(2H-1)/4}$.
In contrast, Cheridito [Che03] has given multiple classes of trading strategies that allow various level of arbitrages (NFLVR, arbitrage in the classical sense and strong arbitrage) under fBM driven assets, and shown that the arbitrages are all eliminated if the intra-transaction time is not zero, i.e., the classes of strategies become arbitrage-free. Such assumption is reasonable in practice, given the physical limit and non-zero transaction cost. For more information on arbitrage theory and its generalization, the reader is referred to [DS94], [Rog97], [Che03].

3.2 Stochastic Volatility Model with fractional Brownian motion

As it was mentioned in the introductory section, the main motivation for fBM is to capture the volatility persistence, the stylized feature observed in empirical data. It makes more sense to model the volatility process with fractional Brownian motion instead, since it is not a tradable quantity, there is no concern about violating arbitrage opportunity. There are several prominent models involving a volatility process with fBM. Here, we just outline several of them.

3.2.1 Stochastic Volatility Model - Truncated Long-Memory Continuous Model

In [CR96], [CR98], Comte and Renault consider the following stochastic volatility model driven by fBM:

$$\begin{cases} \frac{dS(t)}{S(t)} & = rdt + \sigma(t) dB(t) \\ \sigma(t) & = \sigma_0 e^{x(t)} \\ dx(t) & = -kx(t)dt + \nu \widehat{dB^H}(t) \end{cases} \tag{3.1}$$

where the log-volatility term follows a fractional-OU process driven by the truncated fBM (2.5). The asset price process follows a geometric Brownian motion with volatility persistence.
Although Mandelbrot [MVN68] deemed it as signifying the origin too heavily, the model (3.1) is easier and more robust than the ordinary fBMs from the perspective of simulation. A simulation example is explored in Section 6.

3.2.2 Stochastic Volatility Model - Affine Fractional Stochastic Volatility Model

Drawing inspiration from the Heston model (1993) [Hes93], Comte et al. [CCR12] model the overall process:

$$\begin{cases} dS(t) = \mu(t) S(t) dt + \sigma(t) S(t) dB^S(t) \\ dX(t) = k(\theta - X(t)) dt + \gamma \sqrt{X(t)} dB^\sigma(t) \end{cases}$$

Where the squared-volatility process follows the displaced-diffusion of the fractional integrated $X(t)$

$$\sigma^2(t) = \theta + X^{(\alpha)}(t) \tag{3.2}$$

Where

$$X^{(\alpha)}(t) = \int_{-\infty}^{t} \frac{(t-s)^{H-1/2}}{\Gamma(H+1/2)} X(s) ds \tag{3.3}$$

Similar treatment of the fractional integration is outlined in [CR96]. The affine structure in (3.2) is similar to the one originally studied by Duffie et al. [DPS00].
The affine structure is adopted for the extra tractability, and thus better suited for practical option pricing and hedging than the original idea (3.1). In fact, Comte et al. [CCR12] have shown that this model can better depict the difference between the short and long memory properties in the resulting option prices. But there is a drawback of this approach, it didn't fully replicate the framework and features of Heston, because there is no correlation structure imposed within the framework, meaning the resulting option is indifferent to the direction of the volatility return, which, to the common knowledge, does not reflect the reality.

3.2.3 Stochastic Volatility Model - Martingale Expansion

Fukasawa [Fuk11] adopts and expands the asymptotic expansion technique first proposed by Yoshida [Yos01] of European option prices around the Black-Scholes equation by means of perturbation technique and partial Malliavin calculus. It is shown that the logarithm of the asset process can be expressed as

$$lnS_t = Z_t = rt - \frac{1}{2}\int_0^t g(Y_s^n)^2 ds + \int_0^t g(Y_s^n) \left[\theta dW_s + \sqrt{1-\theta^2} dW_s\right]$$

with

$$Y_s^n = y + \epsilon_n W_s^H, \qquad W_t^H = \int_0^t K_H(t,s) dW_s'$$

Here, r is the riskless rate, $\theta \in (-1,1)$, $y \in R$ is a constant, (W, W') is a 2-dimensional standard (independent) Brownian motion, $\epsilon_n \to 0$ is a deterministic sequence for $n \to \infty$, and $g(\cdot)$ is the stochastic volatility process which is an adapted process for the minimal filtration.
Note that W_t^H is a fractional Brownian motion with Hurst index H, where $K_t^H(t,s)$ is the kernel of the stochastic integral representation over a finite interval of Brownian motion. According to [BHOZ08], pertaining to our interest, for the case of $H > 1/2$, the kernel has the following expression:

$$K_H(t,s) = c_H s^{1/2-H} \int_s^t (u-s)^{H-3/2} u^{H-1/2} du$$

where

$$c_H = \left\{ \frac{H(2H-1)}{\beta(2-2H, H-1/2)} \right\}^{1/2}$$

Then, according to Corollary (2.6) of Fukasawa [Fuk11], the implied volatility can be expressed as

$$\sigma \left\{ 1 - \frac{\epsilon_n}{2} \rho_{13} d_2 \right\} + o(\epsilon_n) = aT^{H-1/2} \log(K/s) + \sigma + bT^{H+1/2} + o(\epsilon_n) \tag{3.4}$$

where d_2 is the typical argument in the $N(d_2)$ of the Black-Scholes formula, T is the time-to-maturity and

$$\rho_{13} = \frac{2\theta g'(y) c'_H T^H}{g(y)}, \quad \sigma = g(y), \quad a = \frac{\theta g'(y) c'_H}{\sigma} \epsilon_n, \quad b = -a \left(r - \frac{\sigma^2}{2} \right) \tag{3.5}$$

Equation (3.4) can be seen as an approximation for small $\epsilon_n \to 0$. This model can be considered as expansion of the overall asset process calibrated to the implied volatility surface, though there is a shortcoming of this approach. Since Y_s^n in this case is the instantaneous volatility process, and only depend on W_s^H instead of the full historical realization of the innovation dB_s^H, as it is usually the case. The shape of the volatility surface is limited and the volatility persistence is not correctly captured. This can be seen in Figure 1.

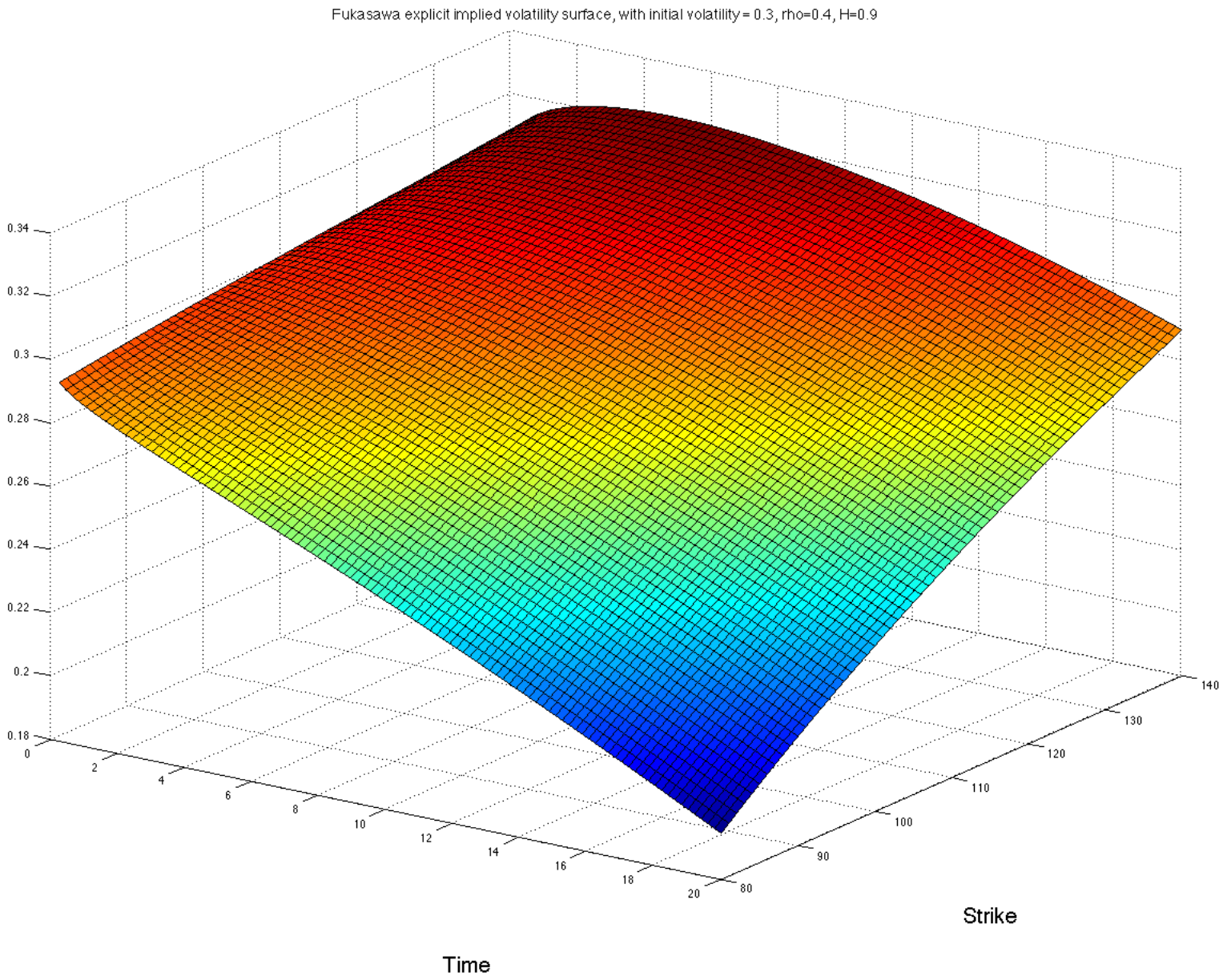

Figure 1: Fukasawa Approximation with $\sigma = 0.3, \rho = 0.4, H = 0.9$

4 Simulation with Exact Methods

In previous section, the definition of fractional Brownian motion is given, and to succinctly put it, it is a Gaussian process with zero-mean, and a general covariance structure that depends on all the past history, making it non-Markovian, this complicates the problem significantly and a robust way to simulate such structure is necessary. In the following two sections we will give detail to how to simulate such a process, starting with the most technically simple, but computationally expensive process, it will give the reader a better understanding of the technical aspect of the simulation procedure, and move on to more sophisticated approaches that is better for practical purposes. In this section we look at exact methods that completely capture the covariance structure and true realization of the fractional Brownian motion (fBM) or fractional Gaussian noise (fGn). Any method described in this section has their starting points at the covariance matrix. While in the next section, approximate schemes, the approaches produce numerically close replication of fBM (or fGn) or asymptotically coincides with the true realization. The collection of algorithm in these two sections is not meant to be exhaustive. For more algorithm and discussion, see [Die02]. In this paper, the Fast-Fourier-Transform simulation is strongly emphasized, because it will serve as the choice of simulation scheme in chapters later on.

4.1 Hosking Method

The Hosking method (also known as the Durbin or Levinson method) utilizes the well-known conditional distribution of the multivariate Gaussian distribution on a recursive scheme to generate samples based on the explicit covariance structure. This method generates a general stationary Gaussian process with given covariance structure, not limited to generating fBMs.
More specifically, this algorithm generates an fGn sequence $\{Z_k\}$ and fBM is recovered by accumulative sum. That is, the distribution of Z_{n+1} conditioned on the previous realization $Z_n, \dots Z_1, Z_0$ can be explicitly computed.

Denote $\gamma(k)$ as the autocovariance function of the zero-mean process $X_{kk=0,1\cdots}$, as seen in (2.2) before:

$$\gamma(k) \equiv \mathbf{E}(X_n X_{n+k}) = \frac{1}{2}[(k+1)^{2H} + (k-1)^{2H} - 2k^{2H}] \tag{4.1}$$

where assuming for convenience that $\gamma(0) = 1$. For $n, k = 0, 1, 2 \dots$, arriving the following recursive relationship for the $(n+1) \times (n+1)$ autocovariance matrix $\Gamma(n) = \{\gamma(i-j)\}_{i,j=0,\dots,n}$:

$$\begin{aligned}
\Gamma(n+1) &= \begin{pmatrix} 1 & \gamma(1) & \gamma(2) & \cdots & \gamma(n+1) \\ \gamma(1) & 1 & \gamma(1) & \cdots & \gamma(n) \\ \gamma(2) & \gamma(1) & \ddots & \vdots & \vdots \\ \vdots & \vdots & \vdots & \ddots & \vdots \\ \gamma(n+1) & \gamma(n) & \cdots & \cdots & 1 \end{pmatrix} \\
&= \begin{pmatrix} 1 & c(n)' \\ c(n) & \Gamma(n) \end{pmatrix} \\
&= \begin{pmatrix} \Gamma(n) & F(n)c(n) \\ c(n)'F(n) & 1 \end{pmatrix}
\end{aligned} \tag{4.2}$$

where $c(n)$ is the $(n+1)$-column vector with elements $c(n)_k = \gamma(k+1), k = 0, \dots, n$
and $F(n) = (\mathbf{1}(i = n - j))_{i,j=0,\dots,n}$ is the $(n+1) \times (n+1)$ 'mirrored' identity matrix:

$$F(n) = \begin{pmatrix} 0 & \cdots & 0 & 1 \\ 0 & \cdots & 1 & 0 \\ \vdots & \ddots & \vdots & \vdots \\ 1 & 0 & 0 & 0 \end{pmatrix}$$

Theorem 4.1. Multivariate Gaussian distribution
Any multivariate Gaussian random vector z can be partitioned into z_1 and z_2 with the mean vector and covariance matrix with the corresponding partition:

$$\mu = \begin{bmatrix} \mu_1 \\ \mu_2 \end{bmatrix} \qquad \Sigma = \begin{bmatrix} \Sigma_{11} & \Sigma_{12} \\ \Sigma_{21} & \Sigma_{22} \end{bmatrix} \tag{4.3}$$

The distribution of z_1 conditioned on $z_2 = a$ is a multivariate normal $(z_1|z_2 = a) \sim N(\bar{\mu}, \bar{\Sigma})$ with

$$\begin{array}{ll} \overline{\mu} & =\mu_1 + \Sigma_{12}\Sigma_{22}^{-1}(a - \mu) \\ \overline{\Sigma} & =\Sigma_{11} - \Sigma_{12}\Sigma_{22}^{-1}\Sigma_{21} \end{array} \tag{4.4}$$

If we substitute equation (4.2) into the partition in (4.4) with $\Sigma_{11} = 1, \mu = 0$, we have the following expression for the conditional distribution:

$$\begin{array}{ll} \mu_{n+1} & = E\left(Z_{n+1}|Z_n, \cdots Z_0\right) = c(n)'\Gamma(n)^{-1} \begin{pmatrix} Z_n \\ \vdots \\ Z_1 \\ Z_0 \end{pmatrix} \\ \sigma_{n+1}^2 & = Var\left(Z_{n+1}|Z_n, \cdots Z_0\right) = 1 - c(n)'\Gamma(n)^{-1}c(n) \end{array} \tag{4.5}$$

With $Z_0 \sim N(0, 1)$, subsequently X_{n+1} for $n = 0, 1, \ldots$ can be generated.

Taking the inverse of $\Gamma(\cdot)$ at every step is computational expensive; the algorithm proposed by Hosking [Hos84] computes the inverse $\Gamma(n+1)^{-1}$ recursively. The next result is due to Dieker [Die02].

Proposition 4.1. Hosking algorithm for simulating fGn
Define $d(n) = \Gamma(n)^{-1}c(n)$, and applying the blockwise method of inversion on equation (4.2):

$$\Gamma(n+1) = \frac{1}{\sigma_n^2} \begin{pmatrix} \sigma_n^2\Gamma(n)^{-1} + F(n)d(n)d(n)'F(n) & -F(n)d(n) \\ -d(n)'F(n) & 1 \end{pmatrix} \tag{4.6}$$

$$= \frac{1}{\sigma_n^2} \begin{pmatrix} 1 & -d\left(n\right)' \\ -d(n) & \sigma_n^2\Gamma\left(n\right)^{-1} + d\left(n\right)d\left(n\right)' \end{pmatrix} \tag{4.7}$$

Also from (4.7), we see that for $x \in \mathbb{R}^{n+1}$, and $y \in \mathbb{R}$, we have the following relationship

$$\begin{pmatrix} y & x \end{pmatrix} \Gamma\left(n+1\right)^{-1} \begin{pmatrix} y \\ x \end{pmatrix} = \frac{\left(y - d\left(n\right)'x\right)^2}{\sigma_n^2} + x\Gamma\left(n\right)^{-1}x$$

So from (4.5), it is apparent that X_{n+1} given $(X_n, \cdots, X_0)$ is indeed Gaussian with mean μ_{n+1} and variance σ_{n+1}^2.

Now we have the distribution canonical representation, it is necessary to simulate sample X_{n+1} for $n = 0, 1, \cdots$ recursively given that X_0 is a standard normal random variable. And this recursive relationship should avoid involving matrix inversion at every step of the way, Hosking put forth the following recursive relationship in his paper [Hos84]:

σ_{n+1}^2 satisfies the recursion

$$\sigma_{n+1}^2 = \sigma_n^2 - \frac{\left(\gamma(n+1) - \tau_{n-1}\right)^2}{\sigma_n^2} \tag{4.8}$$

with $\tau_n = d(n)'F(n)c(n) = c(n)'F(n)d(n)$. Also, the recursion for $d(n+1) = \Gamma(n+1)^{-1}c(n+1)$ is obtained as

$$d(n+1) = \begin{pmatrix} d(n) - \phi_n F(n)d(n) \\ \phi_n \end{pmatrix} \tag{4.9}$$

where

$$\phi_n = \frac{\gamma(n+1) - \tau_n}{\sigma_n^2} \tag{4.10}$$

With $\mu_1 = \gamma(1)Z_0, \sigma_1^2 = 1 - \gamma(1)^2, \tau_1 = \gamma(1)^2, \mu_{n+1}, \sigma_{n+1}^2, \tau_{n+1}$ can be readily computed, and fractional Brownian motion is recovered by the cumulative summation.
This algorithm is also applicable to non-stationary processes (see [BD87] for details), which generates the innovations: $X_{n+1} - \mu_{n+1}$ given $X_n - \mu_n \cdots X_1 - \mu_1, X_0$. Even though this algorithm is very simple and easy to understand and sample paths can be generated on-the-fly, the complexity of this algorithm is of $O(N^2)$ and computational (as well as memory) expense of this algorithm grows at a prohibitive speed.

4.2 Cholesky Method

Given the covariance structure in matrix form, it is natural to go with the Cholesky decomposition: decomposing the covariance matrix into the product of a lower triangular matrix and its conjugate-transpose $\Gamma(n) = L(n)L(n)^*$. If the covariance matrix is proven to be positive-definite (the situation will be addressed in the next subsection), $L(n)$ is a lower triangular matrix with real entries $l_{ij} > 0$ for $j > i$ and $i, j = 0, \cdots, n$ and $\Gamma(n) = L(n)L(n)'$.
Suppose that in matrix form the $(n+1) \times (n+1)$ product is given by

$$\begin{pmatrix} \gamma(0) & \gamma(1) & \gamma(2) & \cdots & \gamma(n) \\ \gamma(1) & \gamma(0) & \gamma(1) & \cdots & \gamma(n-1) \\ \gamma(2) & \gamma(1) & \gamma(0) & \cdots & \gamma(n-2) \\ \vdots & \vdots & \vdots & \ddots & \vdots \\ \gamma(n) & \gamma(n-1) & \gamma(n-2) & \cdots & \gamma(0) \end{pmatrix} = \begin{pmatrix} l_{00} & 0 & 0 & \cdots & 0 \\ l_{10} & l_{11} & 0 & \cdots & 0 \\ l_{20} & l_{21} & l_{22} & \ddots & \\ \vdots & \vdots & \vdots & \ddots & 0 \\ l_{n0} & l_{n1} & l_{n2} & \vdots & l_{nn} \end{pmatrix} \times \begin{pmatrix} l_{00} & l_{10} & l_{20} & \cdots & l_{n0} \\ 0 & l_{11} & l_{21} & \cdots & l_{n1} \\ 0 & 0 & l_{22} & \cdots & l_{n2} \\ \vdots & \vdots & \vdots & \ddots & \vdots \\ 0 & 0 & 0 & 0 & l_{nn} \end{pmatrix}$$

It is easy to see that $l_{00}^2 = \gamma(0)$ for $i = j = 0$
And for $i = 1$, we have (on 2nd row)

$$l_{10} l_{00} = \gamma(1) \qquad \text{and that} \qquad l_{10}^2 + l_{11}^2 = \gamma(0)$$

For $i \geq 1$, the entries of the lower triangular matrix can be determined by

$$\begin{aligned} l_{i,0} &= \frac{\gamma(i)}{l_{0,0}} \\ l_{i,j} &= \frac{1}{l_{j,j}} \left(\gamma(i-j) - \sum_{k=0}^{j-1} l_{i,k} l_{j,k} \right), \qquad 0 < j \leq n \\ l_{i,i}^2 &= \gamma(0) - \sum_{k=0}^{i-1} l_{i,k}^2 \end{aligned}$$

Given independent, identically distributed (i.i.d.) standard normal random variables $(V_i)_{i=0,\ldots,n+1}$, the fGn sequence is generated by

$$Z_{n+1} = \sum_{k=0}^{n+1} l_{n+1,k} V_k$$

Or in matrix form, we have $Z(n) = L(n)V(n)$. If $\Gamma(n)$ is assumed to be positive-definite, the non-negativity of $l_{i,i}^2$ is guaranteed and $L(n)$ is guaranteed to be real. The covariance structure of the process is captured, since

$$Cov(Z(n)) = Cov(L(n)V(n)) = L(n)Cov(V(n))L(n)' = L(n)L(n)' = \Gamma(n) \tag{4.11}$$

Even though the Cholesky method is easy to understand and implement, the computation time is $O(N^3)$, which renders this scheme extremely uneconomical in practice because one has to keep track of $L(n)$ grows at every step and has to be kept in memory, but once the $L(n)$ is calculated, one can quickly generate another sample with only order of $O(N^2)$. To resolve this problem, we will proceed to another exact method. The idea is similar to retain the same relation as equation (4.11), but with a different decomposition. Comparing with Hosking algorithm, they are in the same vein as it involves multiplying a vector of standard normal variables with a pre-calculated matrix to reproduce the covariance structure, but the Hosking algorithm is faster, yet we include the Cholesky method because it is the most simple and direct when it comes to the theoretical basis.

4.3 Fast Fourier Transform Method

Using the Cholesky decomposition seems to be the most straightforward idea to simulate Gaussian process with a given covariance structure; but, it also is the most rudimentary and thus slow. In order to improve upon the speed, the idea of utilizing the fast Fourier transform (FFT) was proposed by Davies and Harte [DH87] and further generalized by Dietrich and Newsam [DN97] and Wood and Chan [WC94]. We list in detail and derivation of this approach because this approach will serve as our choice of simulation tool for the latter chapters.
Similar to the idea before, this method tries to find a decomposition of the covariance matrix as $\Gamma = GG'$ and the sample is generated by $y = Gx$ for given standard normal random variable x. Then, on the given covariance structure, we have

$$Cov(y) = Cov(Gx) = GCov(x)G' = GG\prime = \Gamma$$

The idea is to 'embed' the original covariance matrix a circulant matrix in order to carry out the FFT. Before we outline the idea, we shall give out some detail of the linkage between Fourier transform and the circulant matrix.

Definition 4.1. (Circulant matrix)
Circulant matrix is a special case of the Toeplitz matrix where each row vector is shifted to the right (the last element is shifted back to the beginning of the row). In matrix form, an n-by-n circulant matrix can be written as

$$C = \begin{pmatrix} c_0 & c_{n-1} & c_{n-2} & \cdots & c_1 \\ c_1 & c_0 & c_{n-1} & \cdots & c_2 \\ c_2 & c_1 & c_0 & \cdots & c_3 \\ \vdots & \vdots & \vdots & \ddots & \vdots \\ c_{n-1} & c_{n-2} & \cdots & c_1 & c_0 \end{pmatrix}$$

Remark: As one can see, the first row/column completely describes the whole matrix, and it can be put more succinctly in the following form:

$$c_{j,k} = c_{j-k(modn)}, \qquad \text{where } 0 \leq j, k \leq n-1$$

Note that the indices range from 0 to $n-1$ instead of the usual convention that ranges from 1 to n.

Definition 4.2. (Generating circulant matrix)
We define an n-by-n generating circulant matrix by

$$G = \begin{pmatrix} 0 & 0 & 0 & \cdots & 0 & 1 \\ 1 & 0 & 0 & \cdots & 0 & 0 \\ 0 & 1 & 0 & \cdots & 0 & 0 \\ 0 & 0 & 1 & \cdots & 0 & 0 \\ \vdots & \vdots & \vdots & \ddots & \vdots & \vdots \\ 0 & 0 & 0 & \cdots & 1 & 0 \end{pmatrix}$$

By a simple calculation, we can see that the 'square' of the generating circulant matrix is given by

$$G^2 = \begin{pmatrix} 0 & 0 & 0 & \cdots & 1 & 0 \\ 0 & 0 & 0 & \cdots & 0 & 1 \\ 1 & 0 & 0 & \cdots & 0 & 0 \\ 0 & 1 & 0 & \cdots & 0 & 0 \\ \vdots & \vdots & \vdots & \ddots & \vdots & \vdots \\ 0 & 0 & \cdots & 1 & 0 & 0 \end{pmatrix}$$

From the point of view of row and column operation of the matrix, this can be seen as each row of the matrix being shifted one element forward (or due to the circulant nature of the matrix, it can be consider as element in column being shifted one element down), where the bumped element is replaced to the end of the row. It can also be thought of as the whole row is shifted down and the bumped row is placed back on top (or the whole column is shifted to the left), but this is irrelevant to our interest. Arbitrary power of

the matrix can be deduced accordingly; this operation has a cycle of n iterations. The generating circulant matrix is served as our building block. We have a corresponding polynomial:

$$p(x) = c_0 + c_1 x + c_2 x^2 + \cdots + c_{n-1} x^{n-1} \tag{4.12}$$

Then, the original circulant matrix C can be expressed as:

$$C = \begin{pmatrix} c_0 & c_{n-1} & c_{n-2} & \cdots & c_2 & c_1 \\ c_1 & c_0 & c_{n-1} & \cdots & c_3 & c_2 \\ c_2 & c_1 & c_0 & \cdots & \vdots & c_3 \\ c_3 & c_2 & c_1 & \cdots & \vdots & \vdots \\ \vdots & \vdots & \vdots & \ddots & \vdots & c_{n-1} \\ c_{n-1} & c_{n-2} & c_{n-3} & \cdots & c_1 & c_0 \end{pmatrix}$$

$$C = p(G) = c_0 \mathbf{I}^n + c_1 G + c_2 G^2 + \cdots + c_{n-1} G^{n-1} \tag{4.13}$$

This can be verified by doing the row-operation of arbitrary power on G as shown above. It can be shown that each operation is one-element sub-diagonal compared to the previous power.

Definition 4.3. (Fourier matrix)
The Fourier matrix is introduced as

$$F \equiv \begin{pmatrix} 1 & 1 & 1 & \cdots & 1 & 1 \\ 1 & \xi & \xi^2 & \cdots & \xi^{n-2} & \xi^{n-1} \\ 1 & \xi^2 & \xi^{2\times 2} & \cdots & \vdots & \xi^{2(n-1)} \\ 1 & \xi^3 & \xi^{3\times 2} & \cdots & \vdots & \vdots \\ \vdots & \vdots & \vdots & \ddots & \vdots & \vdots \\ 1 & \xi^{n-1} & \xi^{2(n-1)} & \cdots & \cdots & \xi^{(n-1)^2} \end{pmatrix} = \begin{pmatrix} 1 & 1 & 1 & \cdots & 1 & 1 \\ 1 & \xi & \xi^2 & \cdots & \xi^{n-2} & \xi^{n-1} \\ 1 & \xi^2 & \xi^{2\times 2} & \cdots & \vdots & \xi^{n-2} \\ 1 & \xi^3 & \xi^{3\times 2} & \ddots & \vdots & \vdots \\ \vdots & \vdots & \vdots & \ddots & \vdots & \xi^2 \\ 1 & \xi^{n-1} & \xi^{n-2} & \cdots & \xi^2 & \xi \end{pmatrix} \tag{4.14}$$

Here, we define the n-th unity root as $\omega = e^{2\pi i \frac{1}{n}}$, and $\xi = \bar{\omega} = e^{-2\pi i \frac{1}{n}}$ is the conjugate of the unity root. $i = \sqrt{-1}$, is the basic unit of the imaginary number.
The second equal sign here is given by the De Moivre's formula: $\xi^n = 1$ and $\xi^{2(n-1)} = \xi^n * \xi^{n-2} = \xi^{n-2}$.
The Fourier matrix can be defined using the positive argument ω instead of ξ. Also, as we will see later, some definition includes the normalizing scalar $\frac{1}{\sqrt{n}}$ (or $\frac{1}{n}$).
This is analogous to the duality in Fourier transform, the relationship is uphold by the opposite signs of the exponential power in the original and inverse Fourier transform.
This duality will be restated in the diagonalization representation of the circulant matrix later.

Proposition 4.2. (Unitary Matrix)
If $\frac{1}{\sqrt{n}}$ normalizes the Fourier matrix, then $\frac{1}{\sqrt{n}}F$ is a unitary matrix. It is symmetric (i.e., $F^T = F$), and the inverse of the Fourier matrix is given by

$$\begin{aligned} F^{-1} &= \left(\frac{\sqrt{n}}{\sqrt{n}}F^{-1}\right) \\ &= \frac{1}{\sqrt{n}}\left(\frac{1}{\sqrt{n}}F\right)^{-1} \\ &= \frac{1}{\sqrt{n}}\left(\frac{1}{\sqrt{n}}\bar{F}^T\right) \\ &= \frac{1}{n}\bar{F} = \frac{1}{n}\begin{pmatrix} 1 & 1 & 1 & \cdots & 1 & 1 \\ 1 & \omega & \omega^2 & \cdots & \omega^{n-2} & \omega^{n-1} \\ 1 & \omega^2 & \omega^{2\times 2} & \cdots & \vdots & \omega^{n-2} \\ 1 & \omega^3 & \omega^{3\times 2} & \cdots & \vdots & \vdots \\ \vdots & \vdots & \vdots & \ddots & \vdots & \omega^2 \\ 1 & \omega^{n-1} & \omega^{n-2} & \cdots & \omega^2 & \omega \end{pmatrix} \end{aligned}$$

Proposition 4.3.
If we multiply the Fourier matrix with the generating circulant matrix, we have

$$\begin{aligned} FG &= \begin{pmatrix} 1 & 1 & 1 & \cdots & 1 & 1 \\ 1 & \xi & \xi^2 & \cdots & \xi^{n-2} & \xi^{n-1} \\ 1 & \xi^2 & \xi^{2\times 2} & \cdots & \vdots & \xi^{n-2} \\ 1 & \xi^3 & \xi^{3\times 2} & \ddots & \vdots & \vdots \\ \vdots & \vdots & \vdots & \ddots & \vdots & \xi^2 \\ 1 & \xi^{n-1} & \xi^{n-2} & \cdots & \xi^2 & \xi \end{pmatrix} \begin{pmatrix} 0 & 0 & 0 & \cdots & 0 & 1 \\ 1 & 0 & 0 & \cdots & 0 & 0 \\ 0 & 1 & 0 & \cdots & 0 & 0 \\ 0 & 0 & 1 & \cdots & 0 & 0 \\ \vdots & \vdots & \vdots & \ddots & \vdots & \vdots \\ 0 & 0 & 0 & \cdots & 1 & 0 \end{pmatrix} \\ &= \begin{pmatrix} 1 & 1 & \cdots & 1 & 1 & 1 \\ \xi & \xi^2 & \cdots & \xi^{n-2} & \xi^{n-1} & 1 \\ \xi^2 & \xi^{2\times 2} & \cdots & \vdots & \xi^{n-2} & 1 \\ \xi^3 & \xi^{3\times 2} & \ddots & \vdots & \vdots & 1 \\ \vdots & \vdots & \ddots & \vdots & \xi^2 & 1 \\ \xi^{n-1} & \xi^{n-2} & \cdots & \xi^2 & \xi & 1 \end{pmatrix} \end{aligned}$$

This is the same as shifting (rotating) the first column to the back of the matrix, and is also equivalent to multiplying the first row with $\xi^0 = 1$, the 2nd row with ξ^1, etc.

In matrix operation, it can be seen as:

$$
\begin{aligned}
FG &= \begin{pmatrix}
1 & 1 & \cdots & 1 & 1 & 1 \\
\xi & \xi^2 & \cdots & \xi^{n-2} & \xi^{n-1} & 1 \\
\xi^2 & \xi^{2\times 2} & \cdots & \vdots & \xi^{n-2} & 1 \\
\xi^3 & \xi^{3\times 2} & \ddots & \vdots & \vdots & 1 \\
\vdots & \vdots & \ddots & \vdots & \xi^2 & 1 \\
\xi^{n-1} & \xi^{n-2} & \cdots & \xi^2 & \xi & 1
\end{pmatrix} \\
&= \begin{pmatrix}
1 & 0 & 0 & \cdots & 0 & 0 \\
0 & \xi & 0 & \cdots & 0 & 0 \\
0 & 0 & \xi^2 & \cdots & \vdots & 0 \\
0 & 0 & 0 & \ddots & \vdots & \vdots \\
\vdots & \vdots & \vdots & \ddots & \ddots & 0 \\
0 & 0 & 0 & \cdots & 0 & \xi^{n-1}
\end{pmatrix}
\begin{pmatrix}
1 & 1 & 1 & \cdots & 1 & 1 \\
1 & \xi & \xi^2 & \cdots & \xi^{n-2} & \xi^{n-1} \\
1 & \xi^2 & \xi^{2\times 2} & \cdots & \vdots & \xi^{n-2} \\
1 & \xi^3 & \xi^{3\times 2} & \ddots & \vdots & \vdots \\
\vdots & \vdots & \vdots & \ddots & \vdots & \xi^2 \\
1 & \xi^{n-1} & \xi^{n-2} & \cdots & \xi^2 & \xi
\end{pmatrix} \\
&= \Lambda F
\end{aligned}
$$

where Λ is the diagonal matrix with the k-th diagonal $\Lambda_k = \left\{\xi^k\right\}$, for $0 \leq k \leq n-1$. It follows that

$$FGF^{-1} = \Lambda \tag{4.15}$$

That is, the Fourier matrix diagonalizes the generating circulant matrix with eigenvalues $\left\{\xi^k\right\}_{0\leq k\leq n-1}$.

Theorem 4.2. (Fourier Decomposition of General Circulant Matrix)
The circulant matrix is decomposable by the Fourier matrix, i.e. $C = F^{-1}\Lambda F$ with eigenvalue matrix $\Lambda = \left\{p\left(\xi^k\right)\right\}_{k=0\cdots n-1}$. Also, with equation (4.13), the diagonalization of C can be written as

$$
\begin{aligned}
FCF^{-1} &= F\left(c_0\mathbf{1} + c_1 G + c_2 G^2 + \cdots + c_{n-1}G^{n-1}\right)F^{-1} \\
&= c_0\mathbf{1} + c_1\left(FGF^{-1}\right) + c_2\left(FGF^{-1}\right)^2 + \cdots + c_{n-1}\left(FGF^{-1}\right)^{n-1} \\
&= \begin{pmatrix}
p(1) & 0 & 0 & \cdots & 0 & 0 \\
0 & p(\xi) & 0 & \cdots & 0 & 0 \\
0 & 0 & p(\xi^2) & \cdots & \vdots & 0 \\
0 & 0 & 0 & \ddots & \vdots & \vdots \\
\vdots & \vdots & \vdots & \ddots & \vdots & 0 \\
0 & 0 & 0 & \cdots & 0 & p(\xi^{n-1})
\end{pmatrix}
\end{aligned}
\tag{4.16}
$$

Note that $(FGF^{-1})^2 = FGF^{-1}FGF^{-1} = FGGF^{-1} = FG^2F^{-1}$.
So that, for example $(FGF^{-1})^2 = \Lambda^2$. So that Λ^2 is a main matrix (only the diagonal element is non-zero), where the diagonal element is $l_{kk} = \left\{\xi^k\right\}$, for $0 \leq k \leq n-1$.
Other powers can be deduced iteratively, and the circulant matrix decomposition with polynomial eigenfunctions $p(\xi^k)$, for $0 \leq k \leq n-1$.

Theorem 4.2 gives us the fundamental theoretical framework to build up the FFT exact simulation of fBMs. The basic idea of the simulation is to embed the covariance matrix into a bigger circulant matrix to carry out the discrete Fourier transform as outlined above (with technique of FFT). Such technique is called Circulant Embedding Method (CEM), and is outlined in Dietrich and Newsam [DN97] and Perrin et al. [PHJI02].

Suppose that we need sample size of N (N should be a power of 2, i.e. $N = 2^g$ for some $g \in N$ for the sake of convenience when facilitating FFT). Generate the N-by-N covariance matrix Γ with entries $\Gamma_{j,k} = \gamma(|j-k|)$, where γ is the covariance function given in the definition of fractional Gaussian noise (fGn), by

$$\Gamma = \begin{pmatrix} \gamma(0) & \gamma(1) & \cdots & \gamma(N-1) \\ \gamma(1) & \gamma(0) & \cdots & \gamma(N-2) \\ \vdots & \vdots & \ddots & \vdots \\ \gamma(N-1) & \gamma(N-2) & \cdots & \gamma(0) \end{pmatrix}$$

This approach is generalized by Davies and Harte [DH87], and consists of embedding this covariance matrix into a bigger M-by-M (with $M = 2N$) circulant covariance matrix C such as:

$$C = \begin{pmatrix} \gamma(0) & \gamma(1) & \cdots & \gamma(N-1) & 0 & \gamma(N-1) & \gamma(N-2) & \cdots & \gamma(2) & \gamma(1) \\ \gamma(1) & \gamma(0) & \cdots & \gamma(N-2) & \gamma(N-1) & 0 & \gamma(N-1) & \cdots & \gamma(3) & \gamma(2) \\ \vdots & \vdots & \ddots & \vdots & \vdots & \vdots & \vdots & \ddots & \vdots & \vdots \\ \gamma(N-1) & \gamma(N-2) & \cdots & \gamma(0) & \gamma(1) & \gamma(2) & \gamma(3) & \cdots & \gamma(N-1) & 0 \\ 0 & \gamma(N-1) & \cdots & \gamma(1) & \gamma(0) & \gamma(1) & \gamma(2) & \cdots & \gamma(N-2) & \gamma(N-1) \\ \gamma(N-1) & 0 & \cdots & \gamma(2) & \gamma(1) & \gamma(0) & \gamma(1) & \cdots & \gamma(N-3) & \gamma(N-2) \\ \vdots & \vdots & \ddots & \vdots & \vdots & \vdots & \vdots & \ddots & \vdots & \vdots \\ \gamma(1) & \gamma(2) & \cdots & 0 & \gamma(N-1) & \gamma(N-2) & \gamma(N-3) & \cdots & \gamma(1) & \gamma(0) \end{pmatrix}$$

where the covariance matrix is embedded on the top left hand corner. It is sufficient to point out that

$$C_{0,k} = \begin{cases} \gamma(k) & k = 0, \cdots, N-1 \\ \gamma(2N-k) & k = N+2, \cdots, 2N-1 \end{cases}$$

Remark: As Perrin et al. [PHJI02] have pointed out, the size M can be $M \geq 2(N-1)$, and the case $M = 2(N-1)$ is minimal embedding. For any other choice of M, the choice of $C_{0,N}, \ldots, C_{0,M-N+1}$ is arbitrary and can be conveniently chosen as long as the symmetry of the matrix is upheld; more zeros can be padded if M is bigger to make C circulant. For the rest of the chapter, we will concern ourselves with the case $M = 2N$.

From Theorem 4.2, we know that, given any circulant matrix, it can be decomposed as $C = Q\Lambda Q^*$, where

$$(Q)_{j,k} = \frac{1}{\sqrt{2N}} \exp\left(-2\pi i \frac{jk}{2N}\right) \qquad \text{, for } j,k = 0, \cdots, 2N-1 \tag{4.17}$$

The matrix Λ is the diagonal matrix with eigenvalues

$$\lambda_k = \sum_{j=0}^{2N-1} c_{0,j} \exp\left(2\pi i \frac{jk}{2N}\right) \qquad \text{, for } j,k = 0, \ldots, 2N-1 \tag{4.18}$$

This differs slightly from the previous definition, but similar to the continuous counterpart; the sign of the exponential power in the Fourier transform is just conventional difference. The approach is identical as long as the duality is maintained. That is, if written in the form of $C = Q\Lambda Q^*$, the sign of the exponential power of the component in Q and Λ should be opposite. In the case of the previous theorem where $C = F^{-1}\Lambda F$, it is easy to check that F^{-1} and $\Lambda(\xi)$ indeed have the opposite sign in the exponential power.

It should be noted that C is not guaranteed to be positive-definite. Davies and Harte [DH87] suggest setting zero every negative value that may appear in Λ. In Perrin et al. [PHJI02], they prove that the circulant covariance matrix for fGn is always non-negative definite, so the approach is feasible without any modification. The reader is referred to Dietrich and Newsam [DN97] and Wood and Chan [WC94] for more detail on dealing with this issue.

Assuming that C is positive definite and symmetric, the eigenvalues are positive and real. The 'square root' of C is readily formed, $S = Q\Lambda^{1/2}Q^*$, where $\Lambda^{1/2}$ is the diagonal matrix with eigenvalues $1, \sqrt{\lambda_1}, \cdots, \sqrt{\lambda_{2N-1}}$. It is easy to check that $SS^* = SS' = C$. So, S has the desired properties we look for.

Theorem 4.3. (Simulation of fGn with FFT)
The simulation of the sample path of fGn, we are going to simulate $y = SV$, consists of the following steps:

1. Compute the eigenvalues $\{\lambda_k\}_{k=0,\ldots,2N-1}$ from equation (4.18) by means of FFT. This will reduce the computational time from $O(N^2)$ to $O(N \log N)$.
2. Calculate $W = Q^*V$.
   - Generate two standard normal random variables $W_0 = V_0^{(1)}$ and $W_N = V_N^{(1)}$
   - For $1 \le j < N$, generate two standard normal random variables $V_j^{(1)}$ and $V_j^{(2)}$ and let
     - $W_j = \frac{1}{\sqrt{2}}\left(V_j^{(1)} + iV_j^{(2)}\right)$
     - $W_{2N-j} = \frac{1}{\sqrt{2}}\left(V_j^{(1)} - iV_j^{(2)}\right)$

3. Compute $Z = Q\Lambda^{1/2}W$. This can be seen as another Fourier transform of the vector $\Lambda^{1/2}W$:

   - $Z_k = \frac{1}{\sqrt{2N}} \sum_{j=0}^{2N-1} \sqrt{\lambda_j} W_j \exp\left(-2\pi i \frac{jk}{2N}\right)$
   - It is identical to carry out FFT on the following sequence:

$$w_j = \begin{cases} \sqrt{\frac{\lambda_0}{2N}} V_0^{(1)} & j = 0 \\ \sqrt{\frac{\lambda_j}{4N}} \left(V_j^{(1)} + iV_j^{(2)}\right) & j = 1, \cdots, N-1 \\ \sqrt{\frac{\lambda_N}{2N}} V_N^{(1)} & j = N \\ \sqrt{\frac{\lambda_j}{4N}} \left(V_{2N-j}^{(1)} - iV_{2N-j}^{(2)}\right) & j = N+1, \cdots, 2N-1 \end{cases}$$

   - Due to the symmetric nature of the sequence, the Fourier sum of $\{w_j\} = \{Z_k\}_{k=0}^{2N-1}$ is real. The first N samples have the desired covariance structure. But, since the 2nd half of samples $(N \cdots 2N-1)$ are not independent of the first N samples, this sample cannot be used.

4. Recover fBM from the recursive relationship:

   - $B^H(0) = 0; \qquad B^H(i) = B^H(i-1) + Z_{i-1}, \qquad \text{for } 1 \leq i \leq N$

The Fast-Fourier Transform is of similar vein to the Cholesky decomposition, while utilizing the FFT algorithm thus improve the speed tremendously, in particular, the computation is of order $N \log(N)$ for N sample points. We have here included several sample paths with the same standard normal variables seed, and different Hurst indices:
Figure 2, 3 and 4 are all generated by the same standard normal random vector, but with different Hurst indices, and thus different Fourier matrix. Figure 2 depicts the ordinary Brownian motion case, where figure Figure 3 depicts the fractional case with $H = 0.7$ and figure 4 with $H = 0.85$.

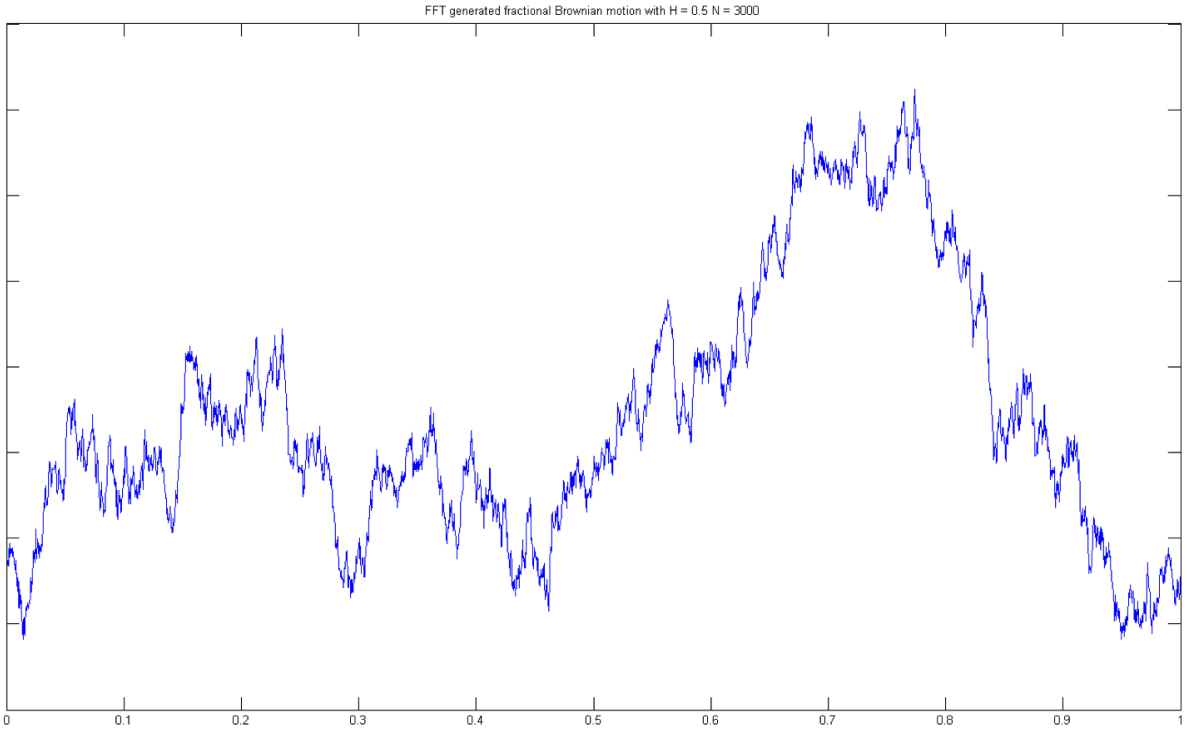

Figure 2: FFT generated Fractional Brownian Motion Path with $H = 0.5$

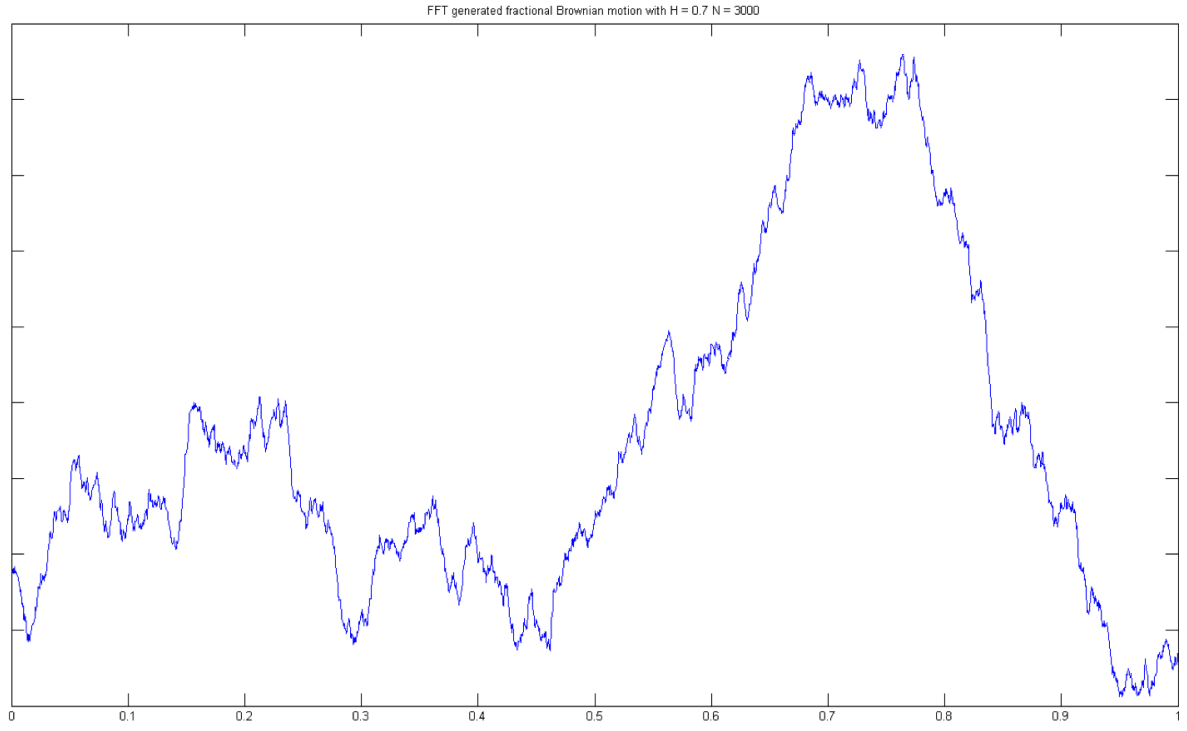

Figure 3: FFT generated Fractional Brownian Motion Path with $H = 0.7$

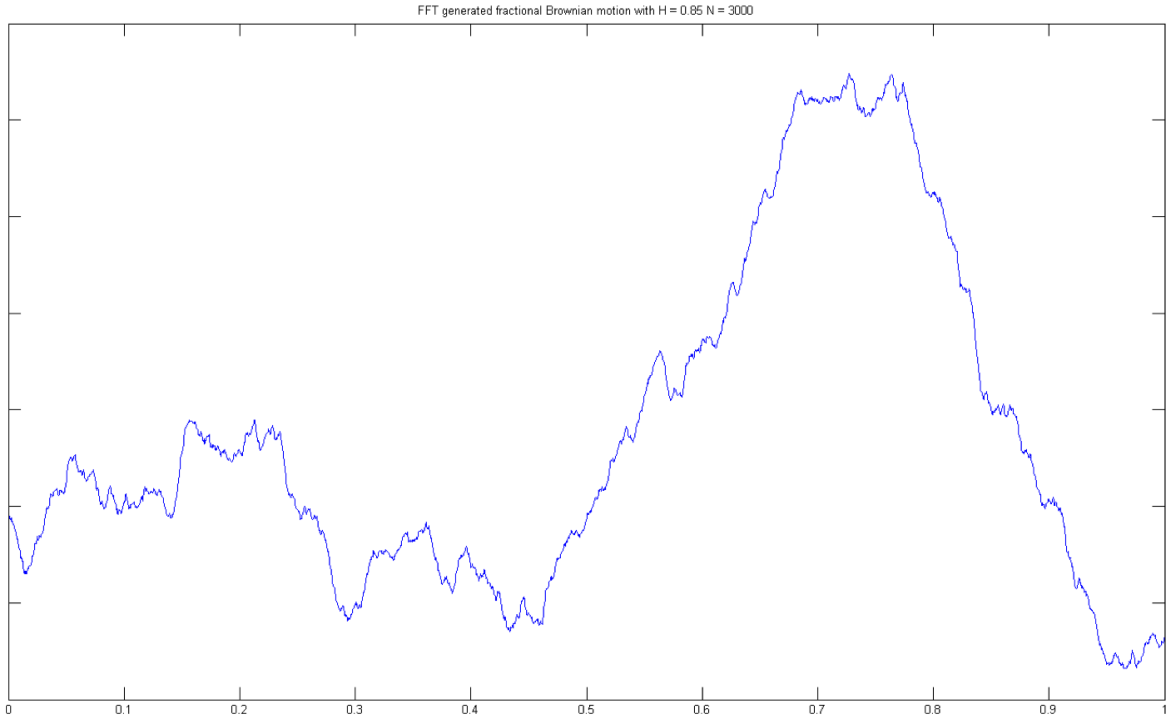

Figure 4: FFT generated Fractional Brownian Motion Path with $H = 0.85$

5 Approximate Methods

As seen in the previous section, the exact methods all take on the covariance structure matrix as starting point and try to reproduce the covariance structure by different decomposition. That can be time and resource consuming, so rather it is preferable to have approximation of the fractional Brownian motion that permits robust simulation.
In this section, starting with the Mandelbrot representation due to historical reason and move onto several other methods that provide us with better understanding of the process and increasing robustness.

5.1 Mandelbrot Representation

Recalling from Section 2.1, fractional Brownian motion permits a stochastic integral representation. To approximate equation (2.3) in the sense of Riemann-type summation, it is natural to truncate the lower limit from negative infinity to some point, say at $-b$ for $\tilde{B}^H(n)$, where $n = 0, 1, \cdots, N$:

$$\tilde{B}^H(n) = C_H \sum_{k=-b}^{0} \left[(n-k))^{H-1/2} - (-k)^{H-1/2} \right] B_1(k) + \sum_{k=0}^{n} (n-k)^{H-1/2} B_2(k) \tag{5.1}$$

Here B_1 and B_2 are $b+1$ and $N+1$ vector of standard Brownian motion respectively, who are mutually independent. Note that the C_H is not the same constant term as in equation (2.3), because one has to re-calculate the normalizing factor due to the truncation, the accuracy of the summation improves as b increases and the grid gets finer, though the computational burden increases tremendously. As pointed out in [Die02], the recommended choice of b is $N^{3/2}$. Even though this is a straightforward way to generate fractional Brownian motion, it is rather inefficient. It is included in this section for the sake of completeness.

5.1.1 Volterra Representation - Euler Hypergeometric Integral

According to [DU99], fBM permits the stochastic integral form involving the Euler hypergeometric integral:

$$B^H(t) = \int_0^t K_H(t,s) dB(s) \tag{5.2}$$

where $B(s)$ is the standard Brownian motion and

$$K_H(t,s) = \frac{(t-s)^{H-1/2}}{\Gamma(H+1/2)} F_{2,1}\left(H - \frac{1}{2}; \frac{1}{2} - H; H + \frac{1}{2}; 1 - \frac{t}{s} \right)$$

is the hypergeometric function, which can be readily computed by most mathematical packages. By discretizing (5.2), at each time index t_j, we have

$$B^H(t_j) = \frac{n}{T} \sum_{i=0}^{j-1} \left(\int_{t_i}^{t_{i+1}} K_H(t_j, s)\, ds \right) \delta B_i$$

where $\delta B_i = \sqrt{\frac{T}{n}} \Delta B_i$ and ΔB_i is drawn according to the standard normal distribution. This means that $\{\delta B_i\}_{i=1\cdots n}$ is the increments of a scaled Brownian motion on $[0, T]$ with quadratic variation T. The inner integral can be computed by the Gaussian quadrature efficiently.

5.2 Construction by Correlated Random Walk

This particular algorithm proposed in [Enr04] of constructing fBM relies on the process of correlated random walks and summation over generated paths. This is similar to the generation of ordinary Brownian method through summation of the sample paths of normal random walk, which is related to the central limit theorem.

Definition 5.1. (Correlated Random Walk)
For any $p \in [0,1]$, denote X_n^p as the correlated random walk with persistence index p. It consists of a jump on each time-step with jump size of either $+1$ or -1 such that:

- $X_0^p = 0, P(X_1^p = -1) = 1/2, P(X_1^p = +1) = 1/2$
- $\forall n \geq 1, \epsilon_n^p \equiv X_n^p - X_{n-1}^p$ which equals either $+1$ or -1
- $\forall n \geq 1, P(\epsilon_{n+1}^p = \epsilon_n^p | \sigma(X_k^p, 0 \leq k \leq n)) = p$

Theorem 5.1.
For any $m \geq 1, n \geq 0$, we have

$$\mathbf{E}\left[\epsilon_m^p \epsilon_{m+n}^p\right] = (2p-1)^n \tag{5.3}$$

In order to add additional randomness into the correlated random walks, we replace the constant persistence index p with a random variable μ, and we denote the resulting correlated random walk as X_n^μ. Or, to put it more formally, denote by P^p the law of X^p for a given persistence index p. Now, consider a probability measure μ on $[0,1]$, which we call the corresponding probability law P^μ, the annealed law of the correlated walk associated to μ. Note that $P^\mu \triangleq \int_0^1 P^p d\mu(p)$

Proposition 5.1.
For all $m \geq 1, n \geq 0$, we have

$$\mathbf{E}\left[\epsilon_m^\mu \epsilon_{m+n}^\mu\right] = \int_0^1 (2p-1)^n \, d\mu(p) \tag{5.4}$$

The next result is due to Enriquez [Enr04]. The proof is based on Lemma 5.1 of Taqqu [Taq75].

Theorem 5.2.
For $1/2 < H < 1$, denote by μ^H the probability on $[1/2, 1]$
with density $(1-H)\, 2^{3-2H}\, (1-p)^{1-2H}$. Let $\left(X^{\mu^H, i}\right)_{i \geq 1}$ be a sequence of independent processes with probability law P^{μ^H}. Then,

$$\mathcal{L}^D \lim_{N\to\infty} \mathcal{L} \lim_{N\to\infty} c_H \frac{X_{[Nt]}^{\mu^H,1} + \cdots + X_{[Nt]}^{\mu^H,M}}{N^H \sqrt{M}} = B_H(t) \tag{5.5}$$

where $c_H = \sqrt{\frac{H(2H-1)}{\Gamma(3-2H)}}$, $\mathcal{L} \lim_{N\to\infty}$ stands for the convergence in law, and $\mathcal{L}^D \lim_{N\to\infty}$ means the convergence in the sense of weak convergence in the Skorohod topology on $D[0,1]$, the space of cadlag functions on $[0,1]$. Here, $[\cdot]$ is the floor function and rounds the argument to the closest lower integer, M is the number of trajectories of correlated random walks and N is number of time steps.

Remark: For $H = 1/2$, there is a similar expression (see [Enr04]). The order of limit in equation (5.5) is important, because if reversed, the sum would result in 0. Theorem 5.2 is mostly for theoretical construction.
In [Enr04], the above theorem is further simplified from double summations into a single summation by applying Berry-Essen bound: As long as $M(N)$ is of order $O\left(N^{2-2H}\right)$,

$$\mathcal{L}^D \lim_{N\to\infty} c_H \frac{X^{\mu^H,1}_{[Nt]} + \cdots + X^{\mu^H,M(N)}_{[Nt]}}{N^H\sqrt{M(N)}} = B_H(t) \tag{5.6}$$

In practice, any probability measure with moment equivalent to $\frac{1}{n^{2-2H}L(n)}$, where L is a slowly varying function, will be used. This could be shown by Karamata's theorem, for which further elaboration is found in [Enr04]. In [Enr04], three families of equivalent measures are provided, and specifically the 2nd family of the measures $\left(\mu'_{H,k}\right)_{k>0}$ is most appropriate for simulation purpose:

For $H > 1/2$, $\mu'_{H,k}$ has the density of $1 - \frac{\left(1-U^{1/k}\right)^{\frac{1}{2-2H}}}{2}$ with the corresponding normalizing factor $c'_{H,k} = \frac{c_H}{\sqrt{k}}$. The error given by the Berry-Essen bound for $H > 1/2$ is given by

$$0.65 \times D_H N^{1-H}/\sqrt{kM} \tag{5.7}$$

where $D_H = \sqrt{\frac{6(2H-1)}{(H+1)(2H+1)}}$. Here, k serves as a control variable of order $k(N) = o(N)$, and the error term contains $\frac{1}{\sqrt{k}}$ which can be seen as a way to restrict error with the price of distortion of the covariance relation in X_N, though it is advisable to keep $k \leq 1$. For more discussion on the choice of k, we refer to Section 4 of [Enr04].

Theorem 5.3. (Simulation of fBM with correlated random walk)
Simulating fBM with correlated random walk for the case of $H > 1/2$ consists of the following steps:

1. Calculate $M(N)$ by the tolerable error level from equation (5.7). Calculate $\lfloor NT \rfloor$, where $\lfloor\cdot\rfloor$ is the floor function, and create time-index $t_i : \{1, 2, \cdots, \lfloor NT \rfloor\}$.

2. Simulate M independent copies of $\left\{\mu^j_{H,k}\right\}_{j=1\cdots M} = 1 - \frac{\left(1-U^{1/k}\right)^{\frac{1}{2-2H}}}{2}$ for M trajectories.

3. Simulate M copies of correlated random walks:

   - If $t_i = 1$, $\epsilon^j_1 = 2 * Bernoulli(\frac{1}{2}) - 1, \quad X^j_1 = \epsilon^j_1$
   - If $t_i > 1$, $\epsilon^j_{t_j} = \epsilon^j_{t_{j-1}} * \left(2 * Bernoulli\left(\mu^j_{H,k}\right) - 1\right), \qquad X^j_{t_j} = X^j_{t_{j-1}} + \epsilon^j_{t_j}$

4. At each t_j, calculate

   - $B^H_{t_j} = c'_H \frac{X^{\mu^H,1}_{\left[Nt_j\right]} + \cdots + X^{\mu^H,M}_{\left[Nt_j\right]}}{N^H\sqrt{M}}$

Remark: For any given time-horizon T, it is easier to simulate the path of $B^H(1)$ with given resolution N and scale it to arrive at $B^H(T) = T^H B^H(1)$.
This algorithm is interesting from a theoretical point of view, since it gives us a construction of fractional Brownian motion reflecting its ordinary Brownian motion counterpart with the help of central limit theorem. But, in practice, it might not be fast enough for simulation purpose that requires large number of simulated paths. We included figures for sample paths.

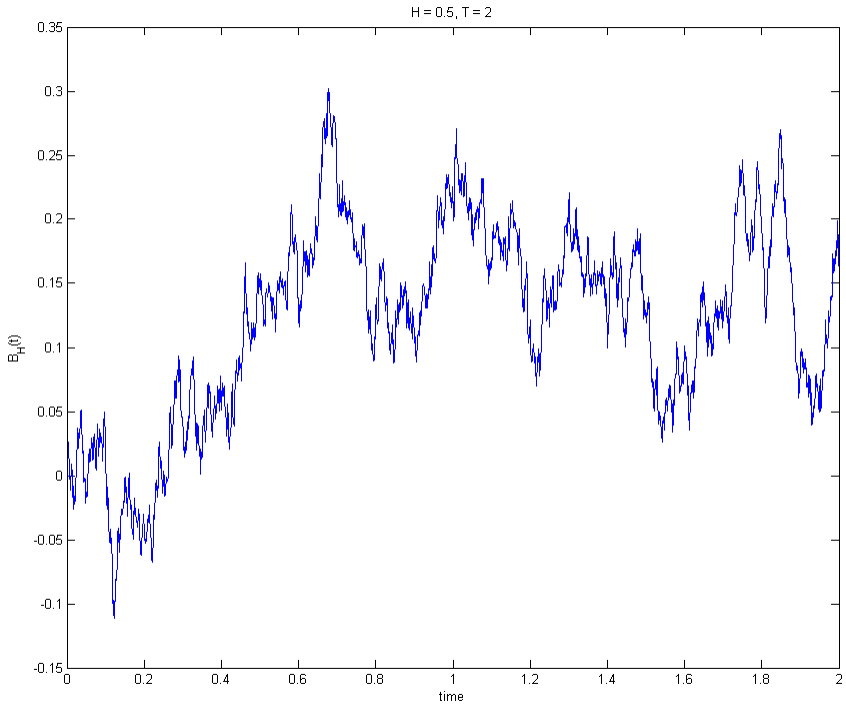

Figure 5: Correlate Random Walk generated Fractional Brownian Motion Path with $H = 0.5$

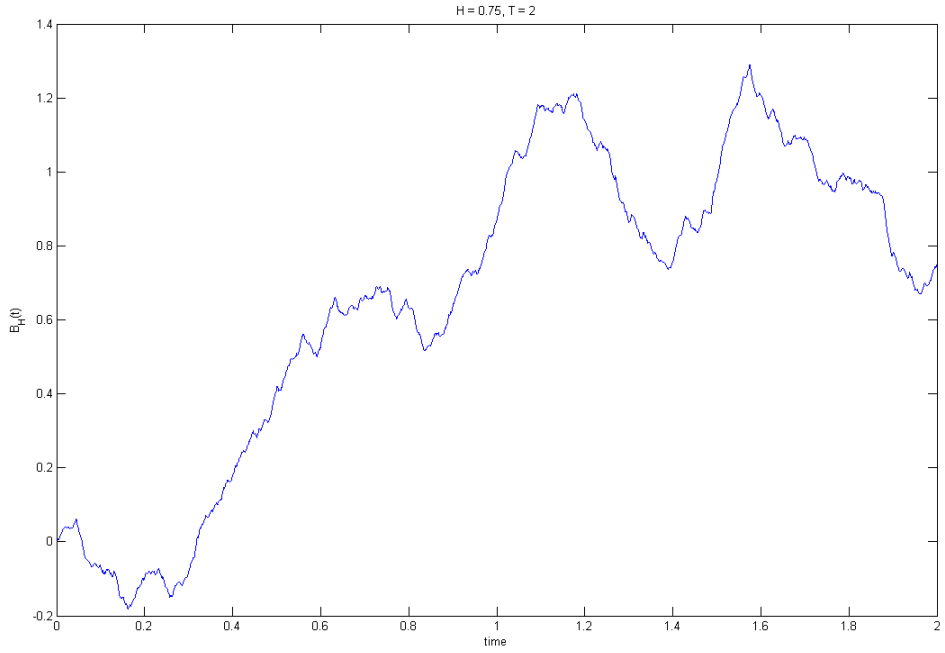

Figure 6: Correlate Random Walk generated Fractional Brownian Motion Path with $H = 0.75$

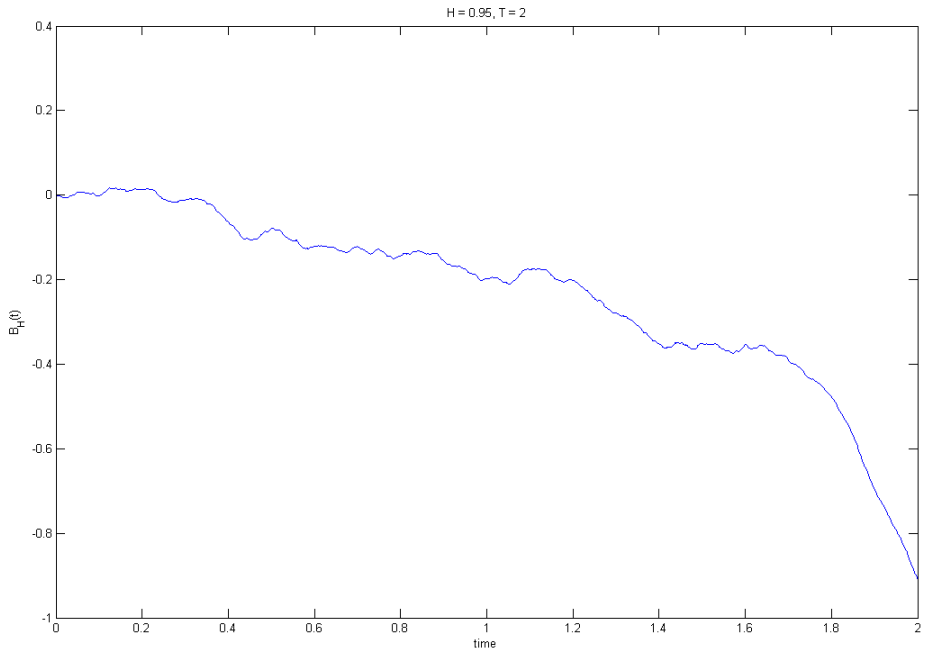

Figure 7: Correlate Random Walk generated Fractional Brownian Motion Path with $H = 0.95$

5.3 Conditional Random Midpoint Displacement

This algorithm is put forth by Norros et al. [NMW99] and uses the similar approach to compute the conditional distribution of the fractional Gaussian noises as we have seen in the Hosking algorithm in Section 4.1. The difference is that this algorithm does not completely capture the covariance of all the sample points, instead it chooses certain number of points of the generated samples and uses a different ordering to do conditioning on (recall that, in the Hosking method, the conditioning is done by chronological order).

Again we are interested in the stationary fractional Gaussian noises and will back out the fractional Brownian motion on the time interval $[0, 1]$, which can be scaled back according to self-similarity relationship. First outlining the idea of bisection method, which will be expanded into the conditional mid-point replacement scheme later on.

5.3.1 Bisection Scheme and Basic Algorithm

In this section the notation is adopted in Norros et al. [NMW99]: $Z(t)$ is the fractional Brownian motion, and $X_{i,j}$ is the fractional Gaussian noise of a certain interval j in a given level i.

The idea is to simulate $Z(t)$ on the interval $[0, 1]$. First, given $Z(0) = 0$ and $Z(1)$ with the standard normal distribution of $N(0, 1)$, we compute the conditional distribution of $\{Z(1/2)|Z(0), Z(1)\} \tilde{} N(\frac{1}{2}Z(1), 2^{-2H} - \frac{1}{4})$. The bisection involves the indices i and j, where i indicates the 'level' and j for the 'position. Let

$$X_{i,j} = Z\left(j \cdot 2^{-i}\right) - Z\left((j-1) \cdot 2^{-i}\right), \qquad \text{for } i = 0, 1, 2, \ldots., j = 1, \cdots, 2^i$$

It is easy to see that, at any given level i, the interval $[0, 1]$ is divided into 2^i sub-intervals.

If we denote $(i-1)$th level as the 'mother-level', it will be divided twice finer in the next level. So given any interval on the mother level, it is easy to observe the relationship

$$X_{i,2j-1} + X_{i,2j} = X_{i-1,j} \tag{5.8}$$

Because of equation (5.8), it is enough to just generate $X_{i,j}$ for odd number j. So, let us proceed from left to right, assuming that the sample points $X_{i,1}, \cdots X_{i,2k}$ have already been generated $k \in \{0, 1, \ldots, 2^{i-1} - 1\}$. Obviously we cannot condition on all the previous generated samples. So, for the point $X_{i,2k+1}$, we only condition on m previous points on the left at current level, and n points on the right on the previous level. Then we have

$$X_{i,2k+1} = \mathbf{e}(i,k) \left[\overbrace{X_{i,\max(2k-m+1,1)}, \cdots, X_{i,2k}}^{\text{Current Level}}, \underbrace{X_{i-1,k+1}, \cdots, X_{i-1,\min(k+n,2^{i-1})}}_{\text{Previous Level}} \right]' + \sqrt{v(i,k)} U_{i,k} \tag{5.9}$$

where $U_{i,k}$ are i.i.d. standard Gaussian random variables $i = 0, 1, \cdots; \quad k = 0, 1, \cdots, 2^{i-1} - 1$. For some vector $= \mathbf{e}(i,k)$, that

$$\begin{aligned} & \mathbf{e}(i,k) \left[X_{i,\max(2k-m+1,1)}, \cdots, X_{i,2k}, X_{i-1,k+1}, \cdots, X_{i-1,\min(k+n,2^{i-1})} \right]' \\ = \quad & \mathbf{E} \left[X_{i,2k+1} | X_{i,\max(2k-m+1,1)}, \cdots, X_{i,2k}, X_{i-1,k+1}, \cdots, X_{i-1,\min(k+n,2^{i-1})} \right] \end{aligned} \tag{5.10}$$

So that $\mathbf{e}(i,k)$ can be considered as the coefficient of regression of $X_{i,2k+1}$on the conditional probability space $X_{i,\max(2k-m+1,1)}, \cdots, X_{i,2k}, X_{i-1,k+1}, \cdots, X_{i-1,\min(k+n,2^{i-1})}$.
Now equation (5.9) can be rewritten as

$$\begin{aligned} X_{i,2k+1} \quad & = \mathbf{e}(i,k) \left[X_{i,(2k-m+1,1)}, \cdots, X_{i,2k}, X_{i-1,k+1}, \cdots, X_{i-1,\min(k+n,2^{i-1})} \right]' + \sqrt{v(i,k)} U_{i,k} \\ & = \mathbf{E} \left[X_{i,2k+1} | X_{i,\max(2k-m+1,1)}, \cdots, X_{i,2k}, X_{i-1,k+1}, \cdots, X_{i-1,\min(k+n,2^{i-1})} \right] + \sqrt{v(i,k)} U_{i,k} \end{aligned} \tag{5.11}$$

For some vector $= \mathbf{e}(i,k)$. Where $v(i,k)$ is the conditional variance:

$$v(i,k) = Var \left[X_{i,2k+1} | X_{i,\max(2k-m+1,1)}, \cdots, X_{i,2k}, X_{i-1,k+1}, \cdots, X_{i-1,\min(k+n,2^{i-1})} \right] \tag{5.12}$$

As mentioned before, this scheme conditions on a fixed number of past samples instead of the whole past, where $(m \geq 0, n \geq 1)$, thus the name Random Midpoint Displacement, RMD(m,n). Looking at (5.11) and (5.12) "$X_{i,(2k-m+1,1)}, \cdots, X_{i,2k}$" indicates that there are at most m neighboring increments to the left of the interval in question $X_{i,2k+1}$, and "$X_{i-1,k+1}, \cdots, X_{i-1,\min(k+n,2^{i-1})}$" indicates that there are at most n neighboring increments to the right of the interval.
Denote by Γ_{ik} the covariance matrix with $X_{i,2k+1}$ as the first entry, and
$X_{i,\max(2k-m+1,1)}, \cdots, X_{i,2k}, X_{i-1,k+1}, \cdots, X_{i-1,\min(k+n,2^{i-1})}$ as the rest of the entries. Then, we have

$$\Gamma_{ik} = Cov \left[X_{i,2k+1}, X_{i,\max(2k-m+1,1)}, \cdots, X_{i,2k}, X_{i-1,k+1}, \cdots, X_{i-1,\min(k+n,2^{i-1})} \right]$$

where

$$Cov([x_1, x_2, \cdots, x_n]) = \begin{pmatrix} Cov(x_1,x_1) & Cov(x_1,x_2) & \cdots & Cov(x_1,x_n) \\ Cov(x_2,x_1) & Cov(x_2,x_2) & \cdots & Cov(x_2,x_n) \\ \vdots & \vdots & \ddots & \vdots \\ Cov(x_n,x_1) & Cov(x_n,x_2) & \cdots & Cov(x_n,x_n) \end{pmatrix}$$

Similar to (4.3)-(4.5), we can partition Γ_{ik} as

$$\Gamma_{ik} = \begin{pmatrix} Var\left(X_{i,2k+1}\right) & \Gamma_{ik}^{(1,2)} \\ \Gamma_{ik}^{(2,1)} & \Gamma_{ik}^{(2,2)} \end{pmatrix}$$

Note that $\Gamma_{ik}^{(1,2)} = \left(\Gamma_{ik}^{(2,1)}\right)'$. Hence, we have

$$\mathbf{e}\left(i,k\right) = \Gamma_{ik}^{(1,2)} \left(\Gamma_{ik}^{(2,2)}\right)^{-1} \tag{5.13}$$

$$v\left(i,k\right) = \frac{\left|\Gamma_{ik}\right|}{\left|\Gamma_{ik}^{(2,2)}\right|} \tag{5.14}$$

By the stationarity of the increment of Z and by self-similarity, $\mathbf{e}\left(i,k\right)$ is independent of i and k when $2k \geq m$ and $k \leq 2^{i-1} - n$ (meaning that the sequence is not truncated by $\max\left(\cdot\right)$ and $\min\left(\cdot\right)$, and it only depends on i only when $2^i < m + 2n$.

5.3.2 On-the-Fly RMD(m,n) Generation

Norros et al. [NMW99] further propose that, instead of having the previous level $(i-1)$ completely generated first, partition and conditioning can be done 'on-the-fly', meaning that there are multiple unfinished levels going at the same time. Unlike the previous RMD(m,n) scheme, the level here is defined differently.

First define the 'resolution' by δ, as the smallest interval that within in this scheme. Note that this is different from the previous sub-section where at the i-th level $\delta = 2^{-i}$, which can be bisected finer indefinitely. Here, for the on-the-fly RMD scheme, the minimum interval length is defined as δ before hand, and cannot be changed afterwards.

At each level i, the interval $[0, 2^i\delta]$ is split finely into interval with length of δ and $X_{i,k}$ samples are generated on each point until all points within the interval are filled. Then, the trace is expanded to the next level $i+1$, the interval $[0, 2^{i+1}]$, and this procedure can be considered as 'enlargement'. So, instead of having a pre-determined time-horizon and zooming in with twice-finer resolution in the original RMD scheme, the new RMD scheme has a pre-determined resolution and expand twice-fold the horizon at each level.

Within the same interval $[0, 2^i\delta]$, the following rules are applied for the inner intervals:

1. On each interval, it must have $n-1$ (or all) right-neighboring intervals (of which, have the same length as the mother-interval).
2. Also, there should be m (or all) left-neighboring intervals (of which, have the same length as the interval being considered).
3. If there are intervals that satisfy both the conditions above, choose the one as left as possible.
4. When all intervals are filled out, expand to the next level by 'enlargement'.

Here we use

$$Y_{i,j} = Z\left(j \cdot 2^i\delta\right) - Z\left((j-1) \cdot 2^i\delta\right), \quad i = 0, 1, \cdots, \quad j = 1, 2, \cdots$$

instead of $X_{i,j}$ to avoid confusion with the original RMD scheme notation.

Similar to the ordinary RMD, we have the following equations from the conditional distribution of multivariate Gaussian processes: The enlargement stage is defined by

$$\begin{aligned} Y_{i,1} &= \mathbf{E}\left[Y_{i,1}|Y_{i-1,1}\right] + \sqrt{Var\left[Y_{i,1}|Y_{i-1,1}\right]}U_{i,1} \\ &= \mathbf{e}\left(i,1\right)Y_{i-1,1} + \sqrt{v\left(i,1\right)}U_{i,1} \end{aligned}$$

Inner interval points are constructed similar to the ordinary RMD scheme (the right-neighboring intervals are of level $i+1$ instead of $i-1$) as

$$Y_{i,2k+1} = \mathbf{e}\left(i,k\right)\left[Y_{i,\max(2k-m+1,1)},\cdots,Y_{i,2k},Y_{i+1,k+1},\cdots,Y_{i+1,\min(k+n,N_{i+1})}\right]' + \sqrt{v\left(i,k\right)}U_{i,k}$$

where N_{i+1} is the last generated increment on the $(i+1)$-th level. The order of splitting for the on-the-fly scheme is given in Figure 8, where its ordinary RMD counterpart's splitting order is also given.

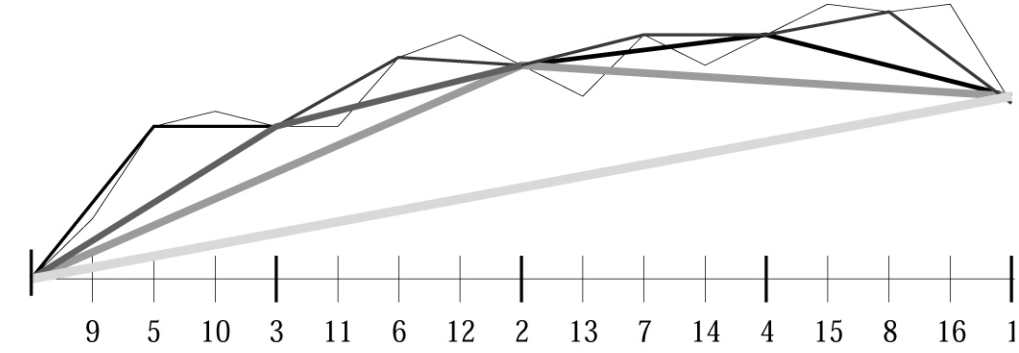

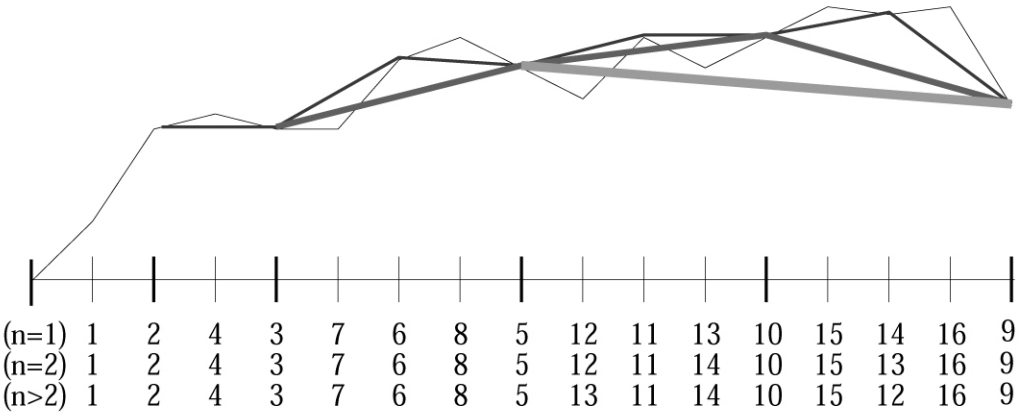

Figure 8: The order of splits by the ordinary RMD(m,n) scheme (top) and the on-the-fly RMD(m,n) scheme (bottom). Note that, for the on-the-fly scheme, the order changes according to the choice of n.

Norros et al. [NMW99] have done an extensive comparison between on-the-fly RMD schemes in terms of accuracy and robustness compared to the FFT and aggregate methods. On-the-fly RMD and FFT are significantly faster than the aggregate method, and on-the-fly RMD can generate samples with no fixed time-horizon, while for FFT the whole trace has to be generated before it can be used. So, RMD seems superior in terms of flexibility.

5.4 Spectral Method

In this subsection, the spectral method of approximating the fractional Gaussian noises is investigated, which has the origin from spectral analysis in physics: A time-domain can be transformed into a frequency-domain without loss of information through Fourier transform. With the typical Fourier-time series, the original input is deterministic and transformed into the spectral density that represents the magnitude of different frequencies in the frequency domain. It is possible to extend this approach to analyzing stochastic processes. Though it is impossible to study all realization, it is possible to analyze in a probabilistic/distribution sense by observing the expected frequency information contained in the autocovariance function.
Spectral density is computed for frequencies, $-\pi \leq \lambda \leq \pi$, as

$$f(\lambda) = \int_{-\infty}^{\infty} \gamma(j) \exp(ij\lambda)\, dj \tag{5.15}$$

The $\gamma(\cdot)$ here is the autocovariance function, which can be recovered by the inverse formula

$$\gamma(j) = \frac{1}{2\pi} \int_{-\pi}^{\pi} f(\lambda) \exp(-ij\lambda)\, d\lambda \tag{5.16}$$

The spectral density of the fGn can be approximated according to [Die02] and [Pax97] as

$$f(\lambda) = 2\sin(\pi H)\,\Gamma(2H+1)\,(1-\cos\lambda)\left[|\lambda|^{-2H-1} + B(\lambda, H)\right] \tag{5.17}$$

where

$$B(\lambda, H) = \sum_{j=1}^{\infty} \left\{ (2\pi j + \lambda)^{-2H-1} + (2\pi j - \lambda)^{-2H-1} \right\} \tag{5.18}$$

Note that the domain is only $-\pi \leq \lambda \leq \pi$, since any frequency higher would only correspond to amplitude between our desired sample points.
The problem with the above expression is that there is no known closed-form for $B(\lambda, H)$, Paxson [Pax97] proposes the following scheme for $B(\lambda, H)$:

$$B(\lambda, H) \cong \tilde{B}_3(\lambda, H) = a_1^d + b_1^d + a_2^d + b_2^d + a_3^d + b_3^d + \frac{a_3^{d'} + b_3^{d'} + a_4^{d'} + b_4^{d'}}{8H\pi} \tag{5.19}$$

where

$$d = -2H - 1, \quad d' = -2H, \quad a_k = 2k\pi + \lambda, \quad b_k = 2k\pi - \lambda \tag{5.20}$$

Moreover, with the help of the Whittle estimator, Paxson [Pax97] shows that

$$\tilde{B}_3(\lambda, H)' = [1.0002 - 0.000134\lambda]\left(\tilde{B}_3(\lambda, H) - 2^{-7.65H-7.4}\right) \tag{5.21}$$

gives a very robust and unbiased approximation for the $B(\lambda, H)$. See Appendix A of [Pax97] for a detailed comparison and justification of this approximation, also Flandrin [Fla89] gives the detail in how to simulate fractional Brownian motion directly with the spectral density, where some problem might arise due to the non-stationary nature of fractional Brownian motion, the issues are addressed by Flandrin in the aforementioned paper.

Theorem 5.4. (Spectral Simulation)
With the approximation scheme for the spectral density at hand, we can now look at the spectral analysis of a stationary discrete-time Gaussian process (fractional Gaussian noise; fGn)
$X = \{X_n : n = 0, \cdots, N-1\}$, which can be represented in terms of the spectral density $f(\lambda)$ as

$$X_n = \int_0^\pi \sqrt{\frac{f(\lambda)}{\pi}} \cos(n\lambda)\, dB_1(\lambda) - \int_0^\pi \sqrt{\frac{f(\lambda)}{\pi}} \sin(n\lambda)\, dB_2(\lambda) \tag{5.22}$$

where B_1 and B_2 are independent standard Brownian motions and the equality is understood in terms of distribution. Define $\xi_n(\lambda) = \sqrt{\frac{f(\lambda)}{\pi}} \cos(n\lambda)$ and fix some integer l. After setting $t_k = \frac{\pi k}{l}$ for $k = 0, \cdots, l-1$, we can approximate it by a simple function $\xi_n^{(l)}$ defined on $[0, \pi]$ for $0 \le n \le N-1$ by

$$\xi_n^{(l)}(\lambda) = \sqrt{\frac{f(t_1)}{\pi}} \cos(nt_1)\, \mathbf{1}_{\{0\}}(\lambda) + \sum_{k=0}^{l-1} \sqrt{\frac{f(t_{k+1})}{\pi}} \cos(nt_{k+1})\, \mathbf{1}_{(t_k, t_{k+1}]}(\lambda)$$

which is similar to the typical construction of stochastic integral.

Define the sine counterpart as $\theta_n^{(l)}(\lambda)$, and then integrate both $\xi_n^{(l)}(\lambda)$ and $\theta_n^{(l)}(\lambda)$ with respect to $dB_1(\lambda)$ and $dB_2(\lambda)$ on $[0, \pi]$ to approximate X_n. Then, we have

$$\hat{X}_n^{(l)} = \sum_{k=0}^{l-1} \sqrt{\frac{f(t_{k+1})}{l}} \left[\cos(nt_{k+1})\, U_k^{(0)} - \sin(nt_{k+1})\, U_k^{(1)}\right]$$

where $U_k^{(\cdot)}$ are i.i.d. standard normal random variables. $U_k^{(0)}$ and $U_k^{(1)}$ are independent, as they are resulted from integration from the two aforementioned independent Brownian motions.
Similar to the Fourier transform approach, the fGns can be recovered by applying the FFT to the sequence of $\hat{X}_n^{(l)}$ efficiently to the following coefficient:

$$a_k = \begin{cases} 0 & k = 1 \\ \frac{1}{2}\left(U_{k-1}^{(0)} + iU_{k-1}^{(1)}\right) & k = i, \cdots, l-1 \\ U_{k-1}^{(0)} \sqrt{\frac{f(t_k)}{l}} & k = l \\ \frac{1}{2}\left(U_{2l-k-1}^{(0)} + iU_{2l-k-1}^{(1)}\right) & k = l+1, \cdots, 2l-1 \end{cases} \tag{5.23}$$

It is easy to check that the covariance structure of fGns can be recovered, with the help of product-to-sum trigonometric identity, as

$$\begin{aligned} Cov\left(\hat{X}_m^{(l)}, \hat{X}_n^{(l)}\right) &= \sum_{k=0}^{l-1} \frac{f(t_{k+1})}{l} \cos\left((m-n)\, t_{k+1}\right) \\ &\cong 2\int_0^\pi \frac{f(\lambda)}{2\pi} \cos(n\lambda)\, d\lambda \\ &= \frac{1}{2\pi} \int_{-\pi}^{\pi} f(\lambda) \exp(-in\lambda)\, d\lambda = \gamma(n) \end{aligned}$$

Paxson [Pax97] has also proposed another method for simulating fGns, where in [Die02] it was proven to be related to (5.23) with the case$l = N/2$:

$$b_k = \begin{cases} 0 & k = 0 \\ \sqrt{\frac{R_k f(t_k)}{N}} \exp\left(i\Phi_k\right) & k = 1, \cdots, N/2 - 1 \\ \sqrt{\frac{f\left(t_{N/2}\right)}{2N}} U_{N/2}^{(0)} & k = N/2 \\ b_k^* & k = N/2 + 1, \cdots, N - 1 \end{cases}$$

Here, R_k is a vector of exponentially distributed random variables with mean 1, and Φ_k are uniformly distributed random variables on $[0, 2\pi]$ independent of R_k. This method is of order $N \log(N)$, and only one FFT is required instead of 2 times compared to the Davis-Harte FFT method. Hence, it is about 4 times faster.

Remark: The Paxson algorithm in (5.23) is improved by Dieker [Die02] to retain the normality of the sequence and its relationship with the original spectral representation.

6 Numerical Example: fBM Volatility Model

This section provides a numerical example of Monte Carlo simulation of fBM volatility model, as shown by [CR98]. In section 3.2.1, as it was briefly mentioned the truncated fractional Brownian motion. Following the example given in [CR98], with the following setup to simulate the volatility process:

$$\begin{cases} \sigma(t) &= \sigma_0 e^{x(t)} \\ dx(t) &= -kx(t)\,dt + \nu d\widehat{B^H}(t) \end{cases} \tag{6.1}$$

where ν is the volatility factor of the log-volatility process $x(t)$. The volatility process is the exponential of an OU-process driven by the truncated fBM. Also, we assume that $x(0) = 0, \quad k > 0, 1/2 < H < 1$. Solving the OU-process with integrating factor, we have

$$x(t) = \int_0^t \nu e^{-k(t-s)} d\widehat{B^H}(s) \tag{6.2}$$

By applying the fractional calculus or using the formulas provided in [CR96], we can formulate $x(t)$ in another way as

$$x(t) = \int_0^t a(t-s)\,dB(s) \tag{6.3}$$

where $B(t)$ is an ordinary standard Brownian motion and

$$\begin{aligned} a(\theta) &= \frac{\nu}{\Gamma(H+1/2)} \frac{d}{dx} \int_0^\theta e^{-ku} (\theta - u)^{H-1/2} du \\ &= \frac{\nu}{\Gamma(H+1/2)} \left(\theta^\alpha - ke^{-\theta} \int_0^\theta e^{ku} u^\alpha du \right) \end{aligned} \tag{6.4}$$

By applying the ordinary discretization scheme to (6.3), we have

$$\tilde{x}(t) = \sum_{j=1}^{N} a(t_N - t_{j-1}) (B(t_j) - B(t_{j-1})) \tag{6.5}$$

For the discretized time vector $0 = t_0 < t_1 < \cdots < t_N = t$. The coefficient $a(\cdot)$ can be calculated by symbolic packages such as Matlab and Mathematica. In our case of OU-process, it is a summation of constant with incomplete gamma function and gamma function.

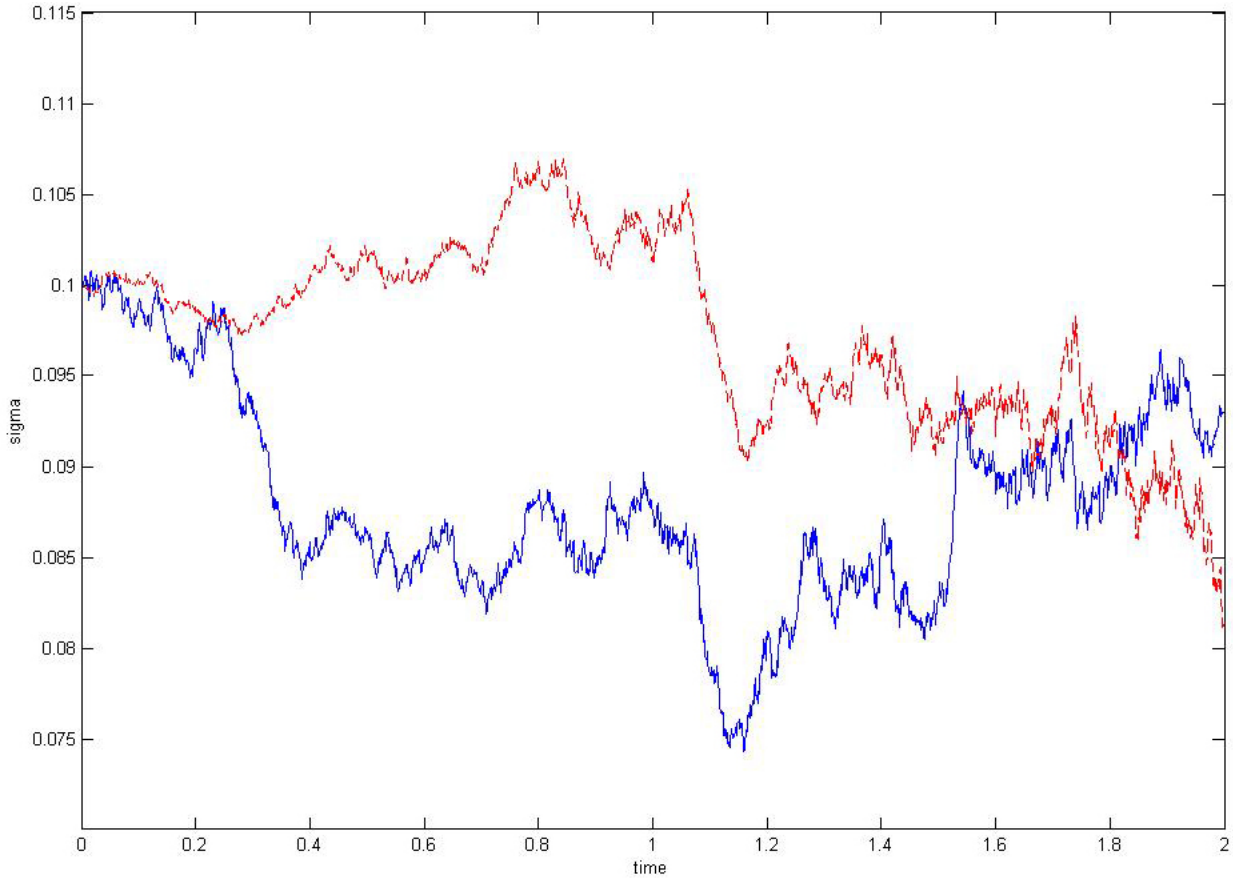

Figure 9: Sample path of $\sigma(t) = \exp(\tilde{x}(t))$ for $k = 1, \sigma_0 = 0.1, \nu = 0.3, H = 0.75, T = 2$, shown as upper red line here. For the sake of comparison, a sample path of the volatility process driven by an ordinary OU-process (the lower blue line) with the same ν and k is shown alongside

The sample path of the fractional-OU driven volatility process has shown more of a persistent trend, i.e. more prominent trend (more smooth and less reversal) compared to the ordinary-OU driven volatility process, which is what to be expected according to [CR96]. Though this approach generates readily available sample path robustly, this is, in a stricter sense of word, not a real fractional Brownian motion, but a truncated process that imitate it asymptotically, and this approximation converges slowly as the grid gets finer and the aggregated effect of the path's previous realization accumulates, and as we have shown in section 3.2.1, this only converges to the real distribution of the fractional Brownian motion asymptotically. Because our simulation starts at $t = 0$, we expect the samples close to the origin actually behaves more similar to an ordinary Brownian motion instead of a fractional Brownian motion; Equation (6.3) shows the approximation can be seen as just a weighted stochastic integral w.r.t ordinary Brownian motion, since $a(\cdot)$ is a smooth function. For more discussion of its statistical property and justification of its stability as compared to the original stationary version, we direct the reader to [CR96] and [CR98]. Also we provide a similar volatility process generated by the FFT-approach as shown in the following figure, showing FFT is a better choice of approximation.

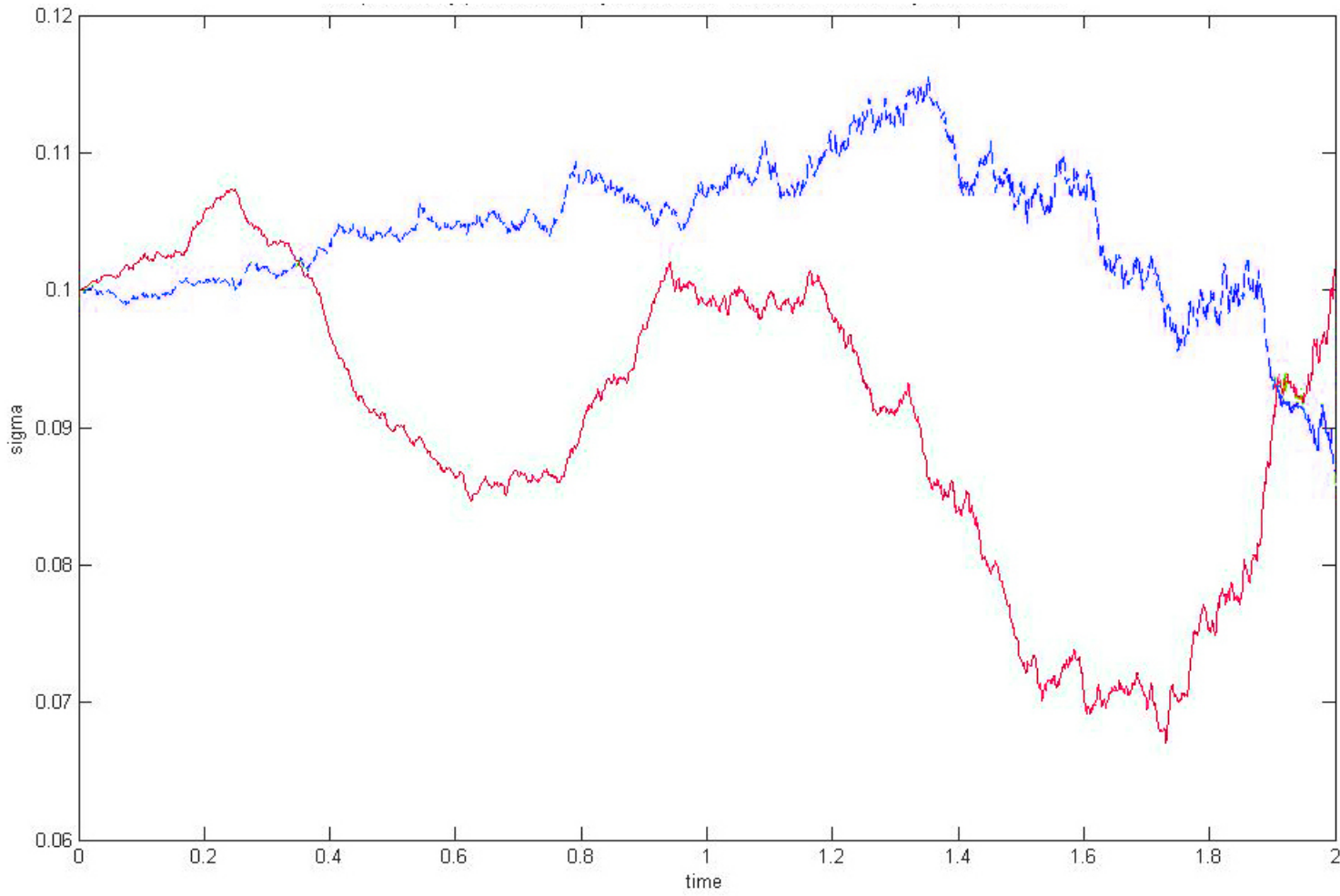

Figure 10: Sample paths with Hurst index $H = 0.75$, FFT generated fractional Brownian Motion shown as lower red line; Truncated fractional Brownian Motion shown as upper blue line.

The Fractional Brownian motion is simulated by the circulant-embedding method, with the same parameters as Figure 9.
Figure 10 shows a sample path of $a(t) = \exp(x(t))$, where x(t) is the fBM generated by the circulant-embedding FFT with the same parameters as figure 9 : $k = 1, \sigma_0 = 0.1, \nu = 0.3, H = 0.75, T = 2$.
In both of these two examples, the fractional Brownian motions are scaled, so that the variance of $B^H(T)$ equals to the ordinary Brownian motion $B^{1/2}(T)$.

7 Full simulation Scheme

In previous section we concluded that the FFT generated fractional Brownian motion is best suited for our simulation purpose, and have looked into the fractional Stochastic volatility process it generates, it is of our general curiosity to see how it will behave in the realm of option pricing. With our robust fractional Brownian motion simulation, the goal is to have a functional pricing algorithm with Monte-Carlo simulation. The result in this section will serve as an reference for the following sections. (Note: We denote W_t as the Brownian Motion, and W_t^H its fractional counterpart starting from this section as to be consistent with the option pricing literature.) Outlining the basic setup:

$$\begin{cases} d\ln S_t = & (r - \frac{1}{2}\sigma_t^2)dt + \sigma_t d\tilde{W}_t \\ dX_t = & \kappa_t(\theta - X_t)dt + \nu_t^H dW_t^H \\ \sigma_t = & \exp(X_t) \\ \text{FFT}\left\{W_t\right\}_{0\le t\le T} = & \left\{W_t^H\right\}_{0\le t\le T} \\ d\left\langle W, \tilde{W}\right\rangle_t = & \rho_t dt \end{cases} \tag{7.1}$$

This setup is the basic setup similar to Comte and Renault's, where the volatility is an exponential of an OU-process. This setup is motivated by the mean-reverting nature of the volatility process observed on the market place. Note here, it does not restrict the stochastic volatility to be driven by a Brownian motion or fractional Brownian motion (i.e. it does not specify the Hurst index besides that it has to be in the region $\left[\frac{1}{2}, 1\right)$. The reason of the lack of restriction will be made clear later on. Here, denoting W_t as the "pre-transformed fBM" for the volatility process, and FFT $(\cdot)$, is the FFT fBM algorithm outlined in Theorem 4.3. The idea of such an imposition is, it is setup this way, in order to impose correlation between the asset process and volatility process. Naturally we want impose it between the asset Brownian motion and the driving random factor behind the stochastic volatility, similar to how the original Heston model captures the leverage effect. The problem here is that, the covariation of fractional Brownian motions with different Hurst indices is zero. This can be shown by looking into the Hermite decomposition of fractional Brownian motion, and for fractional Brownian motion with different Hurst indices, the Hermite function sets between them will be orthogonal, resulting in zero covariation, for detail, readers are encouraged to read the Appendix of [BHOZ08]. So it is naturally to seek another way, intuitively, it is to impose correlation between the Brownian motion driving the asset process, and the independent Brownian motion used in the construction of the fractional Brownian motion for the stochastic volatility(Equation (2.3), (2.5), and theorem 4.3). Looking back at the FFT approach, it involves a 'random seed': the standard normal random variables vector, and impose a linear correlation between this standard normal random variable vector with the one used to drive the asset process itself.
Another way is to go about this, is to generate another path by FFT with $H = \frac{1}{2}$, and then impose correlation with methods such as Cholesky theorem. But it can be seen later on, this is largely unnecessary, the reason will be given later on. It is worth noting that since X_t is a fractionally driven Ornstein-Uhlenbeck process, which is a Gaussian process. Theoretically, one should be able to calculate the distribution of σ_t, and indeed this is the case, as we have included the procedure in Appendix B. The problem with the calculation given by Fink, Kluppelberg, Zahle [FKZ10] is that it adopts the fractional Riemann-Liouville integral, which is similar to the truncated integral given by Paul Levy as mentioned before, putting heavy emphasis on the origin. There exists a singularity at the origin, and it becomes troublesome when it comes to discretizing the integral, as the origin singularity will results in numerical instability, and if it is not properly address, it will either result in unbounded variance or if truncated improperly it will result in similar underestimation, similar to the case of truncated long-memory process by the Comte, Renault framework. Nevertheless it is important to include it for the sake of technical curiosity.

7.1 Full simulation - Stochastic Volatility

7.1.1 Uncorrelated Cases

Simulating the asset process according to scheme as previously stated, the stochastic volatility part of the process is implemented by FFT-generated fBM. This is to captured the volatility persistence phenomenon found in long-maturity option markets. The ordinary stochastic volatility (such as Heston model) cannot sufficiently captured this, as the volatility term-structure decays much faster than expected in the ordinary stochastic volatility model, and fractional Brownian motion random source provides a easy and direct enrichment of the existing and well-developed framework. One of the most direct way to observe volatility persistence is to observe the mean-volatility and the lag-correlation structure, as it was pointed out earlier, volatility persistence displays the behavior of long-range dependence, which can be observed by looking at the autocovariance structure. Figure 11 depicts the lag-autocorrelation between the sigma and its time-lagged counterparts (unit is displayed in years), where the initial volatility is 0.3, and only difference of the two plots is the Hurst index. Between H=0.5 (ordinary Brownian motion) and H=0.9 (fractional Brownian motion). The Long-range dependence can be seen from the plot, because while the ordinary Brownian motion case (H=0.5) quickly dwindled close to zero, the fractional Brownian motion case (H=0.9) stays significantly above zero. So obviously, for the first case the quantity $\sum_{n=1}^{\infty} \gamma(n)$ converges to a number while the 2nd case it does not converge and satisfy the requirement of a long-range dependence.

For the case of full stochastic volatility simulation, the European option (call and put) are calculated and the implied volatility is calculated through root-finding routine with the Black-Scholes formula, subsequently the implied volatility surface is plotted. With the following parameters (unless otherwise specified): $T = 20, \sigma_0 = 0.3, \kappa_t = 0.5, \nu_t^H = 0.75$.

In Figure 12 the implied volatility surface where the stochastic volatility is generated by ordinary Brownian motion. Figure 13 is the same setup only now that H = 0.9, Figure 14 combines both plots for comparison. To put Figure 12 to Figure 14 in context. First, the volatility for the case of fractional Brownian motion driven stochastic volatility persists much longer than the ordinary Brownian motion driven one. Also on the volatility surface, the out-of-money ends of the close-to-maturity display numerical instability, this has to do with the out-of-the money option is very sensitive to path realization that is too 'extreme', as it will distort the average, and through increasing the number of realization does seem to wean the fluctuation a bit, it is worth noting for such deep-in-the-money options, usually path ended up quite far from the mean is considered, resulting in the instability, this is only apparent in close-to-maturity, as the mean-reversion reels in the distribution asymptotically. For market displays long-term maturity smile, under the ordinary Brownian motion stochastic volatility regime, one can try to adapt this by turning up the vol-of-vol, but this is defeating the purpose, and falls under the category of misspecification of the model. This is similar to, for example, if one wants to model a distribution that displays fat-tailed behavior, one can still fit a normal-distribution on the data set, but it will produce a normal distribution with a high variance that seems like a 'overkill', thus, misspecification. Similar story can be told for our case, where it will be much easier to adapt to the slow-decaying volatility smile by implementing the fractionally-driven stochastic volatility process instead of the ordinary stochastic volatility with a much higher vol-of-vol, the effect of this will be elaborated further in the option-pricing section.

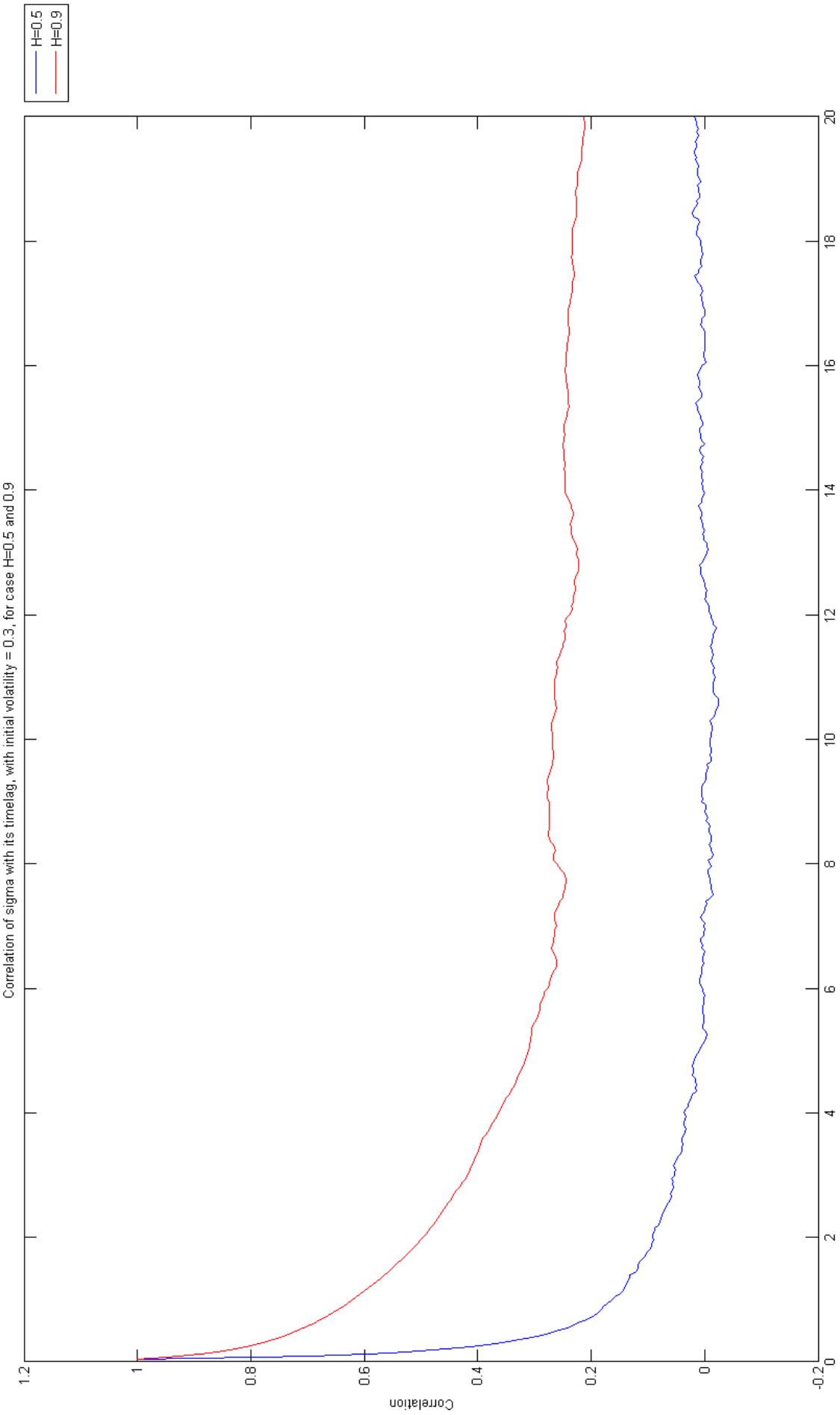

Figure 11: Lag-Autocorrelation of σ (Exponential OU Process).

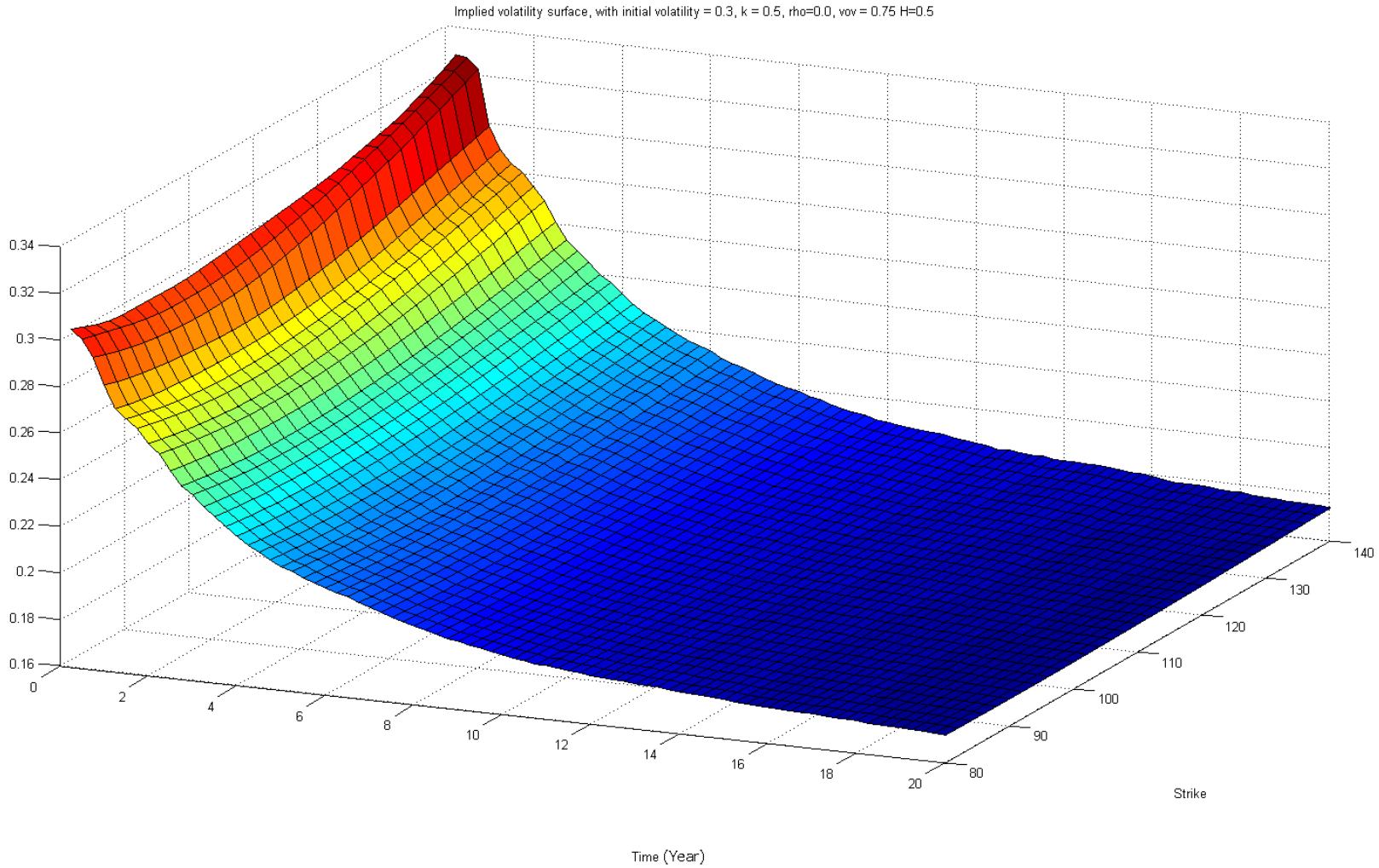

Figure 12: Implied Volatility Surface, $\rho = 0, \nu = 0.75, H = 0.5$.

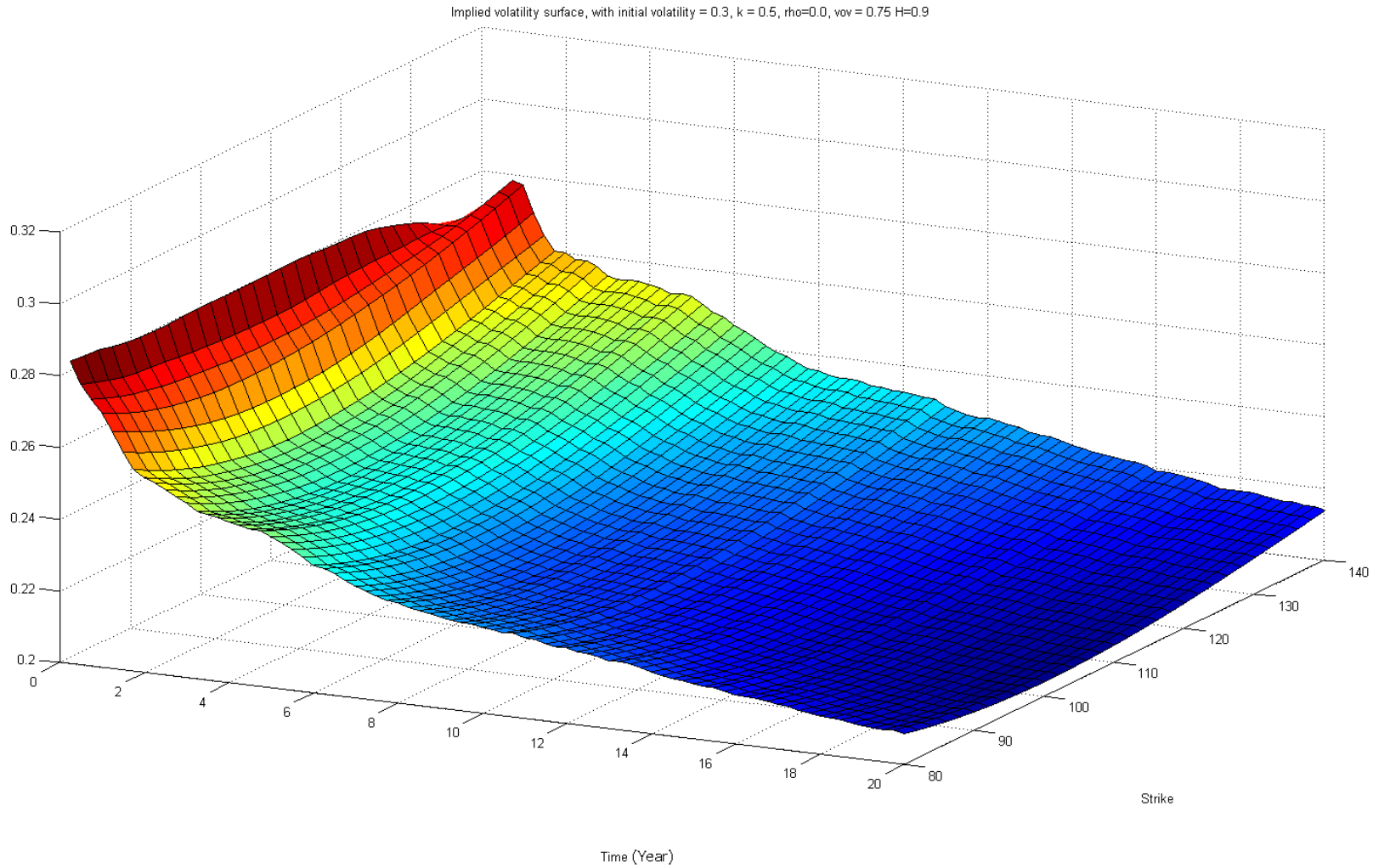

Figure 13: Implied Volatility Surface, $\rho = 0, \nu^H = 0.75, H = 0.9$.

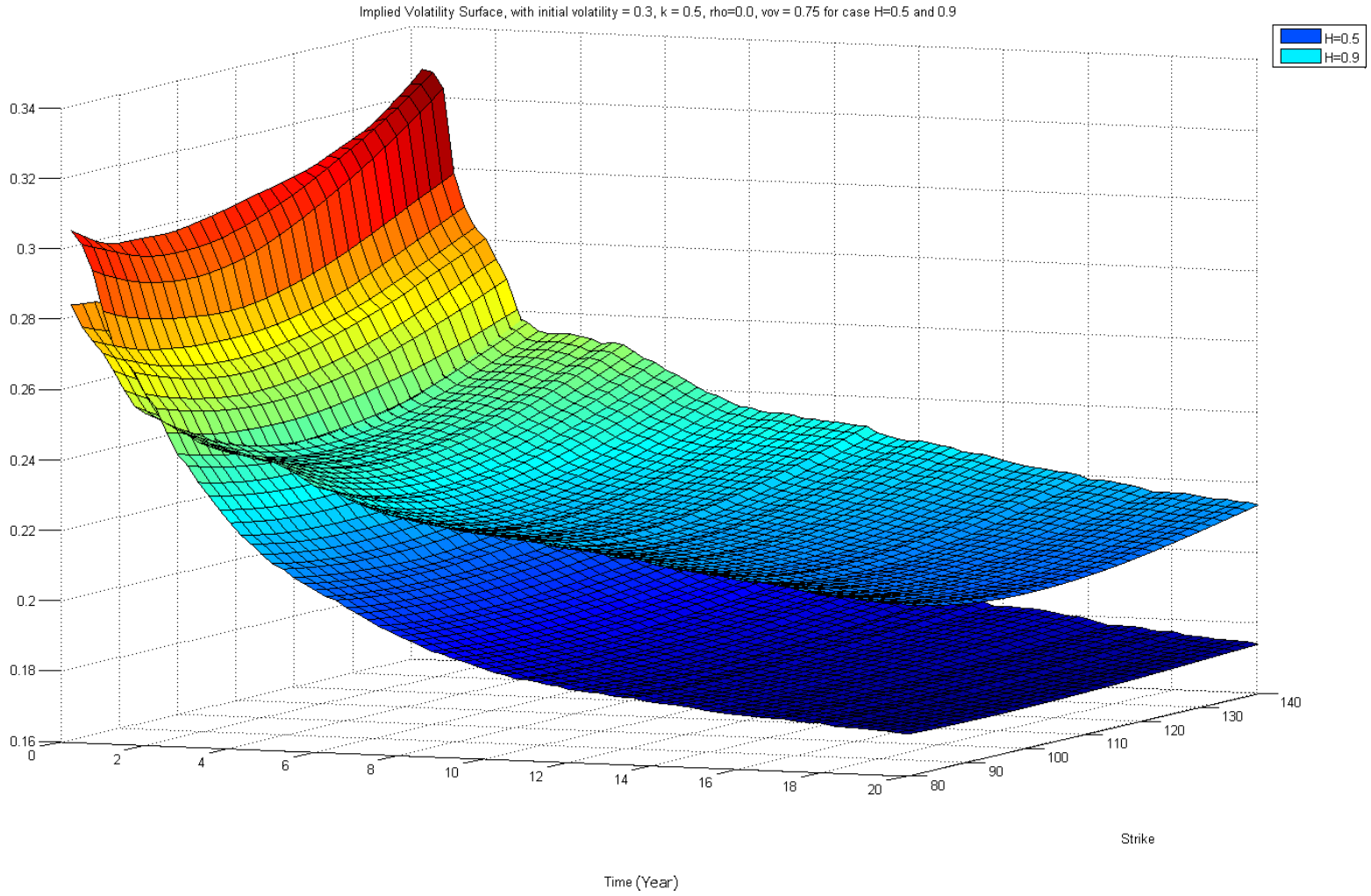

Figure 14: Combined Implied Volatility Surface, $\rho = 0, \nu$ or $\nu^H = 0.75, H = 0.5, 0.9$.

7.1.2 Correlated Case, skewness

It is quite intuitive to impose correlation between the volatility and the asset processes to attempt to display some kind of volatility skewness as mentioned before. When simulating the log-volatility process with the fractional Brownian motion, the "pre-transformed fBM", i.e. the Brownian motion that was used to simulate stochastic volatility fractional Brownian motion, is imposed with linear correlation with the asset's own Brownian motion, similar to the case of the ordinary stochastic volatility simulation.

Looking into Alos, etc. [ALV07] has proved that with Malliavin Calculus that, for the case of $H > \frac{1}{2}$, the skew-slope of the implied volatility surface close to maturity $\tau \to 0$ does not depend on the correlation imposed between the asset's Brownian motion and stochastic volatility's "pre-transformed fBM":
Given that the volatility follows the Comte, Renault setup:

$$x(t) = \int_0^t \nu e^{-k(t-s)} dW^H(s)$$

With the help of the M-operator in equation (A.4), it can be shown that:

$$\begin{aligned}
\int_0^t e^{-k(t-s)} dW^H(s) &= e^{-kt} \int_{\mathbb{R}} \left(\mathbf{1}_{[0,t]}(\cdot) e^{k(\cdot)}\right)(s)\, dW^H(s) \\
&= e^{-kt} \int_{\mathbb{R}} M_-^H \left(\mathbf{1}_{[0,t]}(\cdot) e^{k(\cdot)}\right)(s)\, dW_s \\
&= e^{-kt} \int_{\mathbb{R}} K_H I_-^{H-1/2} \left(\mathbf{1}_{[0,t]}(\cdot) e^{k(\cdot)}\right)(s)\, dW_s \\
&= \frac{K_H}{\Gamma\left(H-\frac{1}{2}\right)} e^{-kt} \int_{\mathbb{R}} \left(\int_s^\infty \mathbf{1}_{[0,t]}(u) e^{ku} (u-s)^{H-\frac{3}{2}} du\right) dW_s \\
&= \frac{K_H}{\Gamma\left(H-\frac{1}{2}\right)} \int_0^t \left(\int_s^t \mathbf{1}_{[0,t]}(u) e^{-k(t-u)} (u-s)^{H-\frac{3}{2}} du\right) dW_s \qquad (7.2)
\end{aligned}$$

Which is the result listed in [AMN01] (suppressing the constant).
And with Malliavin Calculus, it was proved that, the close-to-maturity implied volatility would have the following characteristic:

$$\lim_{T \downarrow 0} \left.\frac{\partial I_T}{\partial K}\right|_{K^*} = -\frac{\lambda \xi}{\sigma(0)} \qquad (7.3)$$

Here λ is the intensity of the Poisson jump-process, and $\xi = \frac{1}{\lambda}\int_{\mathbb{R}} (e^y - 1)\, \mu(dy)$, where μ is the Levy measure. With our setup, it would mean the derivative is 0, that the skewness close-to-maturity is zero. This is a rather surprisingly finding, which is further investigated with numerical simulation.

Similar to previous sub-section, we have the similar setup, and just to check for validity of the claim of Alos, we impose the correlation in the 'pre-transformed fBM' for the case where the correlation is non-zero.
One can see by comparing the Figure 15 and 16 that, the skewness is very pronounced in the ordinary Brownian motion case, but in the case of the fractional Brownian motion, the correlation has little effect on the skewness especially close to maturity, this is indeed a very interesting finding, which is further supported by Alos.

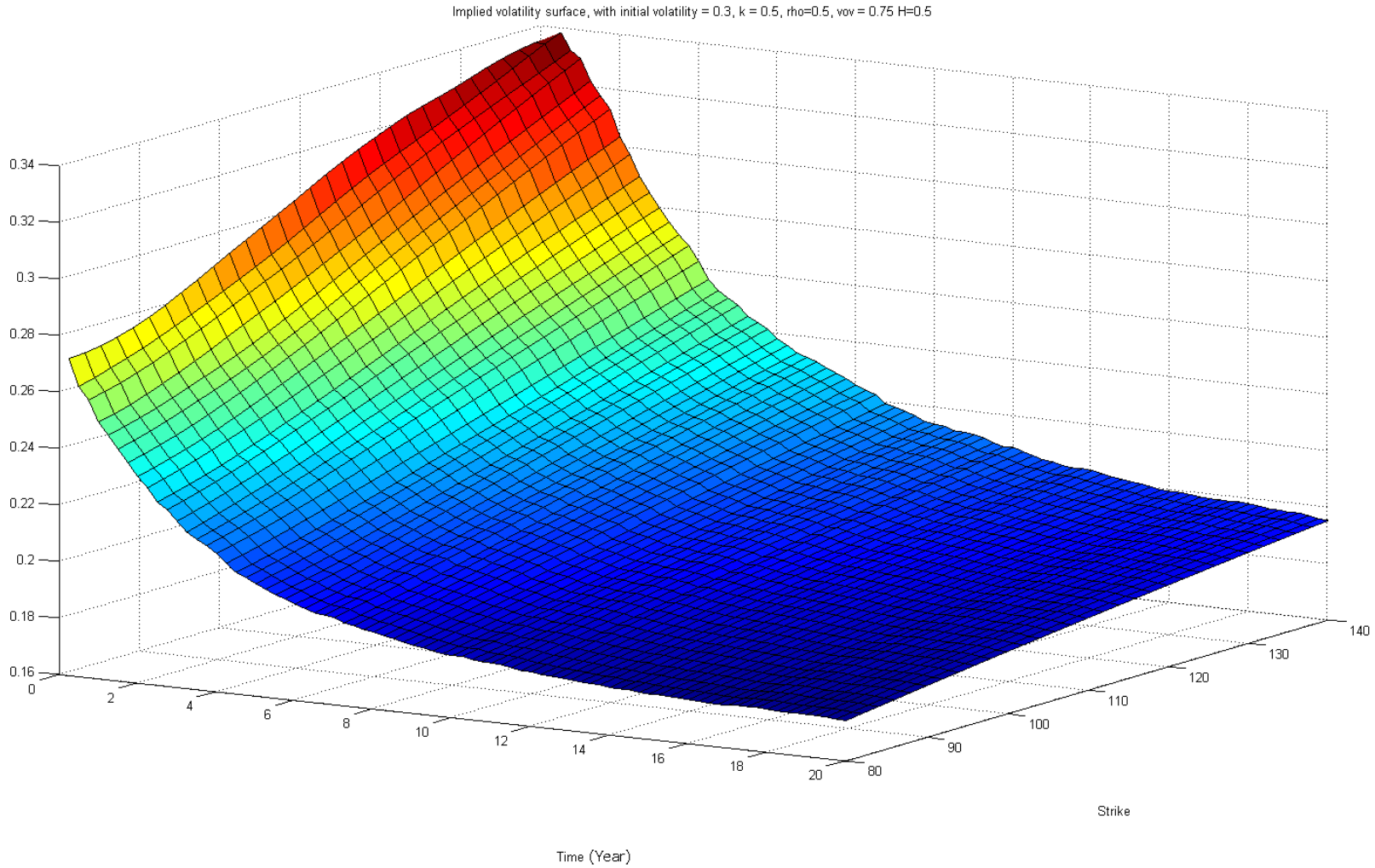

Figure 15: Implied Volatility Surface, $\rho = 0.5, \nu = 0.75, H = 0.5$.

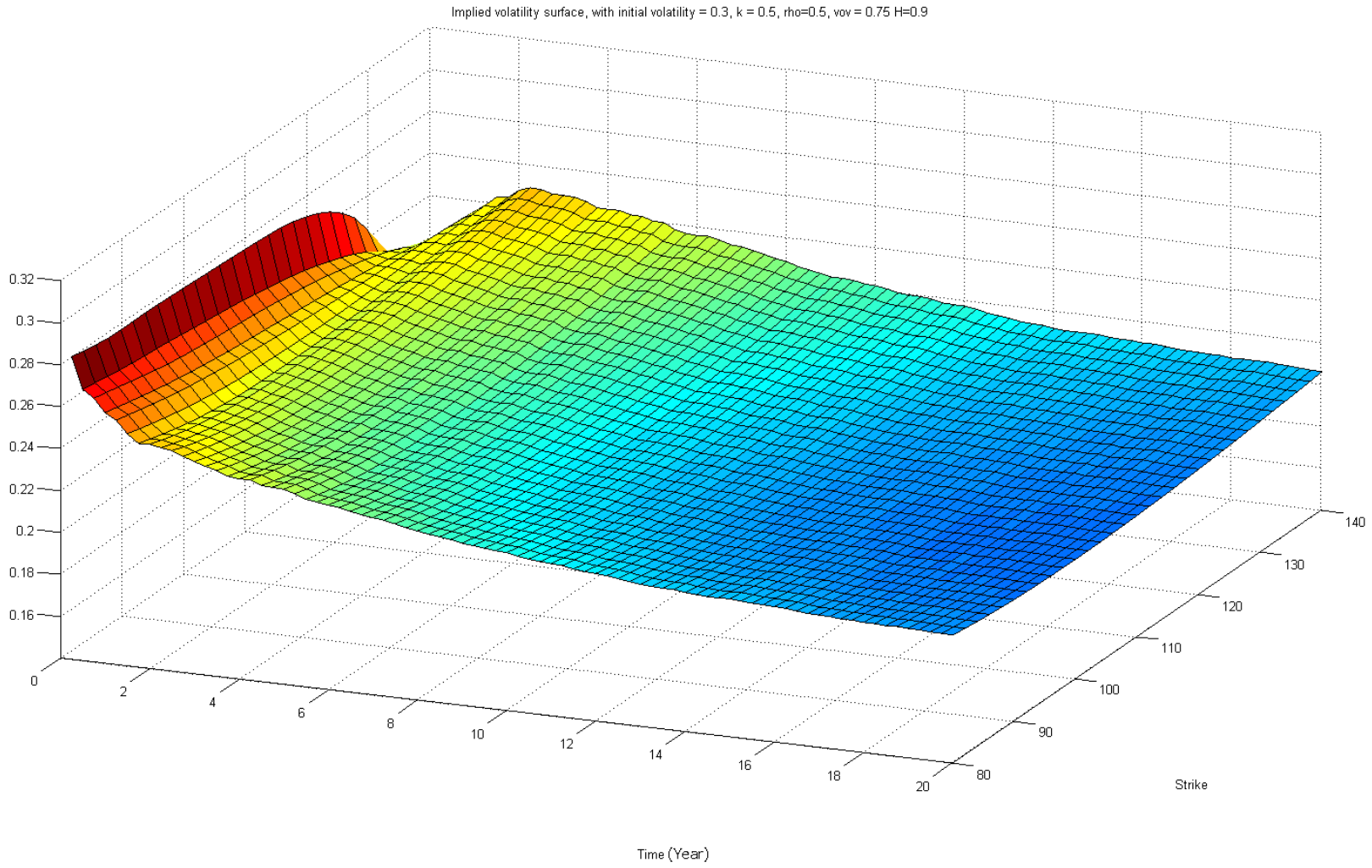

Figure 16: Implied Volatility Surface, $\rho = 0.5, \nu^H = 0.75, H = 0.9$.

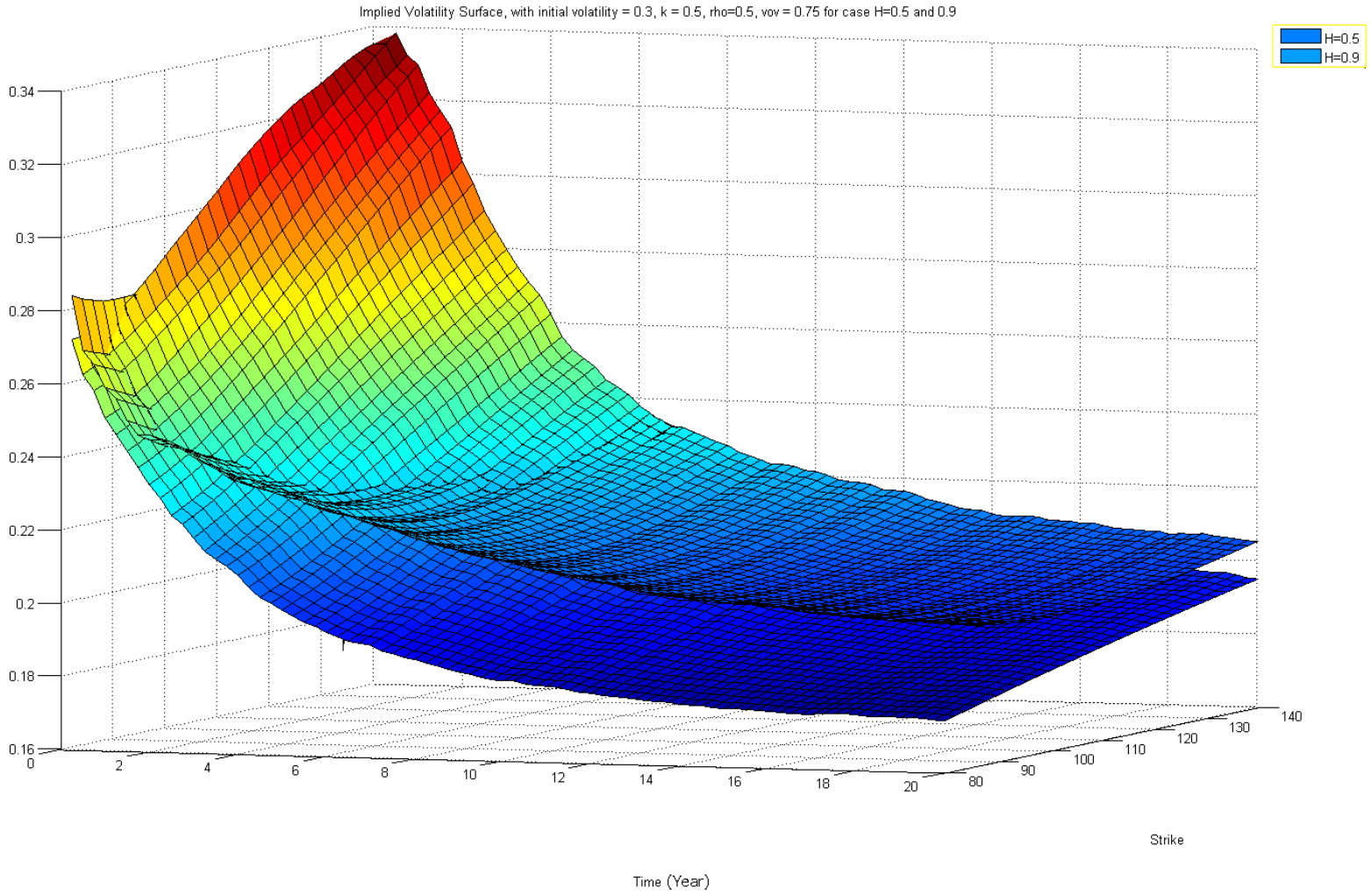

Figure 17: Combined Implied Volatility Surface, $\rho = 0.5, \nu$ or $\nu^H = 0.75, H = 0.5, 0.9$.

7.2 Mixture fBM exponential volatility

Instead of choosing between the ordinary Brownian motion and fractional Brownian motion, in order to capture both the skewness and volatility persistence, both Brownian motion and fractional Brownian motion are utilized in order to capture the volatility persistence and the volatility skewness. Such that the formal setup of the model is outlined as following:

$$\begin{cases} d\ln S_t = & \left(r_t - \frac{1}{2}\sigma_t^2\right)dt + \sigma_t d\widetilde{W_t} \\ dX_t = & \kappa_t\left(\theta - X_t\right)dt + \nu_t dW_t + \nu_t^H dW_t^H \\ \sigma_t = & \exp\left(X_t\right) \\ d\left\langle W, \tilde{W}\right\rangle_t = & \rho_t d_t \end{cases} \tag{7.4}$$

Denoting this process the exponential mixture fractional Ornstein-Uhlenbeck volatility process. The implied volatility surface of this mixture fBM exponential volatility setup is shown in Figure 18 , with parameter $\rho = 0.5, \nu_t = 0.5, \nu_t^H = 0.4, H = 0.9$.
There are some drawbacks of this formulation, but is inherent in all volatility in exponential functional: Large vol-of-vol might lead to big jump in volatility, and causes numerical instability, this is due to the exponential form of the volatility that magnifies the large deviation from the fractional Brownian motion and results in very slow convergence, especially in out-of-money region where most of the realized paths are discarded. Also there might be special difficulty to calibrate due to high similarity of fractional Brownian Motion and ordinary Brownian motion, so it is better to calibrate the vol-of-vol of the fractional Brownian motion part at long-maturity where the volatility smile of the ordinary Brownian motion will be suppressed, more on the issue of calibration will be address later on.

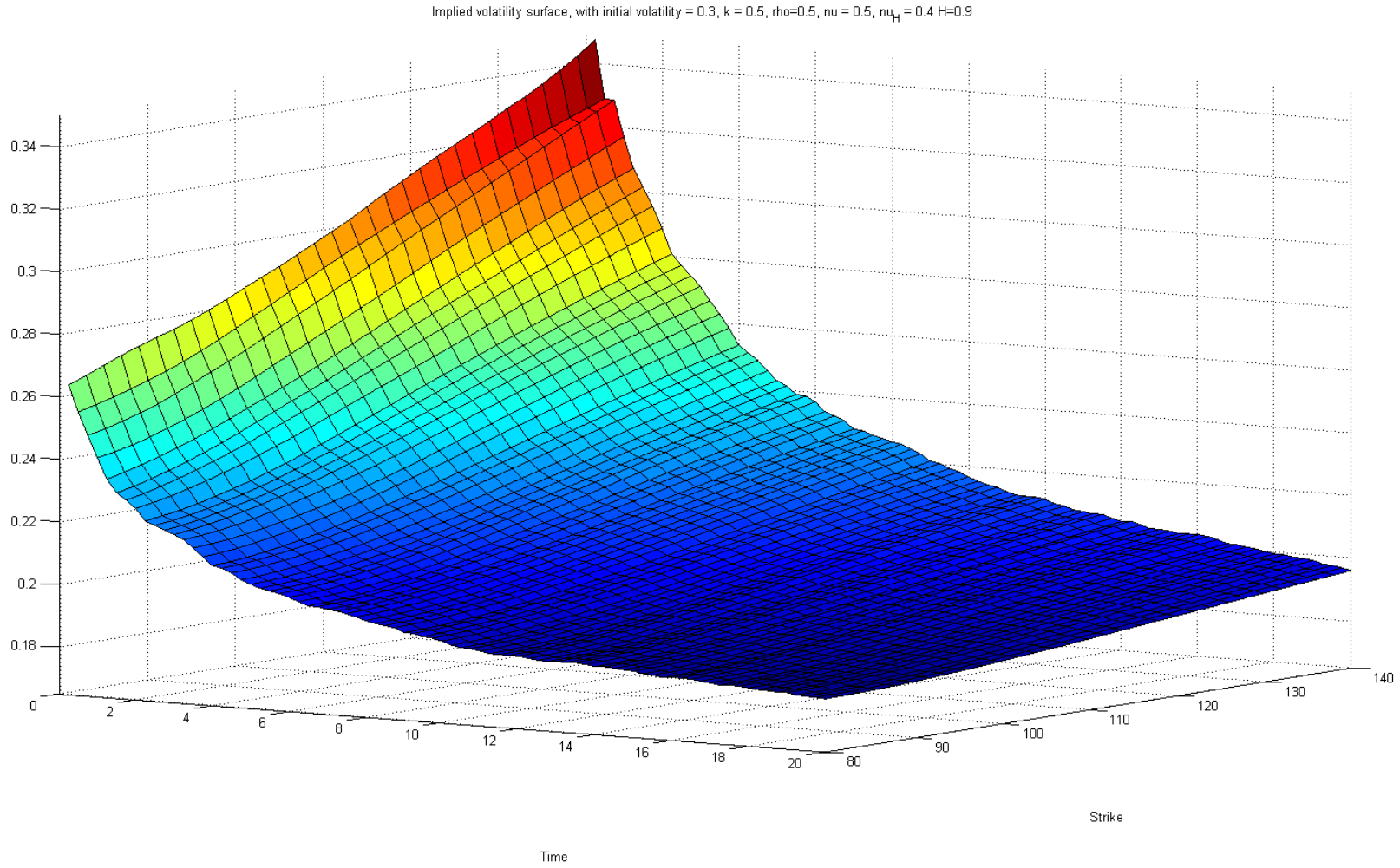

Figure 18: Exponential mixture fractional Ornstein-Uhlenbeck volatility, Implied Volatility Surface, $\rho = 0.5, \nu_t = 0.5, \nu_t^H = 0.4, H = 0.9$.

8 Funahashi Approximation Scheme

In the last section, a full-simulation scheme that involves three-dimensions is investigated: asset's ordinary Brownian motion, stochastic volatility ordinary Brownian motion and stochastic volatility fractional Brownian motion, and finally the mixture fractional Brownian stochastic volatility model that involves both processes. The full simulation involving the mixture Brownian motions is obviously computationally taxing, and is not robust enough for practical purpose. With such complex process it is difficult, if not hopeless to seek an explicit form of the exact solution. So the next best thing is to look for an approximation that will give us reasonable result. Drawing inspiration from several recent computation schemes for complex derivative pricing, it seems natural to first calculate the parts where closed-form solution is readily available, or at least, has easier approximation. Considering this, we adopt the approximation scheme for the hybrid volatility model put forth by Funahashi [FK12], the approximation scheme is capable to calculate European option prices for the stochastic local volatility with general volatility functional, and in our case the functional is of the form of exponential. And in the upcoming section we will show an extension to this approximation scheme so that it is capable of calculating the stochastic volatility setup with the mixture fractional Brownian motions.

8.1 Outline of the Approximation

Funahashi hybrid volatility scheme utilize the Wiener-chaos expansion, by 2nd order successive substitution. It is a robust approximation of the pdf and European option price can be obtained. Iterative stochastic integrals with deterministic integrands are then solved by the Takahashi formulas. And left with approximation where the parameters are calculated by deterministic iterative integrals. The approximation of the pdf is expanded around the normal distribution, similar to Edgeworth approximation.

In order to resolve the normal iterative stochastic integrals into iterative stochastic integrals with deterministic integrand (so that one can apply the Takahashi formulas later), it is necessary to apply Taylor expansion (2nd order as well) around S_t, σ_t, then the iterative stochastic integrals with deterministic integrals is solved by formulas given by Lemma 2.1 in Takahashi [Tak99], where the expectation can be calculated by the deterministic iterative integrals.
Applying this approximation to calculate the exponential-functional structure of the stochastic volatility model for a robust approximation of the European option, we can then further modified this approximation to adapt our mixture fBM model. We will first outline the approximation in this section for a clearer explanation:

8.2 Basic Setup of the approximation

Similar to the previous simulation setup, following is the setup:

$$\begin{cases} \frac{dS_t}{S_t} = & r(t)\,dt + \sigma(S_t, v_t)\,dW_t^S \\ dv_t = & (\theta(t) - \kappa(t)\,v_t)\,dt + \gamma(v_t)\,dW_t^v \end{cases} \tag{8.1}$$

Where $r(t), \theta(t), \kappa(t)$ are deterministic function of time t, and $\sigma(s,v)$ is the stochastic local volatility function, which is a deterministic function of asset price and the function ν_t. $\gamma(v)$ is a deterministic function of volatility and $W^S$and W^v are $\mathbb{Q}$-standard Brownian motion with $d\left\langle W^S, W^v\right\rangle_t = \rho dt$. It is assumed that $\sigma(s,v)$ and $\gamma(v)$ are infinitely differentiable with respect to (s,v)

Solving the differential equations we have the following expression:

$$\left\{\begin{array}{ll} S_t = & F(0,t)\exp\left[\int_0^t \sigma(S_u,v_u)\,dW_u^S - \frac{1}{2}\int_0^t \sigma(S_u,v_u)^2\,du\right] \\ v_t = & V(0,t) + \bar{E}(t)\int_0^t E(u)\,\gamma(v_u)\,dW_u^v \end{array}\right. \tag{8.2}$$

where $F(0,t) = S_0 e^{\int_0^t r(u)du}$, is the forward price of the underlying asset with delivery date t,
$E(t) = e^{\int_0^t \kappa(u)du}$, $\bar{E}(t) = 1/E(t)$, are the integrating factor and its reciprocal.
And the following initial term structure for ν_t:

$$V(0,t) = v_0 e^{-\int_0^t \kappa(u)du} + \int_0^t e^{-\int_u^t \kappa(v)dv}\theta(u)\,du = \bar{E}(t)\left(v_0 + \int_0^t E(u)\,\theta(u)\,du\right) \tag{8.3}$$

Also, denoting the norm and stochastic integrals as: $\|g\|_t^2 = \int_0^t g^2(u)\,du,\ J_t(g) = \int_0^t g(u)\,dW_u^S$
Denoting $L_t(g) = \int_0^t e^{-\int_u^t \kappa(v)dv} g(v_u)\,dW_u^v = \bar{E}(t)\int_0^t E(u)\,g(v_u)\,dW_u^v$, we have

$$\left\{\begin{array}{ll} S_t = & F(0,t)\left[J_t(\sigma) - \frac{1}{2}\|\sigma\|_t^2\right] \\ v_t = & V(0,t) + L_t(\gamma) \end{array}\right. \tag{8.4}$$

8.3 Hermite Polynomial

From the basic setup, the Wiener-Chaos offers an succinct and robust truncation of the asset process by Hermite polynomial. In the following paper we use the probabilists' version of the Hermite polynomial:

$$h_n(x) = (-1)^n e^{x^2/2}\frac{d^n}{dx^n}e^{-x^2/2}, \quad n = 1,2,\cdots$$

Refering to Lemma 3.1 of Funahashi [FK12] or Biagini, etc. [BHOZ08], we know
For any $x \in \mathbb{R}, \lambda > 0$

$$\exp\left[tx - \frac{\left(\sqrt{\lambda}t\right)^2}{2}\right] = \sum_{n=0}^{\infty}\frac{\left(\sqrt{\lambda}t\right)^n}{n!}h_n\left(\frac{x}{\sqrt{\lambda}}\right) \tag{8.5}$$

Putting $t = 1, x = J_t(\sigma)$ and $\lambda = \|\sigma\|_t^2$, we have

$$\exp\left(J_t(\sigma) - \frac{1}{2}\|\sigma\|_t^2\right) = \sum_{n=0}^{\infty}\frac{\|\sigma\|_t^n}{n!}h_n\left(\frac{J_t(\sigma)}{\|\sigma\|_t}\right) \tag{8.6}$$

8.4 Successive Substitution

Initial term-structure for the asset and volatility process:

$$S_t^{(0)} = F(0,t), \quad v_t^{(0)} = V(0,t)$$

and the subsequent successively substitution:

$$\left\{\begin{array}{ll} S_t^{(m+1)} = & F(0,t)\exp\left[J_t(\sigma^m) - \frac{1}{2}\left\|\sigma^{(m)}\right\|_t^2\right] \\ v_t^{(m+1)} = & V(0,t) + L_t\left(\gamma^{(m)}\right) \end{array}\right. \tag{8.7}$$

where the input are updated also successively, similar to the approach of the fixed-pointed theorem:

$$\begin{cases} \sigma^{(m)}(t) = & \sigma\left(S_t^{(m)}, v_t^{(m)}\right) \\ \gamma^{(m)}(t) = & \gamma\left(v_t^{(m)}\right) \end{cases}$$

Under Theorem 5.2.1 of [Oks00], the sufficient condition for the convergence of the volatility process v_t is known, and the convergence of the overall convergence is assumed consequently under Funahashi and Kijima [Fun12], i.e. $\left(S_t^{(m)}, v_t^{(m)}\right) \to (S_t, v_t)$ as $m \to \infty$.
Rearranging (8.7), we have

Theorem 8.1.

$$\frac{S_t^{(m+1)}}{F(0,t)} = \sum_{n=0}^{\infty} \frac{\left\|\sigma^{(m)}\right\|_t^n}{n!} h_n\left(\frac{J_t\left(\sigma^{(m)}\right)}{\left\|\sigma^{(m)}\right\|_t}\right) \tag{8.8}$$

Since the convergence is assumed, $\lim_{m\to\infty} S_t^m = S_t$, and the difference between in each substitution is $I_{m,n}(t)$:

$$S_t = S_t^{(1)} + \sum_{m=1}^{\infty}\left\{S_t^{(m+1)} - S_t^{(m)}\right\} = S_t^{(1)} + F(0,t)\sum_{m,n=1}^{\infty} I_{m,n}(t) \tag{8.9}$$

where

$$I_{m,n}(t) = \frac{1}{n!}\left\{\left\|\sigma^{(m)}\right\|_t^n h_n\left(\frac{J_t\left(\sigma^{(m)}\right)}{\left\|\sigma^{(m)}\right\|_t}\right) - \left\|\sigma^{(m-1)}\right\|_t^n h_n\left(\frac{J_t\left(\sigma^{(m-1)}\right)}{\left\|\sigma^{(m-1)}\right\|_t}\right)\right\} \tag{8.10}$$

n is the exponential-power, and m is the substitution-order.

8.5 Wiener-Ito Expansion

From proposition of 1.14 of Nualart [Nua06], for $f(t) \in L^2[(0,T)]$ be a deterministic function of time, then

$$\frac{\|f(t)\|^n}{n!} h_n\left(\frac{J_t(f)}{\|f\|_t}\right) = \int_0^t \int_0^{t_n} \cdots \int_0^{t_2} f(t_1) f(t_2) \cdots f(t_n)\, dW_{t_1} \cdots dW_{t_n} \tag{8.11}$$

where $\{W_t\}_{t\geq 0}$ is a one-dimensional independent Brownian motions, and this integral is defined on the space $0 \leq t_1 \leq \cdots \leq t_n \leq t$.
For $\sigma^{(0)}(t) = \sigma(F(0,t), V(0,t))$ is a deterministic function, so for the first substitution, it can be represents:

Proposition 8.1.

$$\frac{S_t^{(1)}}{F(0,t)} = 1 + \sum_{n=1}^{\infty} \int_0^t \int_0^{t_n} \cdots \int_0^{t_2} \sigma^{(0)}(t_1)\sigma^{(0)}(t_2) \cdots \sigma^{(0)}(t_n)\, dW_{t_1}^S \cdots dW_{t_n}^S \tag{8.12}$$

This substitution is truncated at $m + n \leq 3$, so the truncated S_t can be written as:

$$S_t \approx \tilde{S}_t^{(1)} + F(0,t) \sum_{m,n\geq 1; m+n\leq 3} I_{m,n}(t) \tag{8.13}$$

where

$$\begin{aligned}\tilde{S}_t^{(1)} &= F(0,t)\left[1+\int_0^t \sigma_0(t_1)\,dW_{t_1}+\int_0^t\int_0^{t_2}\sigma_0(t_1)\,\sigma_0(t_2)\,dW_{t_1}^S dW_{t_2}^S\right. \\ &\quad \left.+\int_0^t\int_0^{t_3}\int_0^{t_2}\sigma_0(t_1)\,\sigma_0(t_2)\,\sigma_0(t_3)\,dW_{t_1}^S dW_{t_2}^S dW_{t_3}^S\right]\end{aligned} \tag{8.14}$$

In [FK12] it has shown this truncation offers an efficient and accurate approximation for S_t, for detail, refers to section 3.5 of the paper.

The approximation involves order only up to $m+n\leq 3,\ m,n\geq 1$. That is, it involves the terms $I_{1,1}(t), I_{1,2}(t), I_{2,1}(t)$, and $I_{2,2}(t)$ and the higher orders are assumed to be zero.

Proposition 8.2. Before expanding $I_{1,1}(t), I_{1,2}(t), I_{2,1}(t)$, we need the following equations for the successive substitution $J_t\left(\sigma^{(m)}\right)$ and $J_t^2\left(\sigma^{(m)}\right)$, (the square is a result of the Hermite polynomial of 2nd order: $n=2$, in $I_{1,2}(t)$). By Taylor expansion up to 2nd order around the last substitution $\sigma^{(m-1)}$ with increment $\left(S^{(m)}-S^{(m-1)}, v^{(m)}-v^{(m-1)}\right)$:

$$\begin{aligned}J_t\left(\sigma^{(m)}\right) &\approx J_t\left(\sigma^{(m-1)}\right) \\ &\quad +\int_0^t \sigma_S^{(m-1)}(u)\left\{S_u^{(m)}-S_u^{(m-1)}\right\}dW_u^S \\ &\quad +\int_0^t \sigma_v^{(m-1)}(u)\left\{v_u^{(m)}-v_u^{(m-1)}\right\}dW_u^S \\ &\quad +\frac{1}{2}\int_0^t \sigma_{SS}^{(m-1)}(u)\left\{S_u^{(m)}-S_u^{(m-1)}\right\}^2 dW_u^S \\ &\quad +\frac{1}{2}\int_0^t \sigma_{vv}^{(m-1)}(u)\left\{v_u^{(m)}-v_u^{(m-1)}\right\}^2 dW_u^S \\ &\quad +\int_0^t \sigma_{Sv}^{(m-1)}\left\{S_u^{(m)}-S_u^{(m-1)}\right\}\left\{v_u^{(m)}-v_u^{(m-1)}\right\}dW_u^S\end{aligned} \tag{8.15}$$

$$\begin{aligned}J_t^2\left(\sigma^{(m)}\right) &\approx J_t^2\left(\sigma^{(m-1)}\right) \\ &\quad +2J_t\left(\sigma^{(m-1)}\right)\int_0^t \sigma_S^{(m-1)}(u)\left\{S_u^{(m)}-S_u^{(m-1)}\right\}dW_u^S \\ &\quad +2J_t\left(\sigma^{(m)}\right)\int_0^t \sigma_v^{(m-1)}(u)\left\{v_u^{(m)}-v_u^{(m-1)}\right\}dW_u^S\end{aligned} \tag{8.16}$$

$I_{1,1}(t), I_{1,2}(t), I_{2,1}(t)$ are expressed as stochastic integrals by expanding the Hermite polynomial, and then expand σ with Taylor expansion around (S, v), just as in equation (8.15):

$$\begin{aligned} I_{1,1}(t) &\approx \int_0^t \sigma_S^{(0)}(u)\left\{S_u^{(1)} - S_u^{(0)}\right\} dW_u^S + \int_0^t \sigma_v^{(0)}\left\{v_u^{(1)} - v_u^{(0)}\right\} dW_u^S \\ &+ \frac{1}{2}\int_0^t \sigma_{SS}^{(0)}(u)\left\{S_u^{(1)} - S_u^{(0)}\right\}^2 dW_u^S + \frac{1}{2}\int_0^t \sigma_{vv}^{(0)}(u)\left\{v_u^{(1)} - v_u^{(0)}\right\}^2 dW_u^S \\ &+ \int_0^t \sigma_{Sv}^{(0)}\left\{S_u^{(1)} - S_u^{(0)}\right\}\left\{v_u^{(1)} - v_u^{(0)}\right\} dW_u^S \end{aligned} \tag{8.17}$$

And in the term $I_{1,2}(t)$, we apply (8.16):

$$I_{1,2}(t) = \frac{1}{2}\left\{\left(J_t^2\left(\sigma^{(1)}\right) - J_t^2\left(\sigma^{(0)}\right)\right) - \left(\left\|\sigma^{(1)}\right\|_t^2 - \left\|\sigma^{(0)}\right\|_t^2\right)\right\} \tag{8.18}$$

$$\begin{aligned} &\approx J_t\left(\sigma^{(0)}\right)\int_0^t \sigma_S^{(0)}(u)\left\{S_u^{(1)} - S_u^{(0)}\right\} dW_u^S + J_t\left(\sigma^{(0)}\right)\int_0^t \sigma_v^{(0)}\left\{v_u^{(1)} - v_u^{(0)}\right\} dW_u^S \\ &- \frac{1}{2}\left(\left\|\sigma^{(1)}\right\|_t^2 - \left\|\sigma^{(0)}\right\|_t^2\right) \end{aligned} \tag{8.19}$$

For $I_{2,1}(t) = J_t\left(\sigma^{(2)}\right) - J_t\left(\sigma^{(1)}\right)$ by definition and equation (8.15):

$$\begin{aligned} I_{2,1}(t) &\approx \int_0^t \sigma_S^{(1)}(u)\left\{S_u^{(2)} - S_u^{(1)}\right\} dW_u^S \\ &+ \int_0^t \sigma_v^{(1)}\left\{v_u^{(2)} - v_u^{(1)}\right\} dW_u^S \\ &+ \frac{1}{2}\int_0^t \sigma_{SS}^{(1)}(u)\left\{S_u^{(2)} - S_u^{(1)}\right\}^2 dW_u^S \\ &+ \frac{1}{2}\int_0^t \sigma_{vv}^{(1)}(u)\left\{v_u^{(2)} - v_u^{(1)}\right\}^2 dW_u^S \\ &+ \int_0^t \sigma_{Sv}^{(1)}\left\{S_u^{(2)} - S_u^{(1)}\right\}\left\{v_u^{(2)} - v_u^{(1)}\right\} dW_u^S \end{aligned} \tag{8.20}$$

where $\sigma_S^{(m)}(t) \coloneqq \partial_s \sigma(s, v)\big|_{s=S_t^{(m)}, v=v_t^{(m)}}$, and other partial derivatives are defined similarly.

Proposition 8.3. With that and applying the Ito lemma and isometry, we have the following iterative integrals with deterministic integrands, for proof we refer to Funahashi [FK12]:

$$\begin{aligned}
I_{1,1}(t) \approx & \int_0^t \sigma_S^{(0)}(s) F(0,s) \left(\int_0^s \sigma^{(0)}(u) dW_u^S \right) dW_s^S \\
& + \int_0^t \sigma_S^{(0)}(s) F(0,s) \left(\int_0^s \sigma^{(0)}(u) \left(\int_0^u \sigma^{(0)}(r) dW_r^S \right) dW_u^S \right) dW_s^S \\
& + \int_0^t \sigma_v^{(0)} \bar{E}(s) \left(\int_0^s E(u) \gamma^{(0)}(u) dW_u^v \right) dW_s^S \\
& + \int_0^t \sigma_{SS}^{(0)}(s) F(0,s)^2 \left(\int_0^s \sigma^{(0)}(u) \left(\int_0^u \sigma^{(0)}(r) dW_r^S \right) dW_u^S \right) dW_s^S \\
& + \frac{1}{2} \int_0^t \sigma_{SS}^{(0)}(s) F(0,s)^2 \left(\int_0^s \left(\sigma^{(0)}(u) \right)^2 du \right) dW_s^S \\
& + \int_0^t \sigma_{vv}^{(0)}(s) \bar{E}(s)^2 \left(\int_0^s E(u) \gamma^{(0)}(u) \left(\int_0^u E(r) \gamma^{(0)}(r) dW_r^v \right) dW_u^v \right) dW_s^S \\
& + \frac{1}{2} \int_0^t \sigma_{vv}^{(0)}(s) \bar{E}(s)^2 \left(\int_0^s E(u)^2 \left(\gamma^{(0)}(u) \right)^2 du \right) dW_s^S \\
& + \int_0^t \sigma_{Sv}^{(0)} F(0,s) \bar{E}(s) \left(\int_0^s \sigma^{(0)}(u) \left(\int_0^u E(r) \gamma^{(0)}(r) dW_r^v \right) dW_u^S \right) dW_s^S \\
& + \int_0^t \sigma_{Sv}^{(0)} F(0,s) \bar{E}(s) \left(\int_0^s E(u) \gamma^{(0)}(u) \left(\int_0^u \sigma^{(0)}(r) dW_r^S \right) dW_u^v \right) dW_s^S \\
& + \int_0^t \sigma_{Sv}^{(0)}(s) F(0,s) \bar{E}(s) \left(\int_0^s \rho E(u) \gamma^{(0)}(u) \sigma^{(0)}(u) du \right) dW_s
\end{aligned} \tag{8.21}$$

$$\begin{aligned}
I_{1,2}(t) \approx & \int_0^t \sigma^{(0)}(s) \left(\int_0^s \sigma_S^{(0)}(u) F(0,u) \left(\int_0^u \sigma^{(0)}(r) dW_r^S \right) dW_u^S \right) dW_s^S \\
+ & \int_0^t \sigma_S^{(0)}(s) F(0,s) \left(\int_0^s \sigma^{(0)}(u) dW_u^S \right)^2 dW_s^S \\
+ & \int_0^t \sigma^{(0)}(s) \left(\int_0^s \sigma_v^{(0)}(u) \bar{E}(u) \left(\int_0^u E(r) \gamma^{(0)}(r) dW_r^v \right) dW_u^S \right) dW_s^S \\
+ & \int_0^t \sigma_v^{(0)}(s) \bar{E}(s) \left(\int_0^s \sigma^{(0)}(u) dW_u^S \right) \left(\int_0^s E(u) \gamma^{(0)}(u) dW_u^v \right) dW_s^S
\end{aligned} \tag{8.22}$$

$$\begin{aligned}
I_{2,1}(t) \approx & \int_0^t \sigma_S^{(0)}(s) F(0,s) \left(\int_0^s \sigma_S^{(0)}(u) F(0,u) \left(\int_0^u \sigma^{(0)}(r) dW_r^S \right) dW_u^S \right) dW_s^S \\
+ & \int_0^t \sigma_S^{(0)}(s) F(0,s) \left(\int_0^s \sigma_v^{(0)}(u) \bar{E}(u) \left(\int_0^u E(r) \gamma^{(0)}(r) dW_r^v \right) dW_u^S \right) dW_s^S \\
+ & \int_0^t \sigma_v^{(0)}(s) \bar{E}(s) \left(\int_0^s \gamma_v^{(0)}(u) \left(\int_0^u E(r) \gamma^{(0)}(r) dW_r^v \right) dW_u^v \right) dW_s^S
\end{aligned} \tag{8.23}$$

For $m+n \leq 4$,

$$I_{m,n}(t) \approx 0$$

To formulate the pdf for the option pricing, we need to formulate $X_t \coloneqq \frac{S_t}{F(0,t)} - 1$, and from the equations (8.13),(8.14):

Theorem 8.2.

$$\begin{aligned} X_t &= \frac{S_t}{F(0,t)} - 1 \approx \left(\frac{\tilde{S}_t^{(1)}}{F(0,t)} - 1 \right) + \sum_{m,n \geq 1; m+n \leq 3} I_{m,n}(t) \\ &= \left[\int_0^t \sigma_0(t_1)\, dW_{t_1} + \int_0^t \int_0^{t_2} \sigma_0(t_1)\, \sigma_0(t_2)\, dW_{t_1}^S dW_{t_2}^S \right. \\ &\quad \left. + \int_0^t \int_0^{t_3} \int_0^{t_2} \sigma_0(t_1)\, \sigma_0(t_2)\, \sigma_0(t_3)\, dW_{t_1}^S dW_{t_2}^S dW_{t_3}^S \right] \\ &\quad + I_{1,1}(t) + I_{1,2}(t) + I_{2,1}(t) \end{aligned} \tag{8.24}$$

by grouping the iterative integral by their order, we have the following

$$\begin{aligned} X_t \approx & \int_0^t p_1(s)\, dW_s^S \\ & + \int_0^t p_2(s) \left(\int_0^s \sigma^{(0)}(u)\, dW_u^S \right) dW_s^S + \int_0^t p_3(u) \left(\int_0^s p_4(u)\, dW_u^v \right) dW_s^S \\ & + \int_0^t p_5(s) \left(\int_0^s \sigma^{(0)}(u) \left(\int_0^u \sigma^{(0)}(r)\, dW_r^S \right) dW_u^S \right) dW_s^S \\ & + \int_0^t p_6(s) \left(\int_0^s p_4(u) \left(\int_0^u p_4(r)\, dW_r^v \right) dW_u^v \right) dW_s^S \\ & + \int_0^t p_7(s) \left(\int_0^s p_4(u) \left(\int_0^u \sigma^{(0)}(r)\, dW_r^S \right) dW_u^v \right) dW_s^S \\ & + \int_0^t p_7(s) \left(\int_0^s \sigma^{(0)}(u) \left(\int_0^u p_4(r)\, dW_r^v \right) dW_u^S \right) dW_s^S \\ & + \int_0^t p_2(s) \left(\int_0^s p_8(u) \left(\int_0^u \sigma^{(0)}(r)\, dW_r^S \right) dW_u^S \right) dW_s^S \\ & + \int_0^t p_2(s) \left(\int_0^s p_3(u) \left(\int_0^u p_4(r)\, dW_r^v \right) dW_u^S \right) dW_s^S \\ & + \int_0^t p_3(s) \left(\int_0^s \gamma_v^{(0)}(u) \left(\int_0^u p_4(r)\, dW_r^v \right) dW_u^v \right) dW_s^S \end{aligned} \tag{8.25}$$

where

$$
\begin{aligned}
p_1(s) \coloneqq\ & \sigma^{(0)}(s) + \left\{ \sigma_S^{(0)}(s) F(0,s) + \frac{1}{2} F(0,s)^2 \sigma_{SS}^{(0)}(s) \right\} \left(\int_0^s (\sigma_0(u))^2 du \right) \\
& + \frac{1}{2} \sigma_{vv}^{(0)}(s) \bar{E}(s)^2 \left(\int_0^s E(u)^2 \gamma^{(0)}(u)^2 du \right) \\
& + \left\{ \sigma_v^{(0)}(s) \bar{E}(s) + \sigma_{Sv}^{(0)}(s) F(0,s) \bar{E}(s) \right\} \left(\int_0^s \rho E(u) \gamma^{(0)}(u) \sigma^{(0)}(u) du \right) \\
p_2(s) \coloneqq\ & \sigma^{(0)}(s) + F(0,s) \sigma_S^{(0)}(s) \\
p_3(s) \coloneqq\ & \sigma_v^{(0)}(s) \bar{E}(s) \\
p_4(s) \coloneqq\ & E(s) \gamma^{(0)}(s) \\
p_5(s) \coloneqq\ & \sigma^{(0)}(s) + 3\sigma_S^{(0)}(s) F(0,s) + \sigma_{SS}^{(0)}(s) F(0,s)^2 \\
p_6(s) \coloneqq\ & \sigma_{vv}^{(0)}(s) \bar{E}(s)^2 \\
p_7(s) \coloneqq\ & \sigma_v^{(0)}(s) \bar{E}(s) + \sigma_{Sv}^{(0)} F(0,s) \bar{E}(s) \\
p_8(s) \coloneqq\ & \sigma_S^{(0)}(s) F(0,s)
\end{aligned}
\tag{8.26}
$$

Note that all the functions are deterministic, thus the integrands are all simple stochastic integrals with deterministic integrands.

To put it more succinctly, $X_t = a_1(t) + a_2(t) + a_3(t)$,where

$$
\begin{aligned}
a_1(t) &= \int_0^t p_1(s) dW_s^S \\
a_2(t) &= \int_0^t p_2(s) \left(\int_0^s \sigma^{(0)}(u) dW_u^S \right) dW_s^S + \int_0^t p_3(s) \left(\int_0^s p_4(u) dW_u^v \right) dW_s^S \\
a_3(t) &= \int_0^t p_5(s) \left(\int_0^s \sigma^{(0)}(u) \left(\int_0^u \sigma^{(0)}(r) dW_r^S \right) dW_u^S \right) dW_s^S \\
&\quad + \int_0^t p_6(s) \left(\int_0^s p_4(u) \left(\int_0^u p_4(r) dW_r^v \right) dW_u^v \right) dW_s^S \\
&\quad + \int_0^t p_7(s) \left(\int_0^s p_4(u) \left(\int_0^u \sigma^{(0)}(r) dW_r^S \right) dW_u^v \right) dW_s^S \\
&\quad + \int_0^t p_7(s) \left(\int_0^s \sigma^{(0)}(u) \left(\int_0^u p_4(r) dW_r^v \right) dW_u^S \right) dW_s^S \\
&\quad + \int_0^t p_2(s) \left(\int_0^s p_8(u) \left(\int_0^u \sigma^{(0)}(r) dW_r^S \right) dW_u^S \right) dW_s^S \\
&\quad + \int_0^t p_2(s) \left(\int_0^s p_3(u) \left(\int_0^u p_4(r) dW_r^v \right) dW_u^S \right) dW_s^S \\
&\quad + \int_0^t p_3(s) \left(\int_0^s \gamma_v^{(0)}(u) \left(\int_0^u p_4(r) dW_r^v \right) dW_u^S \right) dW_s^S
\end{aligned}
\tag{8.27}
$$

a_1 denotes the single-order stochastic integral terms, a_2 for second-order, and a_3 for the third-order terms. This is a necessary setup for

The significance of equation (8.25) is that the asset process itself, completed with the stochastic local volatility structure, can be expressed as a iterative integral where the integrands are all deterministic, so that the moments of X_t can be calculated explicitly, albeit complicated. And indeed, because of the moments are calculatable, the probably distribution function (pdf), can be inverted from the process, or at least approximated.

8.6 Probability Distribution Function approximation

As mentioned previously, it is possible to approximate the probability distribution function, and integrate it against the payoff function to get the European option formula, this is a relatively typical treatment to invert the probability distribution function:

$$\begin{aligned}
\Psi(\xi) &= \mathbb{E}\left[e^{i\xi X_t}\right] && (8.28)\\
&= \mathbb{E}\left[e^{i\xi\{a_1(t)+a_2(t)+a_3(t)\}}\right] \\
&= \mathbb{E}\left[e^{i\xi a_1(t)}e^{i\xi\{a_2(t)+a_3(t)\}}\right] && (8.29)\\
&\approx \mathbb{E}\left[e^{i\xi a_1(t)}\left(1+i\xi a_2(t)+i\xi a_3(t)-\frac{1}{2}\xi^2 a_2(t)^2+R\right)\right]
\end{aligned}$$

where R consists of fourth or higher-order multiple stochastic integrals. Taking conditional expectation based on $a_1(t)$:

$$\begin{aligned}
\Psi(\xi) \approx\ & \mathbb{E}\left[e^{i\xi a_1(t)}\right]+i\xi\mathbb{E}\left[e^{i\xi a_1(t)}\mathbb{E}\left[a_2(t)\,|a_1(t)\right]\right] && (8.30)\\
&+i\xi\mathbb{E}\left[e^{i\xi a_1(t)}\mathbb{E}\left[a_3(t)\,|a_1(t)\right]\right]-\frac{1}{2}\xi^2\mathbb{E}\left[e^{i\xi a_1(t)}\mathbb{E}\left[a_2(t)^2\,|a_1(t)\right]\right]
\end{aligned}$$

Now define the quantity

$$\Sigma_t \coloneqq \mathbb{E}\left[\int_0^t p_1(s)\,dW_s^S\right]^2 = \int_0^t p_1^2(s)\,ds \tag{8.31}$$

Which is the variance of the $a_1(t)$ (it has zero-mean).

Theorem 8.3. From the lemma of B.1 of [FK12], it is known that if X follow a normal distribution with zero mean and variance Σ. Then for any polynomial function $h(x)$ and $g(x)$:

$$\frac{1}{2\pi}\int_{\mathbb{R}} e^{-iky}g(-ik)\,\mathbb{E}\left[h(X)\,e^{ikX}\right]dk = g\left(\frac{\partial}{\partial y}\right)\left[h(y)\,n(y;0,\Sigma)\right] \tag{8.32}$$

Here $n(x;a,b)$ is the normal density function with mean a and variance b. $g(\cdot)$ is the polynomial of the operator $\frac{\partial}{\partial y}$, for example, in the last term, $g(-ik)=(-ik)^2$, so $g\left(\frac{\partial}{\partial y}\right)[\cdots]=\frac{\partial^2}{\partial y^2}[\cdots]$

Differentiating both side with respect to y, we can obtain

$$\frac{1}{2\pi}\int_{\mathbb{R}} e^{-iky}\mathbb{E}\left[h\left(X\right)e^{ikX}\right]dk = h\left(y\right)n\left(y;0,\Sigma\right)$$

For example and proof, please refers to Takahashi [Tak99], and Fujikoshi, etc. [FMKT82].

Applying this to each term of (8.30):

$$\begin{aligned} f_{X_t} &= n\left(x;0,\Sigma_t\right) - \frac{\partial}{\partial x}\left\{\mathbb{E}\left[a_2\left(t\right)|a_1\left(t\right)=x\right]n\left(x;0,\Sigma_t\right)\right\} \\ &\quad -\frac{\partial}{\partial x}\left\{\mathbb{E}\left[a_3\left(t\right)|a_1\left(t\right)=x\right]n\left(x;0,\Sigma_t\right)\right\} \\ &\quad +\frac{1}{2}\frac{\partial^2}{\partial x^2}\left\{\mathbb{E}\left[a_2\left(t\right)^2|a_1\left(t\right)=x\right]n\left(x;0,\Sigma_t\right)\right\}+\cdots \end{aligned} \tag{8.33}$$

The conditional expectation can be solved by Lemma 2.1 in [Tak99]. Which is included in Appendix C, resulting in the following conditional expectation:

$$\begin{aligned} \mathbb{E}\left[a_2\left(t\right)|a_1\left(t\right)=x\right] &= q_1\left(t\right)\left(\frac{x^2}{\Sigma_t^2}-\frac{1}{\Sigma_t}\right) \\ \mathbb{E}\left[a_3\left(t\right)|a_1\left(t\right)=x\right] &= q_2\left(t\right)\left(\frac{x^3}{\Sigma_t^3}-\frac{3x}{\Sigma_t^2}\right) \\ \mathbb{E}\left[a_2^2\left(t\right)|a_1\left(t\right)=x\right] &= q_3\left(t\right)\left(\frac{x^4}{\Sigma_t^4}-\frac{6x^2}{\Sigma_t^3}+\frac{3}{\Sigma_t^2}\right)+q_4\left(t\right)\left(\frac{x^2}{\Sigma^2}-\frac{1}{\Sigma_t}\right)+q_5\left(t\right) \end{aligned} \tag{8.34}$$

where

$$\begin{aligned} q_1\left(t\right) &= \int_0^t p_1\left(s\right)p_2\left(s\right)\left(\int_0^s \sigma^{(0)}\left(u\right)p_1\left(u\right)du\right)ds + \int_0^t p_1\left(s\right)p_3\left(s\right)\left(\int_0^s \rho p_1\left(u\right)p_4\left(u\right)du\right)ds \\ q_2\left(t\right) &= q_{2,1}\left(t\right)+q_{2,2}\left(t\right)+q_{2,3}\left(t\right) \\ q_3\left(t\right) &= q_1^2\left(t\right) \\ q_4\left(t\right) &= q_{4,1}\left(t\right)+q_{4,2}\left(t\right)+q_{4,3}\left(t\right) \\ q_5\left(t\right) &= \int_0^t p_2^2\left(s\right)\left(\int_0^s \left(\sigma^{(0)}\left(u\right)\right)^2 du\right)ds + \int_0^t p_3^2\left(s\right)\left(\int_0^s p_4^2\left(u\right)du\right)ds \\ &\quad +2\int_0^t p_2\left(s\right)p_3\left(s\right)\left(\int_0^s \rho\sigma^{(0)}\left(u\right)p_4\left(u\right)du\right)ds \end{aligned} \tag{8.35}$$

And $q_{2,1}\left(t\right), q_{2,2}\left(t\right), q_{2,3}\left(t\right), q_{4,1}\left(t\right), q_{4,2}\left(t\right), q_{4,3}\left(t\right)$.

$$
\begin{aligned}
q_{2,1}(t) &= \int_0^t p_1(s)\,p_5(s)\left(\int_0^s \sigma^{(0)}(u)\,p_1(u)\left(\int_0^u \sigma^{(0)}(r)\,p_1(r)\,dr\right)du\right)ds \qquad (8.36)\\
&\quad+\int_0^t p_1(s)\,p_2(s)\left(\int_0^s p_1(u)\,p_8(u)\left(\int_0^u \sigma^{(0)}(r)\,p_1(r)\,dr\right)du\right)ds\\
q_{2,2}(t) &= \int_0^t p_1(s)\,p_3(s)\left(\int_0^s \rho p_1(u)\,\gamma_v^{(0)}(u)\left(\int_0^u \rho p_1(r)\,p_4(r)\,dr\right)du\right)ds\\
q_{2,3}(t) &= \int_0^t p_1(s)\,p_6(s)\left(\int_0^s \rho p_1(u)\,p_4(u)\left(\int_0^u \rho p_1(r)\,p_4(r)\,dr\right)du\right)ds\\
&\quad+\int_0^t p_1(s)\,p_7(s)\left(\int_0^s \rho p_1(u)\,p_4(u)\left(\int_0^u \sigma^{(0)}(r)\,p_1(r)\,dr\right)du\right)ds\\
&\quad+\int_0^t p_1(s)\,p_7(s)\left(\int_0^s \sigma^{(0)}(u)\,p_1(u)\left(\int_0^u \rho p_1(r)\,p_4(r)\,dr\right)du\right)ds\\
&\quad+\int_0^t p_1(s)\,p_2(s)\left(\int_0^s p_1(u)\,p_3(u)\left(\int_0^u \rho p_1(r)\,p_4(r)\,dr\right)du\right)ds\\
q_{4,1}(t) &= 2\int_0^t p_1(s)\,p_2(s)\left(\int_0^s p_1(u)\,p_2(u)\left(\int_0^u (\sigma(r))^2\,dr\right)du\right)ds\\
&\quad+2\int_0^t p_1(s)\,p_2(s)\left(\int_0^s \sigma^{(0)}(u)\,p_2(u)\left(\int_0^u \sigma^{(0)}(r)\,p_1(r)\,dr\right)du\right)ds\\
&\quad+\int_0^t p_2(s)^2\left(\int_0^s \sigma^{(0)}(u)\,p_2(u)\,du\right)^2 ds\\
q_{4,2}(t) &= 2\int_0^t p_1(s)\,p_3(s)\left(\int_0^s p_1(u)\,p_3(u)\left(\int_0^u p_4(r)^2\,dr\right)du\right)ds\\
&\quad+2\int_0^t p_1(s)\,p_3(s)\left(\int_0^s \rho p_3(u)\,p_4(u)\left(\int_0^u \rho p_1(r)\,p_4(u)\,dr\right)du\right)ds\\
&\quad+\int_0^t p_3(s)^2\left(\int_0^s \rho p_1(u)\,p_4(u)\,du\right)^2 ds\\
q_{4.3}(t) &= 2\int_0^t p_1(s)\,p_2(s)\left(\int_0^s p_1(u)\,p_3(u)\left(\int_0^u \rho\sigma^{(0)}(r)\,p_4(r)\,dr\right)du\right)ds\\
&\quad+2\int_0^t p_1(s)\,p_3(s)\left(\int_0^s p_1(u)\,p_2(u)\left(\int_0^u \rho\sigma^{(0)}(r)\,p_4(r)\,dr\right)du\right)ds\\
&\quad+2\int_0^t p_1(s)\,p_2(s)\left(\int_0^s \sigma^{(0)}(u)\,p_3(u)\left(\int_0^u \rho p_1(r)\,p_4(r)\,dr\right)du\right)ds\\
&\quad+2\int_0^t p_1(s)\,p_3(s)\left(\int_0^s \rho p_2(u)\,p_4(u)\left(\int_0^u \sigma^{(0)}(r)\,p_1(r)\,dr\right)du\right)ds\\
&\quad+2\int_0^t p_2(s)\,p_3(s)\left(\int_0^s \sigma^{(0)}(u)\,p_1(u)\,du\right)\left(\int_0^s \rho p_1(u)\,p_4(u)\,du\right)ds
\end{aligned}
$$

Proposition 8.4. Therefore we obtain the following proposition:

$$\begin{aligned} f_{X_t(x)} &\approx \frac{1}{2} n\left(x; 0, \Sigma_t\right) \left[\frac{q_3\left(t\right)}{\Sigma_t^3} h_6\left(\frac{x}{\sqrt{\Sigma_t}}\right) + \frac{\left(2q_2\left(t\right) + q_4\left(t\right)\right)}{\Sigma_t^2} h_4\left(\frac{x}{\sqrt{\Sigma_t}}\right)\right. \\ &\quad \left. + \frac{2q_1\left(t\right)}{\left(\sqrt{\Sigma_t}\right)^3} h_3\left(\frac{x}{\sqrt{\Sigma_t}}\right) + \frac{q_5\left(t\right)}{\Sigma_t} h_2\left(\frac{x}{\sqrt{\Sigma_t}}\right) + 2\right] \end{aligned} \tag{8.37}$$

8.7 Option Pricing

The European call option with strike K and maturity t on the asset S_t can be written as:

$$C\left(t\right) = \mathbb{E}\left[e^{-\int_0^t r(s)ds}\left(S_t - K\right)^+\right] = F\left(0,t\right)\mathbb{E}\left[e^{-\int_0^t r(s)ds}\left(X_t + K'\right)^+\right] = S\left(0\right)\int_{-K'}^{+\infty}\left(x + K'\right) f_{X_t}\left(x\right) dx \tag{8.38}$$

where $K^{'} \coloneqq 1 - \frac{K}{F(0,t)}$, and can be approximated by integrating the above equation against the approximated probability distribution function.

Theorem 8.4.
Truncating the higher-orders, we have the following approximation or the European Call option:

$$\begin{aligned} C\left(t\right) &\approx \frac{S_0 n\left(K'; 0, \Sigma\right)}{2\Sigma^4}\left[q_3\left(t\right)\left(K'^4 - 6K'^2\Sigma + 3\Sigma^2\right)\right. \\ &\quad +\Sigma^2\left(q_4\left(t\right) + 2q_2\left(t\right)\right)\left(K'^2 - \Sigma\right) \\ &\quad \left. + \Sigma^3\left\{-2q_1\left(t\right)K' + q_5\left(t\right)\Sigma + 2\Sigma^2\right\}\right] \\ &\quad +S_0 K'\left(1 - \Phi\left(-\frac{K'}{\sqrt{\Sigma}}\right)\right) \end{aligned} \tag{8.39}$$

Here the $n\left(x; 0, \Sigma\right)$ is the zero-mean normal probability distribution function with standard deviation Σ. And $\Phi\left(\cdot\right)$ is the standard normal probability cumulative distribution function.

Theorem 8.4 will serve as our jumping point for the extension to incorporate the fractional Brownian motion.

9 Approximation scheme with mixture fBM model

In the mixture fractional Brownian motion setup from equation (7.4), it looks very similar to the hybrid volatility model approximated by the Funahashi scheme from the previous section. Indeed the only extra part in the volatility term is the fractional Brownian motion, where it can be robustly obtained by FFT approach. So the volatility process is in the functional form of $\sigma(t) = \exp(X_t)$, where X_t is an OU process that has both ordinary Brownian motion and fractional Brownian motion:

$$X(t) = X^{(0)}(t) + \int_0^t \nu_u e^{-\kappa(t-u)} dW_u + \int_0^t \nu_u^H e^{-\kappa(t-u)} dW_u^H \tag{9.1}$$

where

$$X^{(0)}(s) = X_0 e^{-\int_0^s \kappa(u)du} + \int_0^s e^{-\int_u^s \kappa(v)dv} \theta du \tag{9.2}$$

Due to the independence of fractional Brownian motion and Brownian motion with different Hurst indices, it is relatively easy to separate the ordinary Brownian motion and fractional Brownian motion parts, now our volatility process can be written as:

$$\hat{\sigma}^{(i)}(t) = \sigma_{BM}(t) * K_t^i \tag{9.3}$$

where

$$K_t^{(i)} = \exp\left(\int_0^t \nu_u^H e^{-\kappa(t-u)} dW_u^{H,i} \right) \tag{9.4}$$

Which $\left\{ W_s^{H,(i)} \right\}_{0 \le s \le T}$ is the i'th path of a fractional Brownian motion with Hurst index H, $K_t^{(i)}$ follows a log-normal distribution, and $\sigma_{\text{BM}}(t)$ is the original stochastic local volatility process from section 8.

The approximation has the input of $\sigma(t)$, and also the corresponding partial derivative with respect to the state-variables (S_t, v_t), but not with respect to time. So $K_t^{(i)}$, being an time-dependent random variable only, can be treated as a constant, multiplied to the log-volatility process. For the input parameters in the approximation, it can be simply modified by multiplying $K_t^{(i)}$ appropriately, take $p_2(s)$ for example, the original version:

$$p_2(s) = \sigma^{(0)}(s) + F(0,s)\, \sigma_S^{(0)}(s) \tag{9.5}$$

where $\sigma^{(0)}(s)$ is the deterministic initial term-structure of the stochastic volatility depends on the deterministic vol-of-vol $X^{(0)}(s) = X_0 e^{-\int_0^s \kappa(u)du} + \int_0^s e^{-\int_u^s \kappa(v)dv} \theta du$
So now substituting Equation (9.3) into $p_2(s)$:

$$\hat{p}_2^{(i)}(s) = K_s^{(i)} \sigma^{(0)}(s) + K_s^{(i)} F(0,s)\, \sigma_S^{(0)}(s) \tag{9.6}$$

We have the following modified formula for the call option,

$$\begin{aligned}
\hat{C}(t) &= E\left[C(t)|\left\{W_s^H\right\}_{0\leq s\leq T}\right] && (9.7)\\
&= \frac{1}{N}\sum_{i=1}^{N}\left[C(t)|\left\{W_s^{H,i}\right\}_{0\leq s\leq T}\right] && (9.8)\\
&= \frac{1}{N}\sum_{i=1}^{N}\left[C(t)|\,\Sigma_t, p_1^i(t), p_2^i(t), \cdots, p_8^i(t)\right]
\end{aligned}$$

$\left[C(t)|\,\Sigma_t, p_1^i(t), p_2^i(t), \cdots, p_8^i(t)\right]$ is the Call option price calculated by Theorem (8.4), with input parameters $\Sigma_t, p_1^i(t), p_2^i(t), \cdots, p_8^i(t)$, which are generated by the path $\left\{W_s^{H,i}\right\}_{0\leq s\leq T}$.
The reason of choosing this approach instead of calculating the explicit higher moment of K_t in the approximation is because equations for cross-term $\mathbb{E}[K_t K_s]$ is not yet known, which is necessary to do. if one is to replicate the stochastic local volatility asymptotic expansion around the volatility function for a fully analytical approximation scheme, resulting in iterative fractional stochastic integrals $E\left[\int_0^T y_3(t)\left(\int_0^t y_2(s)\,dW_s^H\right)dW_t^H\middle|\int_0^T y_1(t)\,dW_t^H = X\right]$, similar to those in [Tak99], but instead it is iterative fractional stochastic integrals, which no known explicit formulas have been found yet.

9.1 Simulated result

Here, three cases are included of the comparison between the Funahashi approximated mixture fBM model and the simulated counterpart, as well as the error terms of the full mixture fBM model.

The general setup is $\kappa = 1, \rho = -0.5, H = 0.9$ for all three cases:

- $\nu = 0.95, \nu^H = 0.0$
- $\nu = 0.0, \nu^H = 0.30$
- $\nu = 0.95, \nu^H = 0.30$

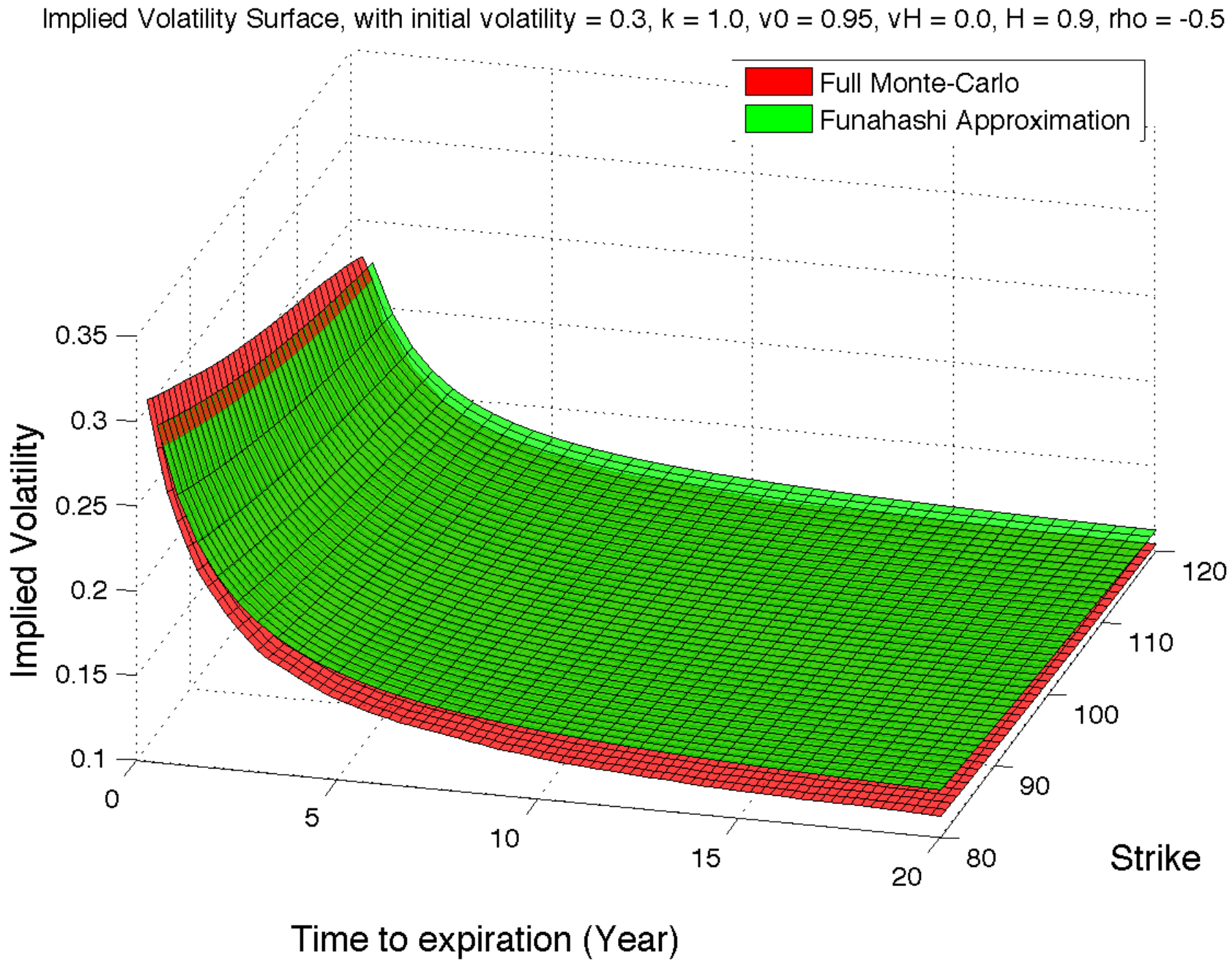

Figure 19: Approximated and Simulated Volatility Surface. $\nu = 0.95, \nu^H = 0.0$.

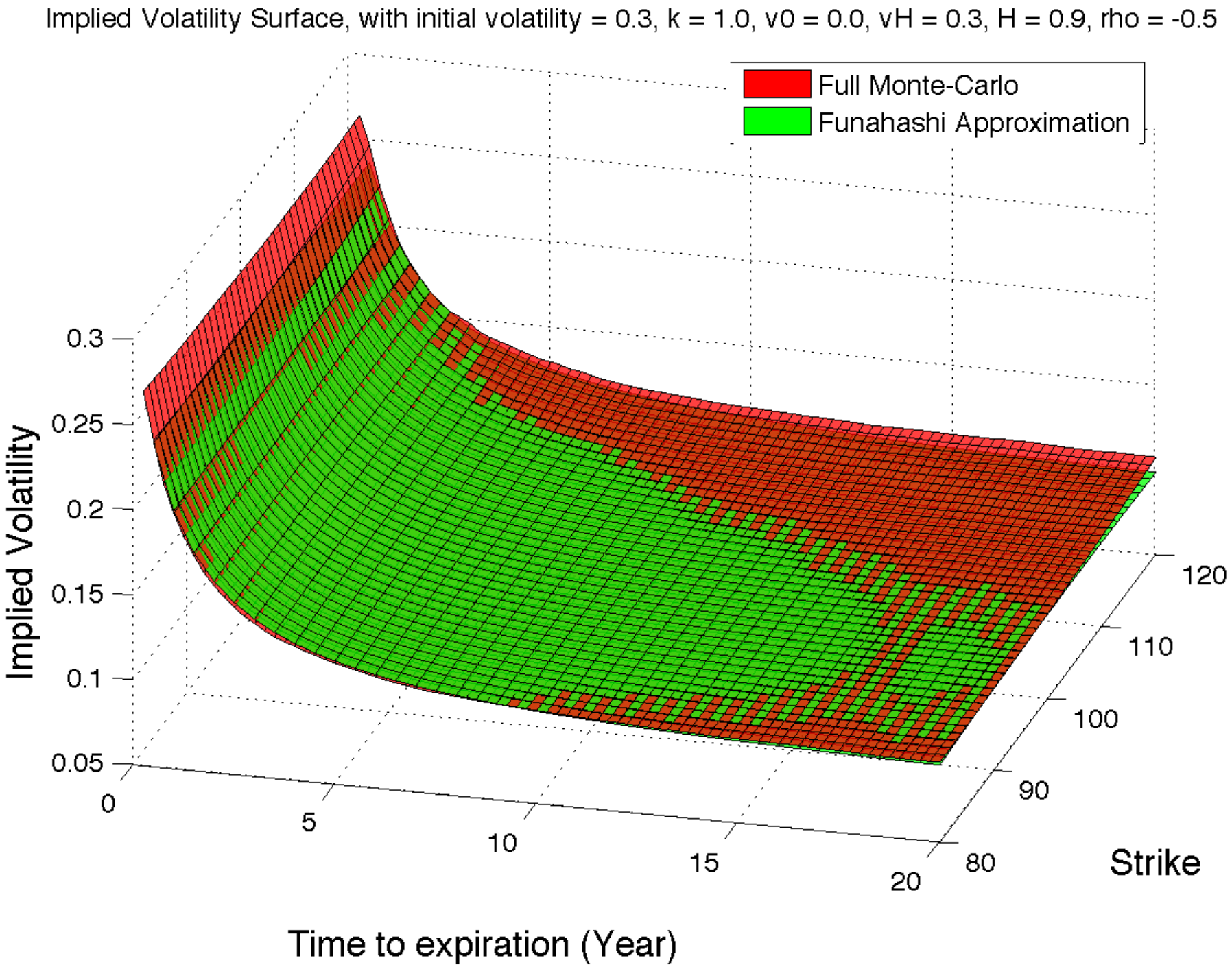

Figure 20: Approximated and Simulated Volatility Surface. $\nu = 0.0, \nu^H = 0.3$.

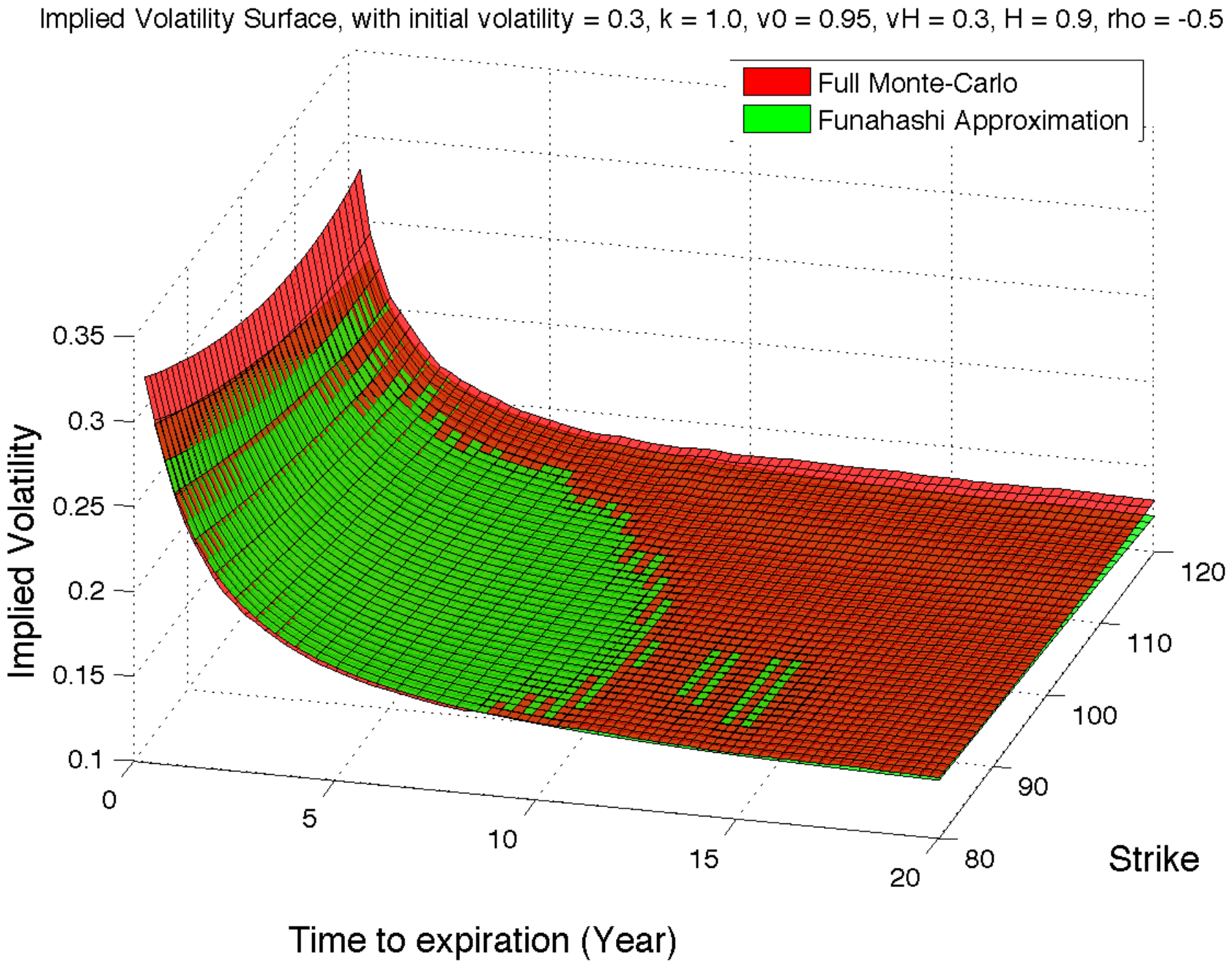

Figure 21: Approximated and Simulated Volatility Surface. $\nu = 0.95, \nu^H = 0.3$.

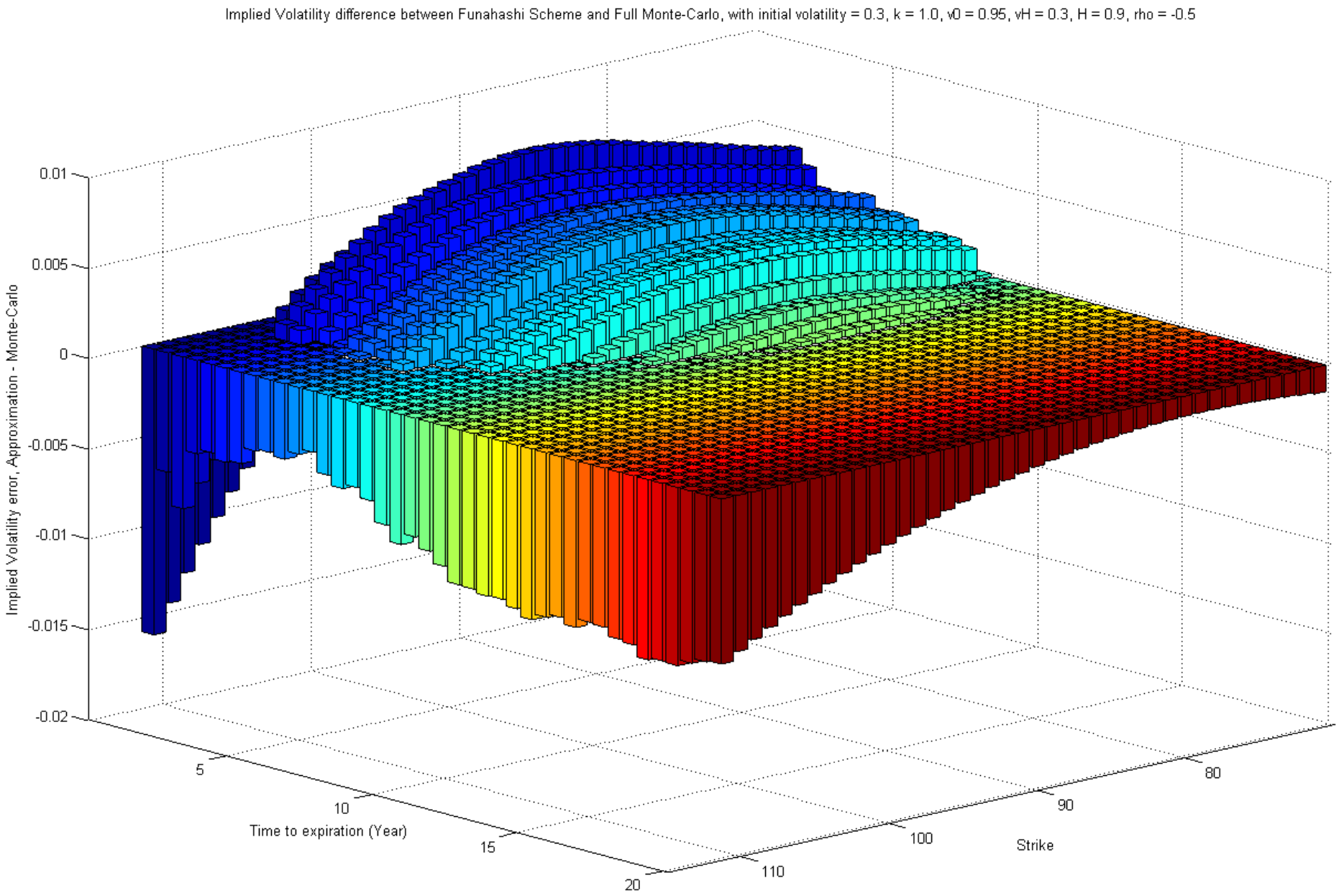

Figure 22: Error between Approximated and Simulated Volatility Surface. $\nu = 0.95, \nu^H = 0.35$.

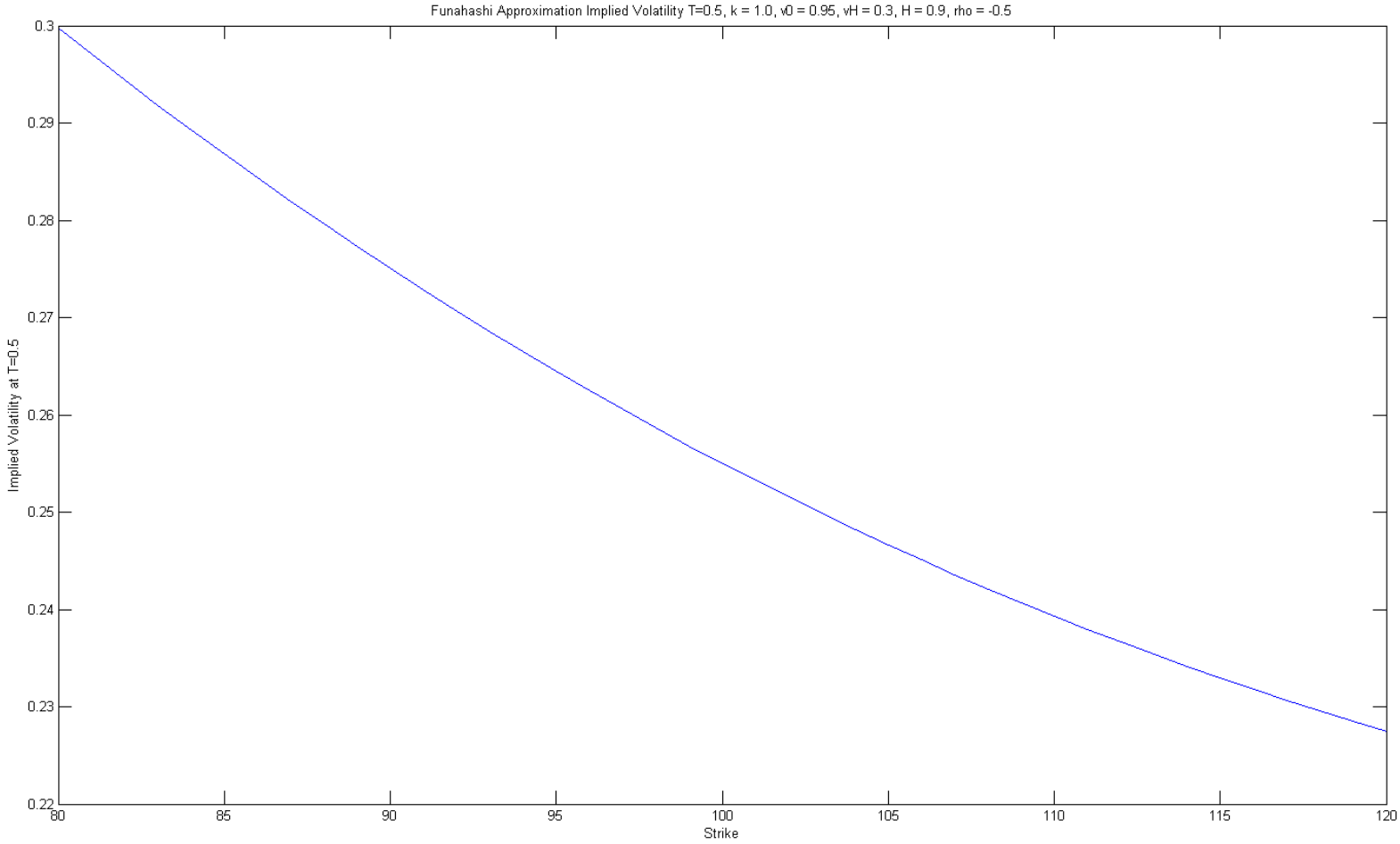

Figure 23: Volatility skewness displayed by the Approximated implied volatility at $T = 0.5, \nu = 0.95, \nu^H = 0.35$.

The scheme is a pretty good approximation for the mixture Brownian motion, as it can capture the simulated result quite accurately, besides some of the very far away strikes. The stylized features such as volatility smiles and skewness are captured. To emphasize the feature of the volatility persistence captured in this approximation.

In order to emphasize the vantage of fractional Brownian motion, cases with various level of vol-of-vol for both the ordinary Brownian motion and fractional Brownian motion are also included. And plot the volatility curves at different time-to-maturity horizons to emphasize the effect of the fractional Brownian motion on the implied volatility surfaces.

The numerical result from the approximation scheme under different Hurst indices are included: Backbone of the volatility surface (At-The-Money implied volatility), and three implied volatility curve across strikes at different point of time-to-maturity.

Figure 24 to 27, plot the case where there is zero-correlation. This is one of the main result of this paper, the volatility decays quickly for the purely ordinary Brownian motion stochastic volatility (the top plots), and the purely fractionally Brownian motion stochastic volatility structure (bottom plots) has resilient volatility smile. The curvature of the fractional Brownian motion driven stochastic volatility model remains prominent compared to the ordinary Brownian motion counterpart.

Observing figure 28 to 31, the case where the correlation coefficient is set at $\rho = -0.8$. We can see that the correlation is actually a much stronger factor than the stochastic volatility in the beginning, and the slope remains to be the more prominent factor throughout for the purely ordinary Brownian motion case. From the middle plot of Figure 31, we see as the temporal aggreation takes hold, the skewness is suppressed, and the volatility persistence causes the curvature become significant again. In order to emphasize this trait, the vol-of-vol is increased for the fractional Brownian motion in the last part, (from Figure 32 to Figure 36), showing significant long-term curvature and skewness at the same time. where the volatility smile remains prominent throughout the horizon as well as the skewness. As pointed out before, the long-maturity volatility smile is best attributed to the fractional Brownian motion, this is an important point to bear in mind during the calibration routine in the next chapter.

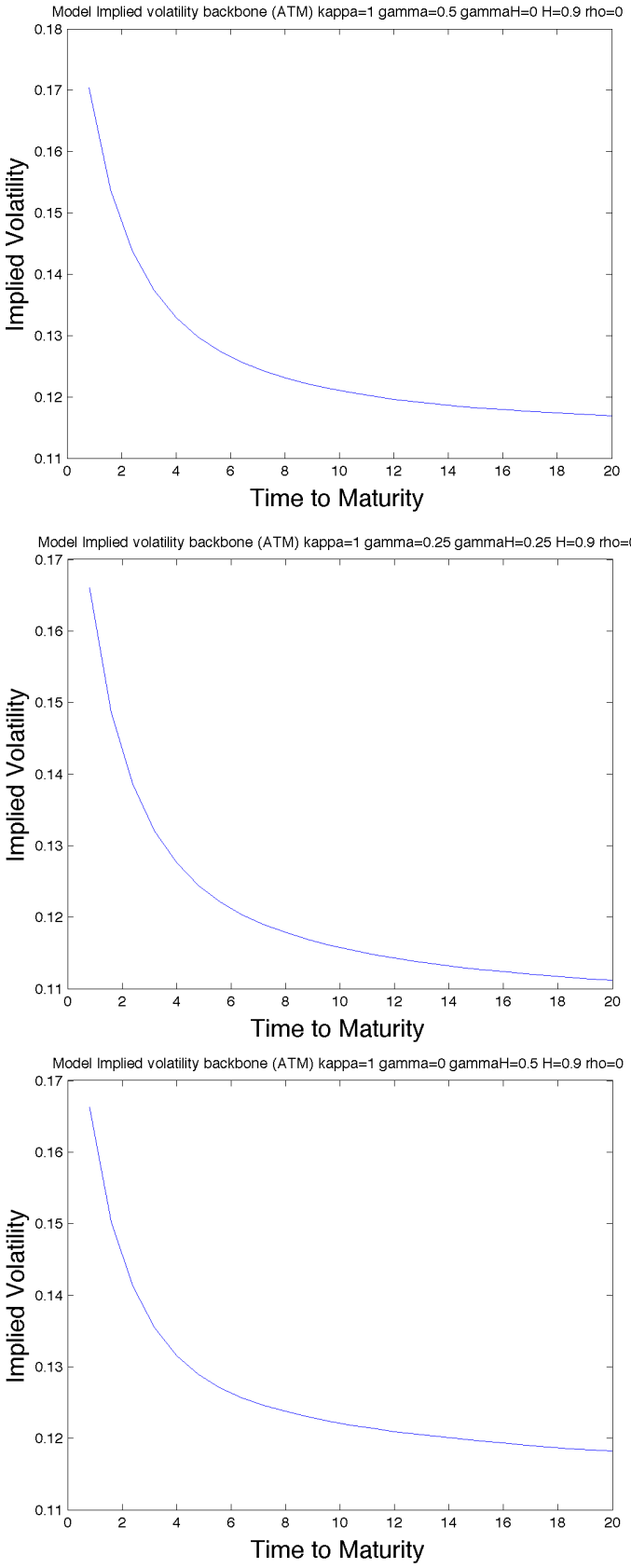

Figure 24: ATM Implied Volatility Curve (BackBone), $\kappa = 1, \rho = 0$

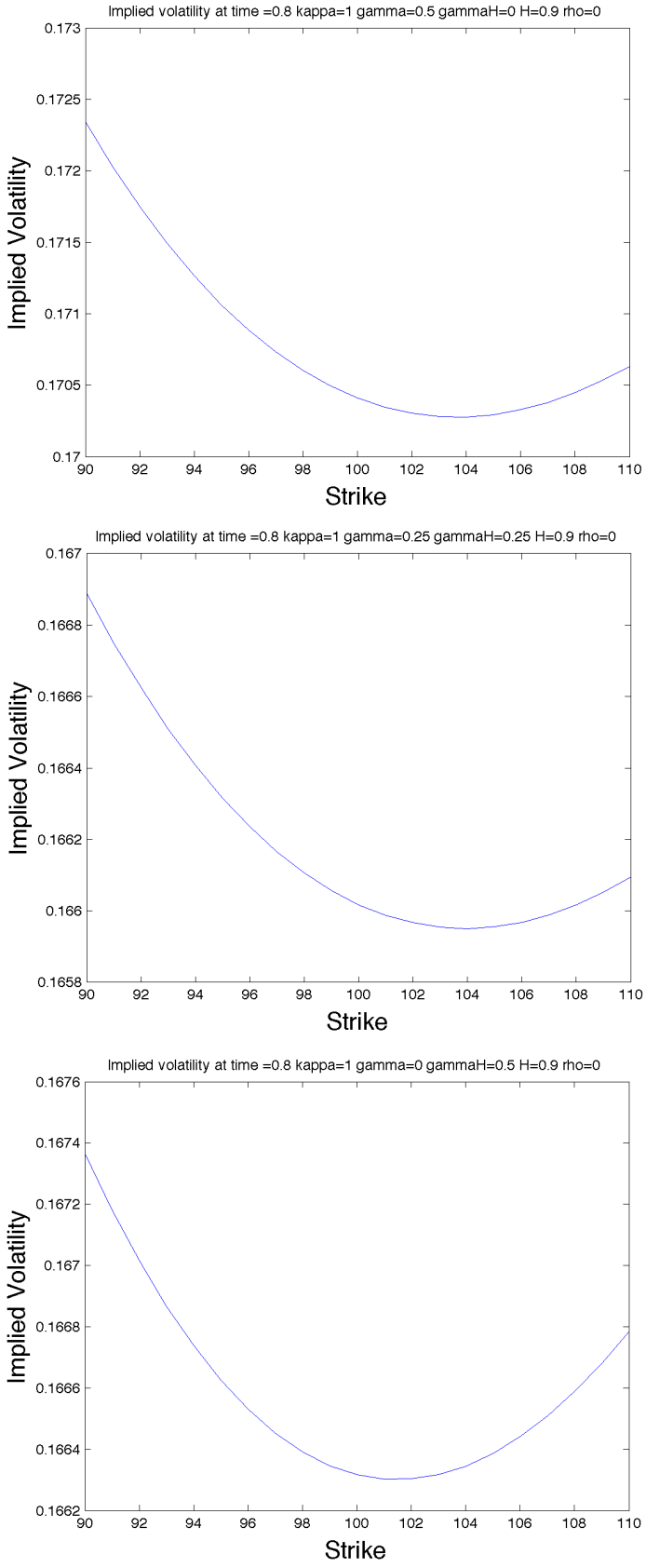

Figure 25: Implied Volatility Curve at $t = 0.8$, $\kappa = 1, \rho = 0$

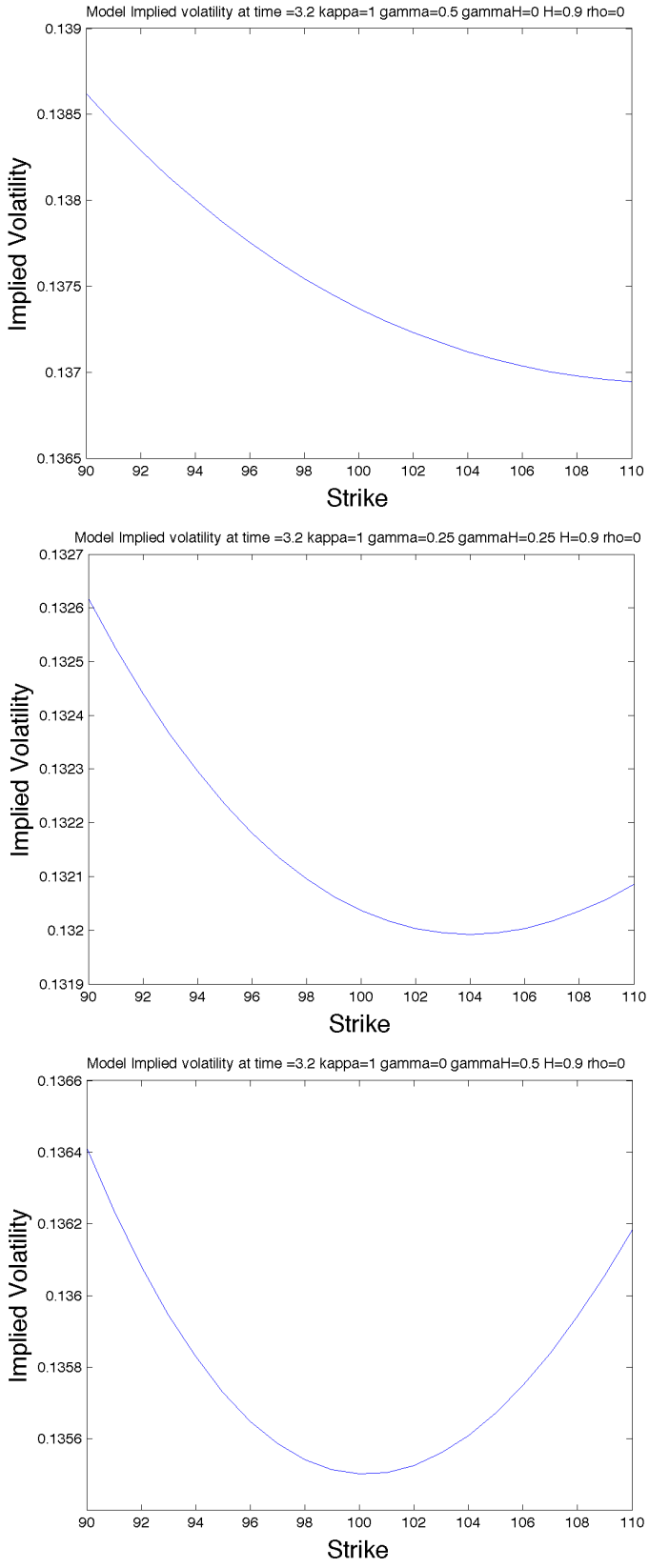

Figure 26: Implied Volatility Curve at $t = 3.2$, $\kappa = 1, \rho = 0$

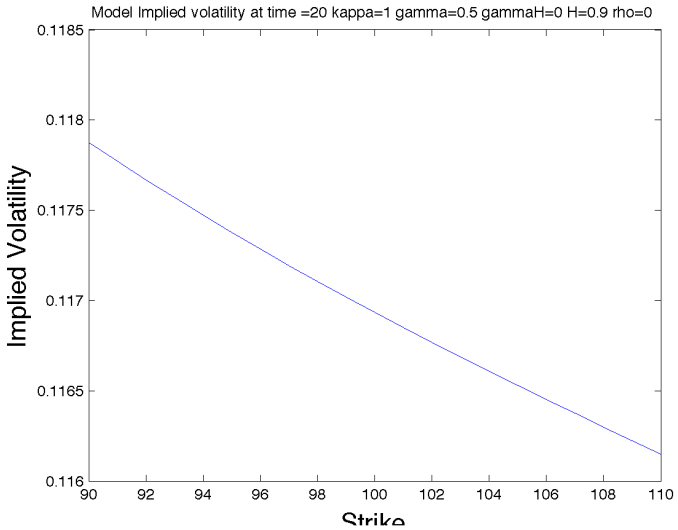

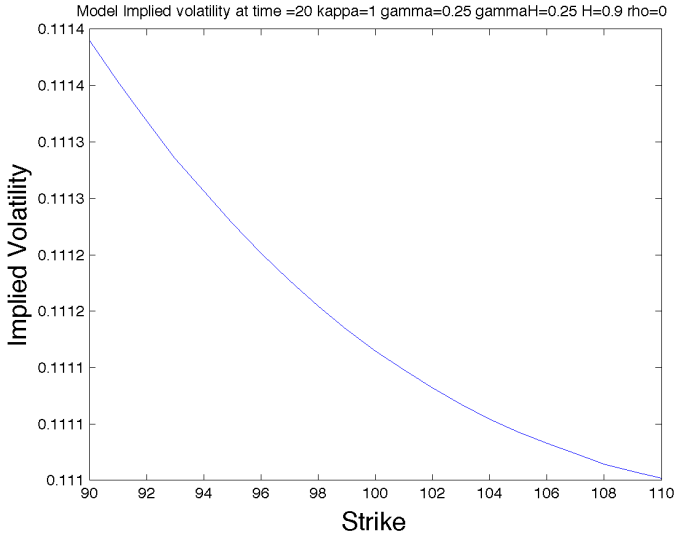

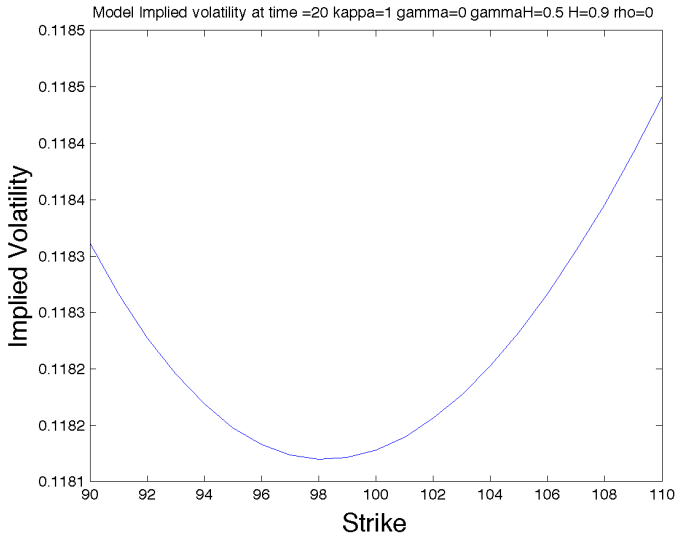

Figure 27: Implied Volatility Curve at $t = 20$, $\kappa = 1, \rho = 0$

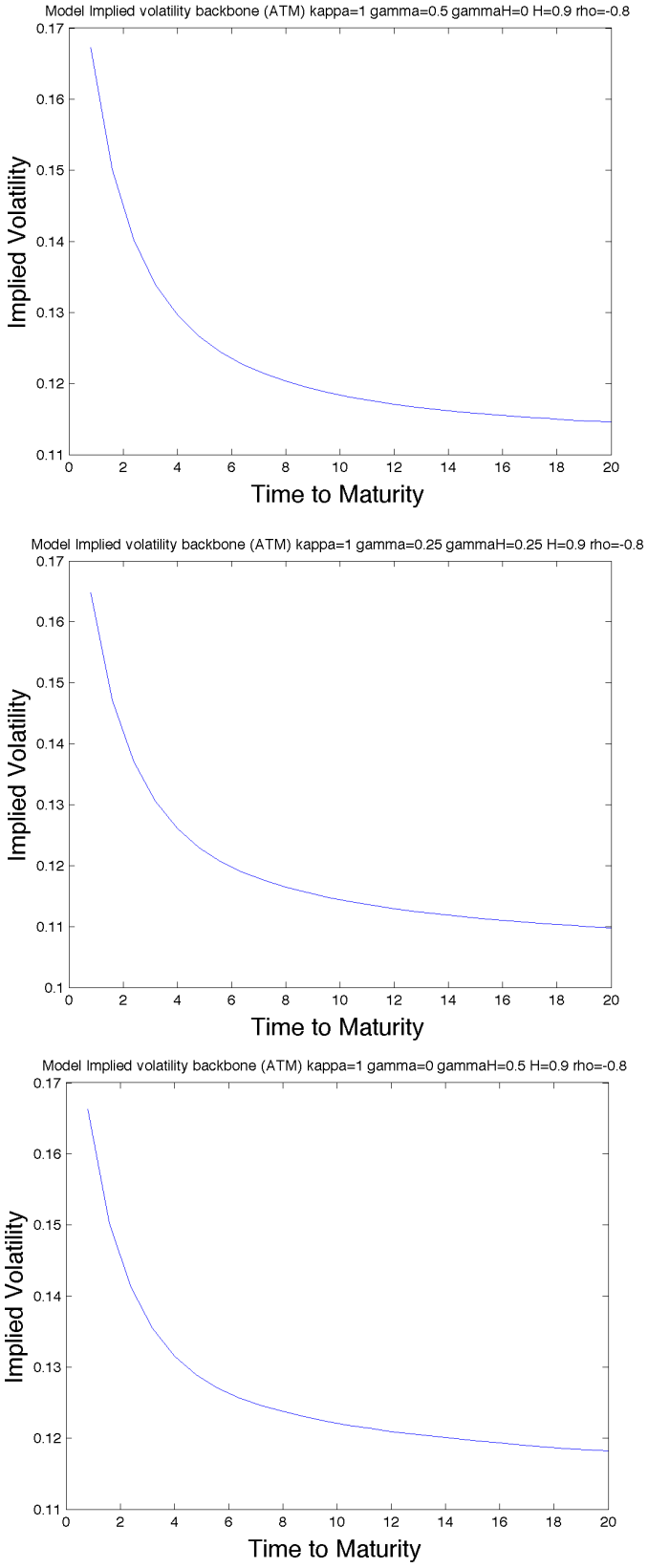

Figure 28: ATM Implied Volatility Curve (BackBone), $\kappa = 1, \rho = -0.8$

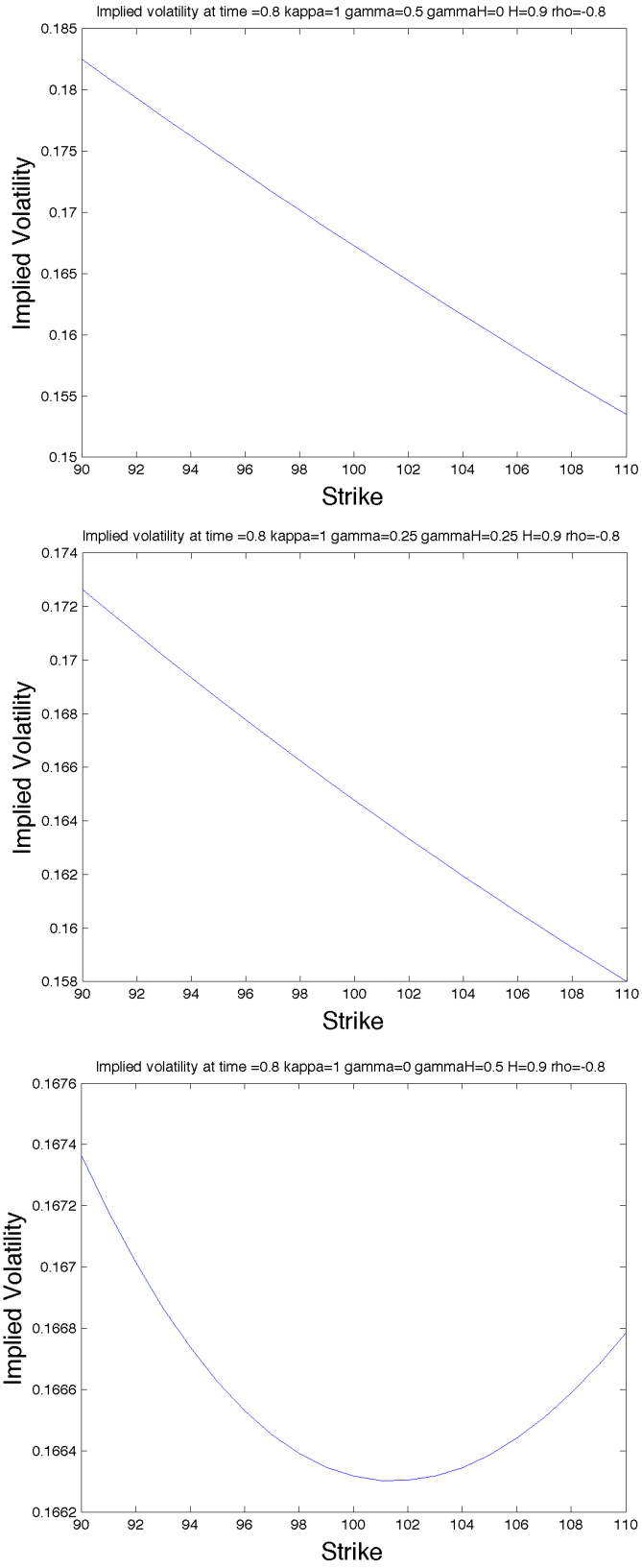

Figure 29: Implied Volatility Curve at $t = 0.8$, $\kappa = 1, \rho = -0.8$

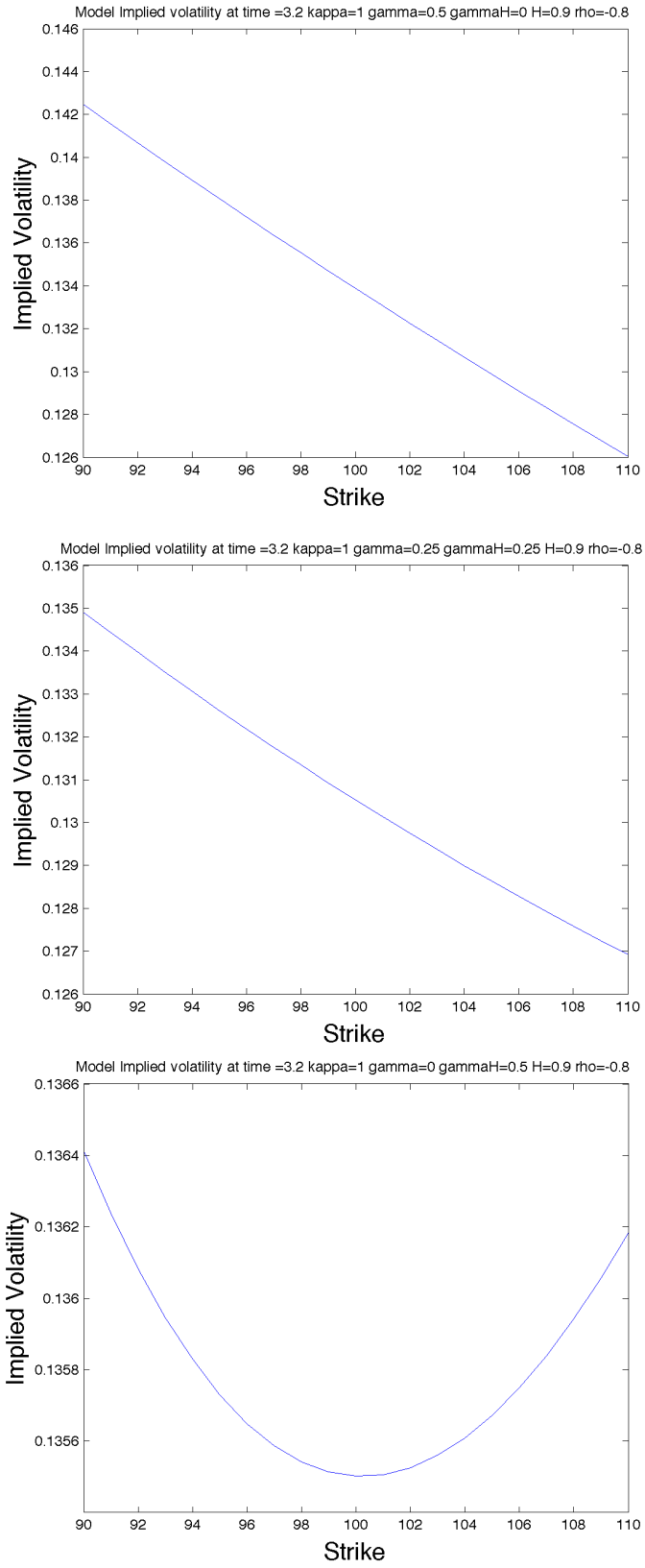

Figure 30: Implied Volatility Curve at $t = 3.2$, $\kappa = 1, \rho = -0.8$

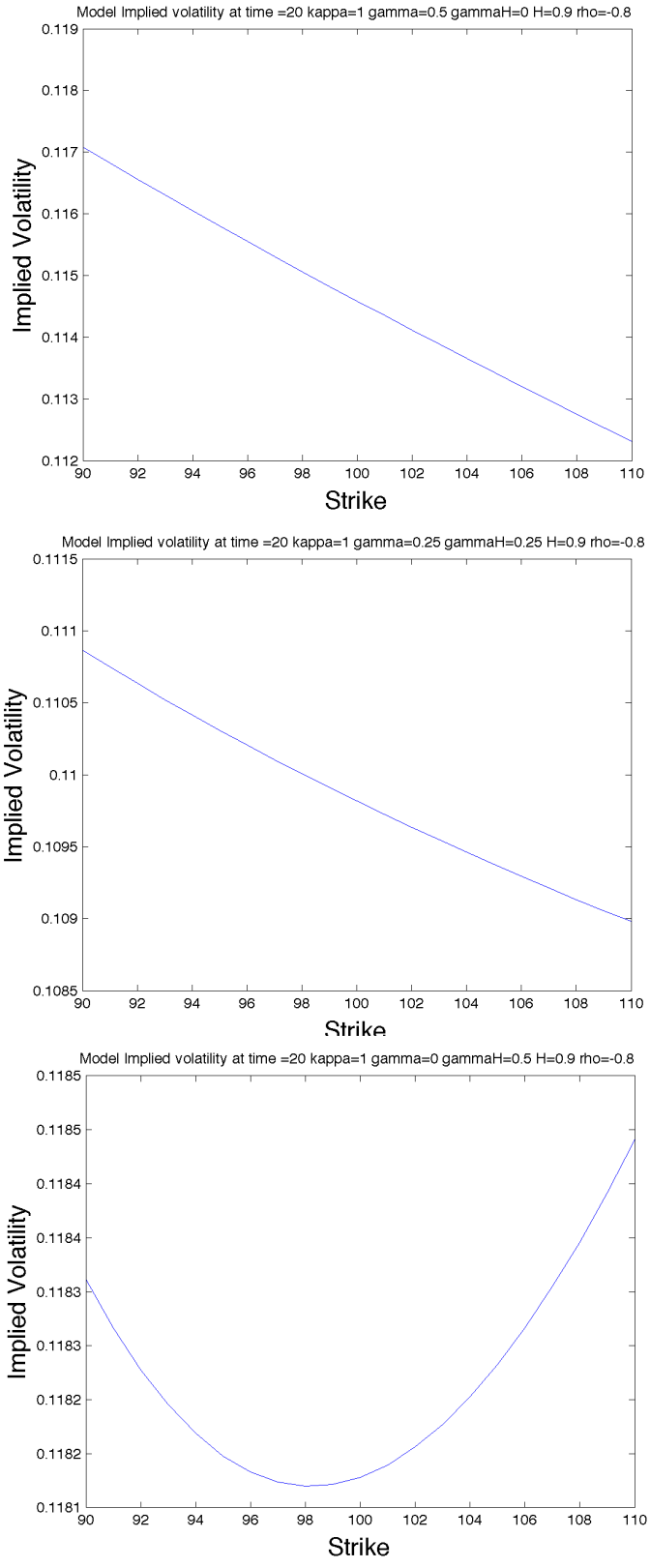

Figure 31: Implied Volatility Curve at $t = 20$, $\kappa = 1, \rho = -0.8$

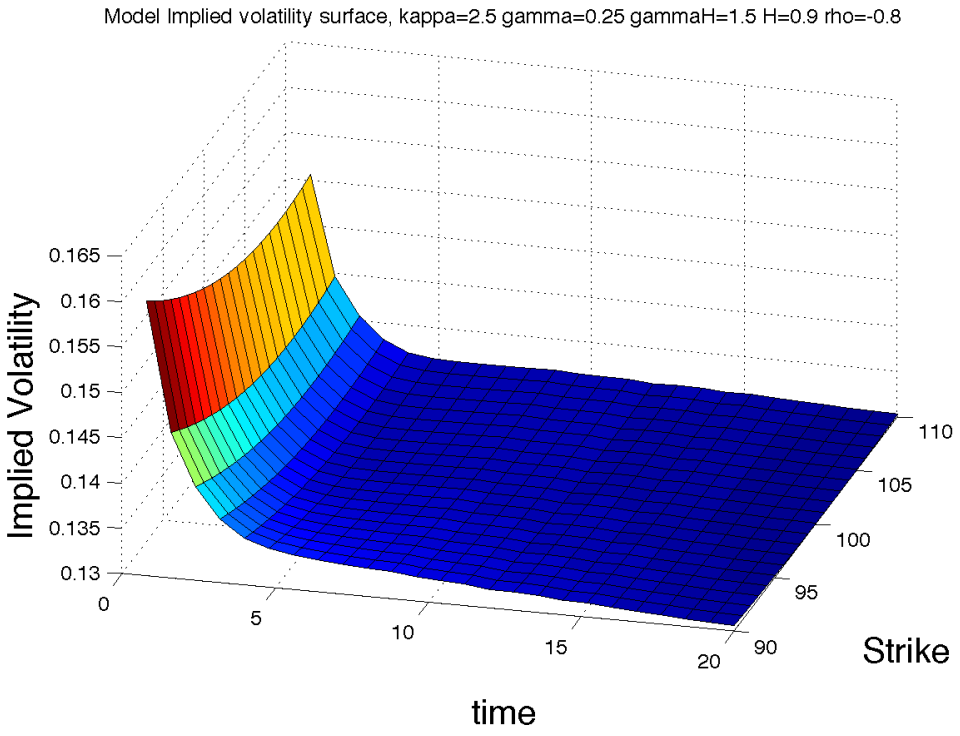

Figure 32: Model Implied Volatility Surfaces, $\kappa = 2.5, \rho = -0.8, \nu = 0.25, \nu^H = 1.5, H = 0.9$

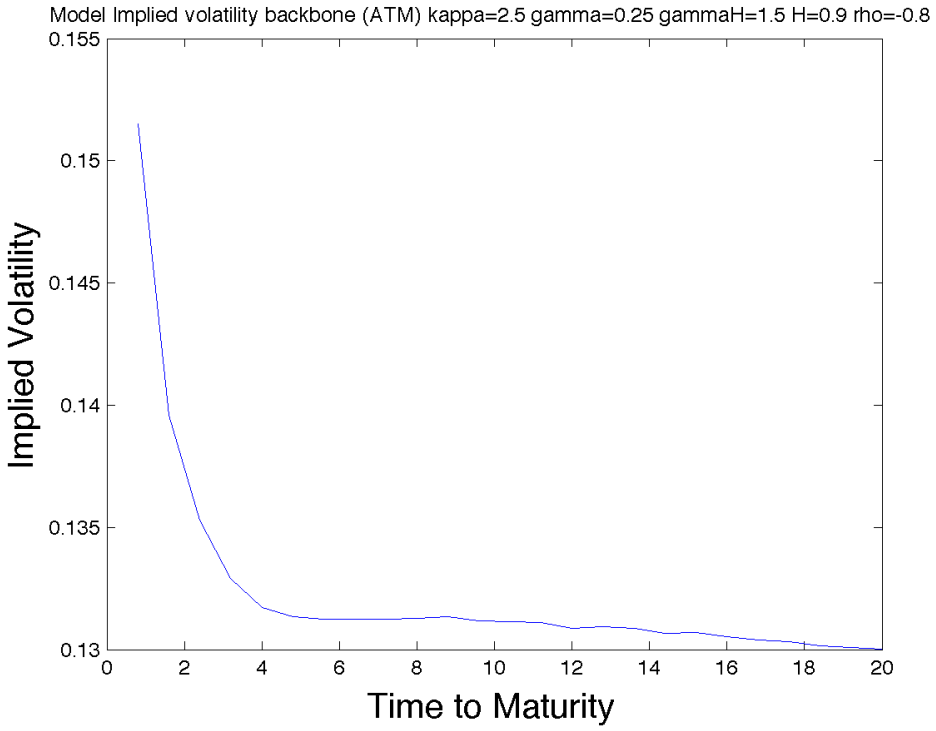

Figure 33: ATM Implied Volatility Curve (BackBone), $\kappa = 2.5, \rho = -0.8, \nu = 0.25, \nu^H = 1.5, H = 0.9$

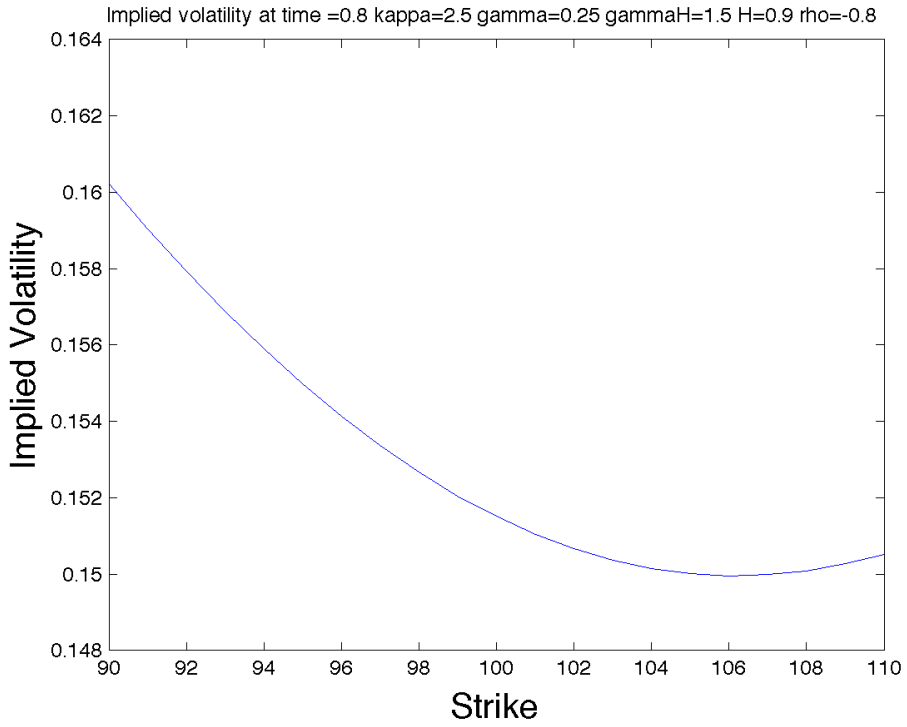

Figure 34: Implied Volatility Curve at $t = 0.8$, $\kappa = 2.5, \rho = -0.8, \nu = 0.25, \nu^H = 1.5, H = 0.9$

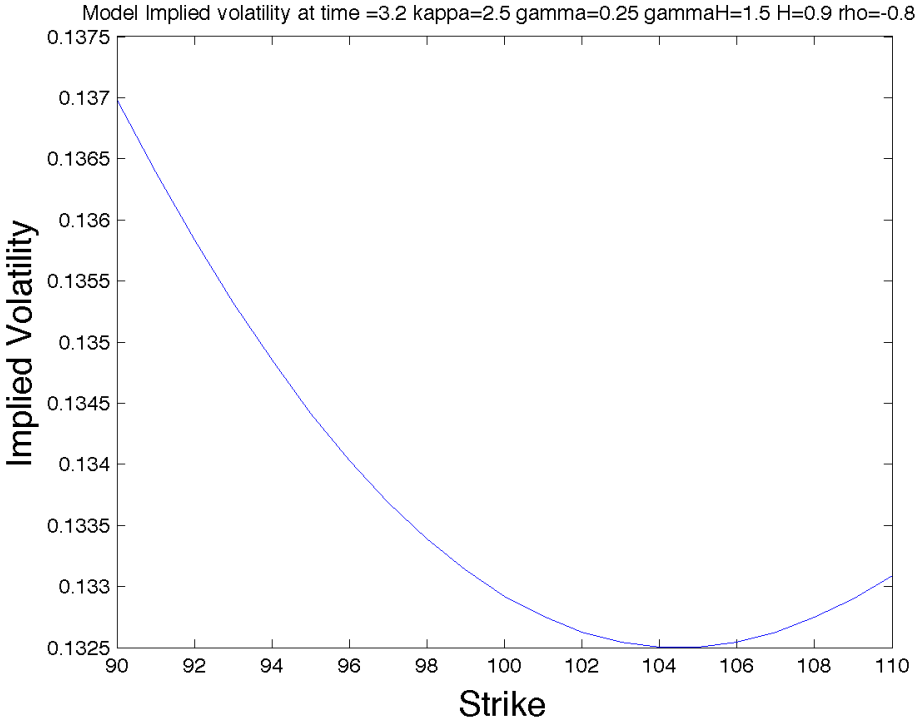

Figure 35: Implied Volatility Curve at $t = 3.2$, $\kappa = 2.5, \rho = -0.8, \nu = 0.25, \nu^H = 1.5, H = 0.9$

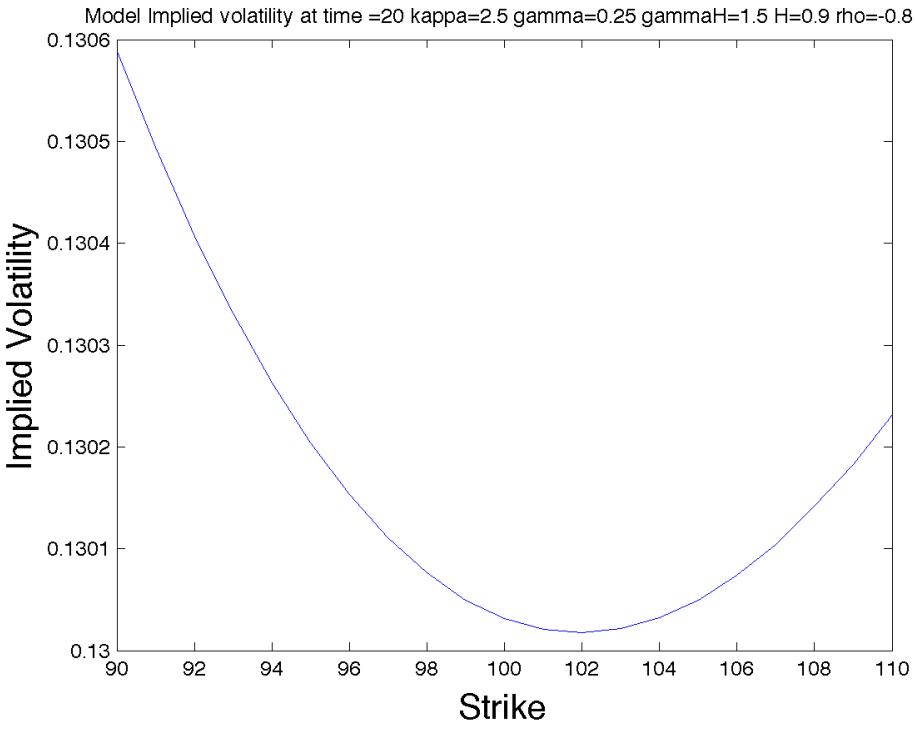

Figure 36: Implied Volatility Curve at $t = 20$, $\kappa = 2.5, \rho = -0.8, \nu = 0.25, \nu^H = 1.5, H = 0.9$

10 Calibration

In this section, using the call option pricing formula from (9.7), the parameters are calibrated to the SPX equity option market dated Jan 04, 2010. Here is the outline of the calibration scheme, of which the methodology is adapted from Christoffersen, Heston and Jacobs [CHJ09], and Cont, Tankov [CT04].

Proposition 10.1. Estimation Methodology

We have the structural parameter set $\Theta = \left\{\rho, \kappa, \theta, \nu, \nu^H, \sigma\left(0\right)\right\}$, and we seek the set of parameters that minimizes the sum of squared implied volatility difference between the model implied volatility and market implied volatility, i.e.:

$$\begin{aligned}\sum_{i=1}^{N}\left(\sigma_{\text{model}}^{\text{imp}}\left(T_i;\Theta\right)-\sigma_{\text{mkt}}^{\text{imp}}\right)^2 &\approx \sum_{i=1}^{N}\left(\left(\frac{\partial C_{BS}}{\partial\sigma}\bigg|_{\sigma=\sigma_{mkt}^{imp}}\right)^{-1}\left|C_{\text{model},T_i}\left(K;\Theta\right)-C_{BS,T_i}\left(K;\sigma_{\text{mkt}}^{\text{imp}}\right)\right|\right)^2 \\ &= \sum_{i=1}^{N}\frac{\left(C_{\text{model},T_i}\left(K;\Theta\right)-C_{BS,T_i}\left(K;\sigma_{\text{mkt}}^{\text{imp}}\right)\right)^2}{\left(\text{Vega}_{BS}\left(\sigma_{\text{mkt}}^{\text{imp}}\right)\right)^2} \qquad (10.1)\end{aligned}$$

Here C_{model,T_i} is the Model Call Price with maturity T_i given by equation (9.7), and C_{BS,T_i} and Vega_{BS} is the Black-Scholes Call option price and Black-Scholes Vega respectively.

One might notice, the Hurst index itself is excluded from the list of calibration, this is because every time the Hurst index is changed, the paths have to be completely re-simulated, and this is very time-consuming and not at all robust. Also it is observed in Figure 5 of [CV12], the produced Black-Scholes option prices are not sensitive to the change of Hurst indices, and in simulation Hurst index is shown to be non-simulation-robust as well. One way around this is to choose a fixed constant for the Hurst index, this is similar to the approach adopted by Multi-scale stochastic volatility models, where the 'fast' and 'slow' reversion are often hard to distinguish making it difficult to calibrate both directly, so instead, two mean reversion speeds are imposed through observation and macroeconomic argument. The effect of different Hurst indices on calibrated parameters is also observed.
There is also the problem of stability, it is undesirable to have parameters that is very sensitive to change of the market data, in order to find a relative stable parameter set, we follow the methodology in [CT04]: Suppose after the calibration according to (10.1), and nonlinear least-square method as the mean of optimization (for example, *lsqnonlin* package in Matlab), we have the structural parameter set Θ', i.e.

$$\Theta' = \arg\inf_{\Theta} \sum_{i=1}^{N} \left(\sigma_{\text{model}}^{\text{imp}} \left(T_i; \Theta \right) - \sigma_{\text{mkt}}^{\text{imp}} \right)^2 \tag{10.2}$$

Then ϵ_0^2 is the corresponding squared error for the model error:

$$\epsilon_0^2 = \sum_{i=1}^{N} \left(\sigma_{\text{model}}^{\text{imp}} \left(T_i; \Theta' \right) - \sigma_{\text{mkt}}^{\text{imp}} \right)^2 \tag{10.3}$$

Θ' is our *a prior* parameters set, and ϵ_α calculates the modified squared error function, given a regularization parameter $\alpha > 0$:

$$\epsilon_\alpha^2 \left(\Theta \right) = \sum_{i=1}^{N} \left(\sigma_{\text{model}}^{\text{imp}} \left(T_i; \Theta \right) - \sigma_{\text{mkt}}^{\text{imp}} \right)^2 + \alpha \left| \Theta - \Theta' \right|^2 \tag{10.4}$$

For some $\delta > 1$,(for example $\delta = 1.1$), through re-calibration:

$$\delta\epsilon_0 = \epsilon_\alpha \left(\Theta \right)$$

Results in a more data-stable parameter set Θ . The idea is to seek a slightly perturbed parameter set that is not 'too far' from the *a prior* parameter set that still numerically produce error term that is close to the model error, i.e.: $\epsilon_0 \approx \epsilon_\alpha \left(\Theta \right)$. This also has to do with such a high-dimensional parameter space, the squared-error function is not necessarily convex, so the optimization might lead several local minimum based on the initial guess, so we penalize the optimization if it stray too far from the *a prior* parameters.

Since there are 6 parameters with different sensitivities, it is hopeless to try to calibrate all of them simultaneously. So instead, the calibration process is dissected into three steps:

Given an initial guess for the parameters $\left\{\rho, \kappa, \theta, \nu, \nu^H, \sigma\left(0\right)\right\}$, and a given Hurst index H:

1. "Backbone": calibrate $\left\{\kappa, \theta, \nu, \sigma\left(0\right)\right\}$ with the ATM options.
2. "Skewness": calibrate $\left\{\rho, \nu\right\}$ while fixing the $\left\{\kappa, \theta, \nu, \sigma\left(0\right)\right\}$ from Step 1 constant.
3. "Overall": calibrate all the parameters $\left\{\rho, \kappa, \theta, \nu, \nu^H, \sigma\left(0\right)\right\}$

Testing multiple Hurst indices, against the following optimized parameters:

Table 1: Parameters Calibrated to Jan 4, 2012 SPX Options

	ρ	κ	θ	ν	ν^H	H	$\sigma\left(0\right)$	Residual(ϵ)
Initial Guess	-0.9281	9.7532	0.2160	1.5907	0.00	0.5	0.1408	-
$H = 0.75$	-0.8155	4.1613	0.2022	1.4689	0.5489	0.75	0.1685	5.5593×10^{-5}
$H = 0.90$	-0.7826	4.0917	0.2011	1.5001	0.3778	0.90	0.1681	5.6884×10^{-5}
$H = 0.975$	-0.7852	4.2168	0.2028	1.5109	0.3335	0.975	0.1677	5.7050×10^{-5}

There are several observation that can be deduced from the optimized parameter set:

i. The correlation coefficient decreases as the effect of long-memory increases (Hurst index goes up), this can be explained that the longer maturity smile effects are partially captured by the volatility persistence, and higher the Hurst index, more effective this becomes.

ii. Reversion speed is roughly halved, because of the volatility persistence kicks in and produce a trough at the ATM-backbone, making the corresponding κ necessary to fit the backbone lower.

iii. As the Hurst index increase, the fitted fractional vol-of-vol decreases, as it was explained before, the long-maturity volatility smile increases in prominence along the Hurst index, and the necessary fractional vol-of-vol to capture this lowers.

We decided to compare the case for $H = 0.9$ by pricing the option prices and implied volatility surfaces based on the parameter given in table 1:

Table 2: Market and Calibrated Market Call Options on Jan 04, 2010, $H = 0.9$, $S_0 = 1132.99$

K/S_0	0.8	0.9	0.95	0.975	1	1.025	1.05	1.1	1.25
$C_{\text{Model},T=0.25}$	231.05	127.5496	82.0461	62.0529	44.4591	29.698	18.1045	4.4659	0.3274
$C_{\text{Mkt},T=0.25}$	230.9365	128.6257	82.7271	62.4855	44.7733	30.056	18.6545	5.4549	0.2353
$\sigma^{\text{imp}}_{\text{Model},T=0.25}$	0.2929	0.2431	0.2191	0.2074	0.1958	0.1844	0.1732	0.151	0.1563
$\sigma^{\text{imp}}_{\text{Mkt},T=0.25}$	0.2911	0.2504	0.2225	0.2094	0.1972	0.186	0.1759	0.1598	0.1501
$C_{\text{Model},T=1}$	261.6978	174.9606	136.9637	119.5477	103.278	88.2185	74.4253	50.7941	19.2869
$C_{\text{Mkt},T=1}$	263.8868	176.3388	137.7263	120.0143	103.4697	88.1761	74.2328	50.527	19.6906
$\sigma^{\text{imp}}_{\text{Model},T=1}$	0.2724	0.2474	0.2353	0.2294	0.2236	0.2178	0.2122	0.2012	0.181
$\sigma^{\text{imp}}_{\text{Mkt},T=1}$	0.2801	0.2509	0.2371	0.2305	0.224	0.2177	0.2117	0.2006	0.1823
$C_{\text{Model},T=2}$	304.4254	227.0084	192.5325	176.4223	161.0847	146.532	132.7737	107.6624	67.0026
$C_{\text{Mkt},T=2}$	307.1073	227.5601	191.8026	175.0455	159.0698	143.911	129.5939	103.5269	61.8525
$\sigma^{\text{imp}}_{\text{Model},T=2}$	0.2655	0.2497	0.2423	0.2387	0.2352	0.2317	0.2283	0.2216	0.209
$\sigma^{\text{imp}}_{\text{Mkt},T=2}$	0.2714	0.2507	0.2411	0.2365	0.2319	0.2276	0.2233	0.2151	0.2002

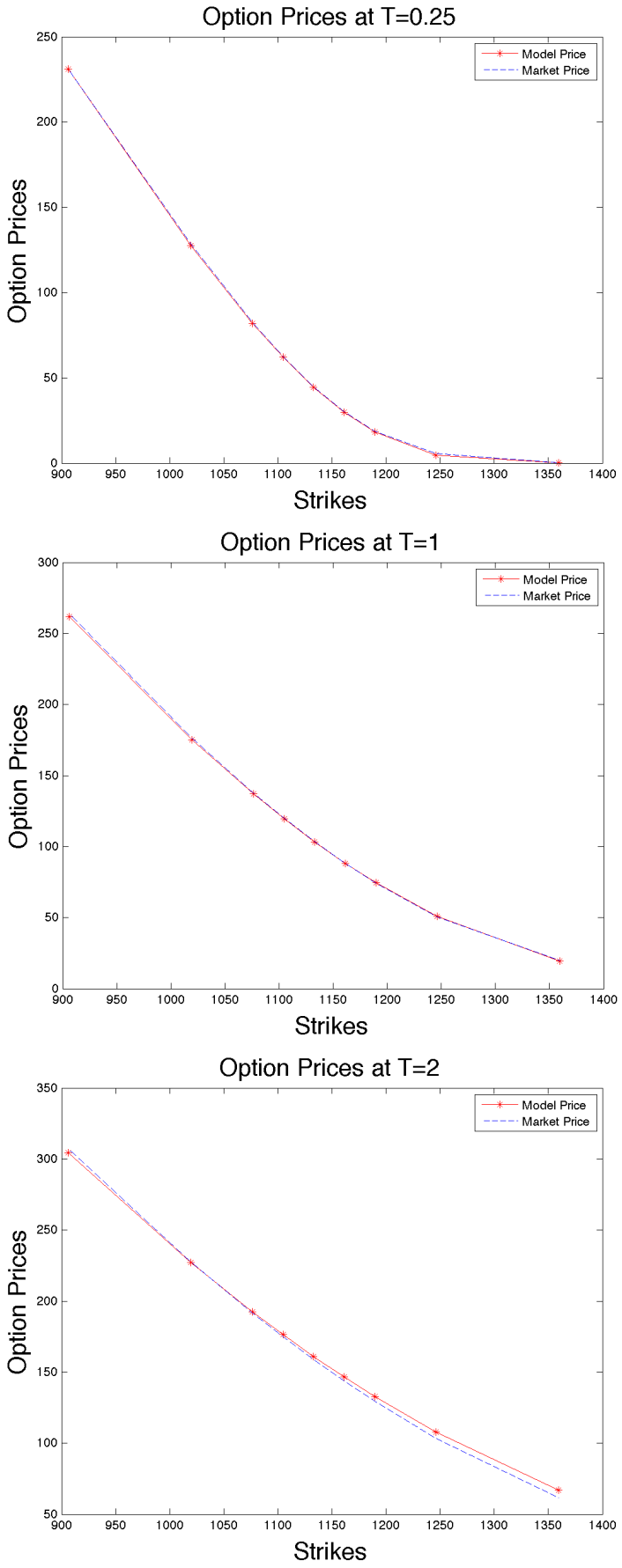

Figure 37: Market and Calibrated Option Prices, $H = 0.9$, for Jan 04, 2010 SPX options

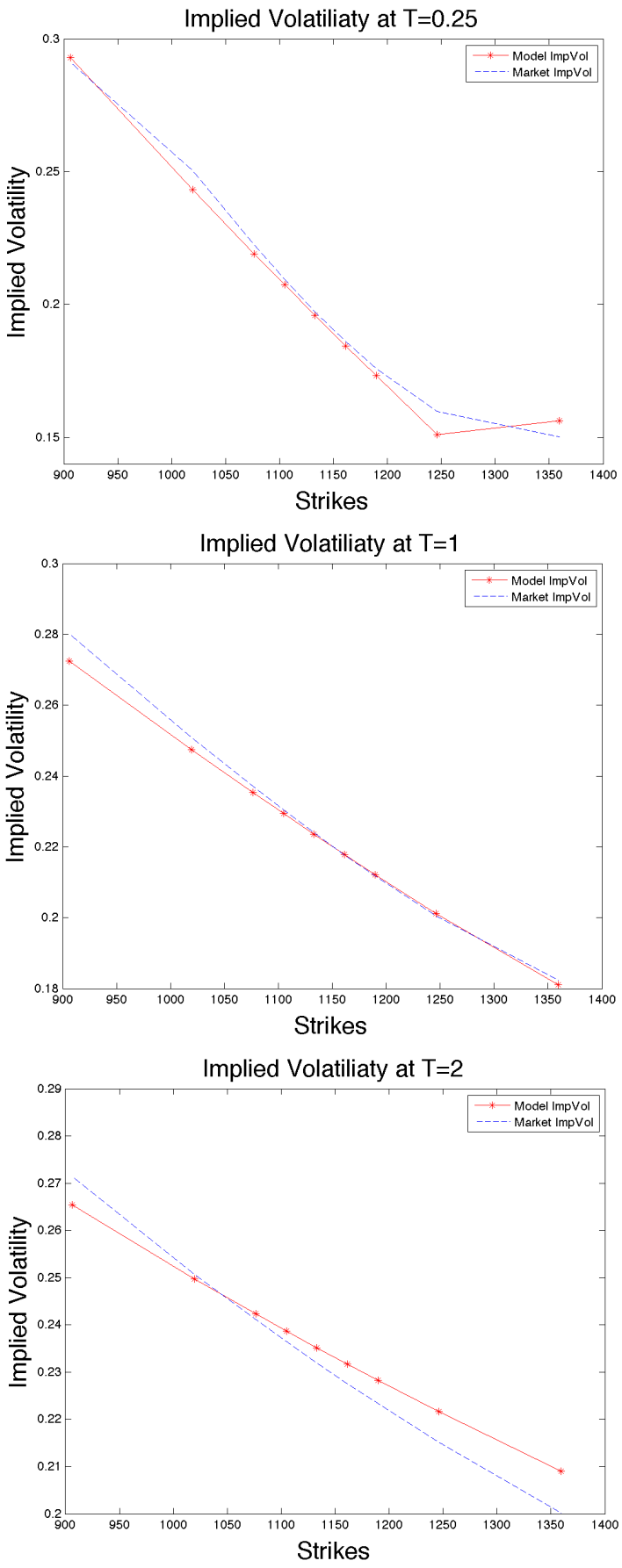

Figure 38: Market and Calibrated Implied Volatility, $H = 0.9$, for Jan 04, 2010 SPX options

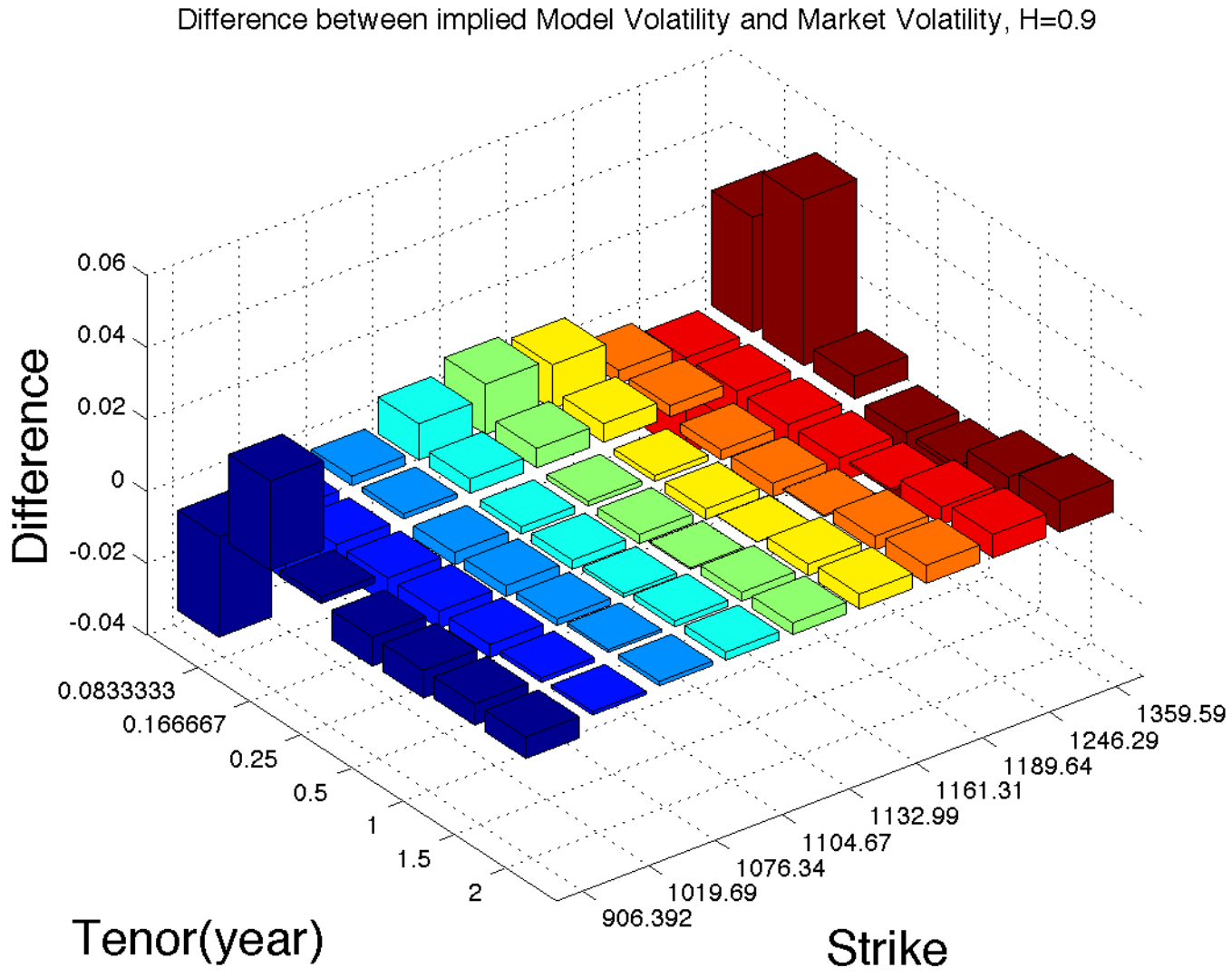

Figure 39: Difference between Model and Market Implied Volatility, $H = 0.9$, for Jan 04, 2010 SPX options

From the bar-chart in Figure 39, it can be seen that for the longer maturity the calibrated model is a pretty good fit for the implied volatility surface, but the very close-to-expiration $\left(T = \frac{1}{12}\right)$ with strikes far away from the spot, there is a significant discrepancy between the model and market implied volatility. This can be explained by the lowered correlation coefficient after the introduction of the fractional stochastic volatility term after the overall calibration. Bear in mind that we only have a constant correlation term, so after adjusting to options that are not close to maturities $(T \geq 0.25)$, which have smaller skewness due to the temporal aggregation, then the skewness from the implied volatility curve that is very close to maturity will not be as adequately accounted for. This is not a major concern of our model, since it is our goal to capture the long-term phenomenon of the volatility surface.

In order to capture all the stylized features observed on the volatility surface, one might have to resort to multi-scale models, distinguishing the long and short term factors in the model. But incorporating fractional Brownian motion in such a multi-factor model will significantly complicates the problem. One easier fix to this problem, is instead of a constant correlation coefficient, one can impose a time-dependent correlation coefficient: $\rho_t = \alpha e^{-\beta t} + \xi$, where $\alpha + \xi$ is the initial correlation level and approaches to ξ with exponential rate β. But even with such simple modification we will need to revamp the whole derivation of the model, so unless one's position is significantly exposed to both short and long term volatility Greeks, our model is more than adequate for a large variety of scenarios.

There are more to note about the calibration scheme, as mentioned before, since the calibration squared error function is unlikely to be convex across the parameters space, one can end up in different calibrated parameters set based on the initial parameter guess, nevertheless, with reasonable upper and lower bound of the parameters, one should be able to find a set of parameters that minimize the squared error with respect to the choice of option sets, i.e., if one wish to calibrate to options with longer maturity, one should not be too concern with the very-close-to-maturity options, in that case, one of the choice is to not calibrate to the options with short maturities. Or if one is inclined to price variance or volatility swap, then options that are not ATM are of little importance. It is a fool's errand to try and find the holy grail of model that will fit to every single stylized phenomenon in market data, and one should only strive for model that fits the particular problem at hand, this rings true in calibration as well.

11 Conclusion

Motivated by the inadequacy in capturing long-dependence feature in volatility process of the traditional stochastic volatility framework, the possibility of fractional Brownian motion (fBM) in financial modeling and various schemes of the Monte Carlo simulation is explored. Starting from the general definition, fBM can be considered as an extension of the ordinary Brownian motion with an autocovariance function that depends on both time indices instead of just the minimum between the two. With different values of Hurst index, we can distinguish fractional Brownian motion into three different cases: $H < 1/2, H = 1/2$ and $H > 1/2$. For only $H > 1/2$ displays a long-dependence behavior, that is the only case considered.

Several prominent examples of fBM in financial modeling are given in chapter 3. Simulation schemes are divided into the exact schemes and approximate schemes in chapter 4 and 5. While the former will capture the complete structure for the whole length of sample size, the latter either approximates the value of the real realization or truncates the covariance structure for robustness. We start with the exact scheme of Hosking algorithm that utilizes the multivariate Gaussian distribution of fractional Gaussian noises and simulates the sample points conditioned on the previous samples. Alternatively, instead of simulating each conditioned on the past sample points, we can first construct the covariance matrix of the size of the sample we want, and proceed to find the 'square root' of the covariance matrix and multiply with a standard normal variable vector, for which the product vector will be the fractional Gaussian noise (fGn) with exact covariance structure as the covariance matrix. To find the 'square root', we first investigate the Cholesky decomposition, but the computational and memory expense is too large to be feasible in practice. In contrast, fast Fourier transform (FFT) simulation embeds the original covariance matrix in a larger circulant matrix and simulates by diagonalizing the circulant matrix into the product of eigenvalue matrix and unitary matrix. The FFT method is significantly more robust than the previous schemes.

We then look into the approximate schemes; namely the construction of fBM with correlated random walks, which can be viewed as an extension of construction of Brownian motion with ordinary random walk. This method gives us interesting insight into the true working of fBM, especially the idea of long-range dependence. This approach is not only interesting and easy to implement, but also the error can be calculated explicitly. The drawback of this approach is that the speed slows down significantly with large sample points, and the trade-off is made based on the error function. The last simulation approach we look at is the conditional random midpoint displacement (RMD) scheme, which is mathematically similar to the Hosking scheme, but with fixed number of past sample points it conditions on. The on-the-fly version of RMD scheme can indefinitely generate sample points with given resolution. Finally, we include the spectral method for approximating fBM. Comparing all the schemes and also referring the studies done in [NMW99], we conclude that if the time-horizon is known beforehand, the FFT/spectral schemes would be the best scheme due to the high speed and accuracy. Alternately, if samples should be generated indefinitely, the on-the-fly conditioned RMD scheme seems to offer similar level of accuracy and speed as the FFT scheme.

Instead of the usual definition of fBM as in [MVN68], the truncated version of fBM proposed in [CR96], [CR98] is also investigated in chapter 6, which is generally not equivalent to the fBM, but it retains some important features such as self-similarity and long-range dependence for $H > 1/2$. The volatility process that is driven by a fractional-OU process is included as an example, numerical result shows that the truncated fBM is not robust enough for pricing purpose. In chapter 7, discoveries are made through full simulation of the fBM driven Stochastic volatility process: even if correlation between the asset

and volatility process is imposed, it would not affect the skewness of the implied volatility surface, this fact is further supported by E.Alos's work by Malliavin Calculus in the paper [ALV07]. So we propose the mixture-fBM model, which has both the ordinary Brownian motion and the fractional Brownian motion in the stochastic volatility process. Due to the high dimensional nature of the process, it is quite uneconomical to simulate all 3 dimensions for option pricing purpose. With the help of the approximation scheme provided in chapter 8, provided by my colleague Funahashi in [Fun12], it is possible to reduce the simulation dimension to just the fractional Brownian motion, resulting in a robust simulation-based-approximation scheme as outlined in chapter 9. Numerical result from the robust simulation scheme shows that the volatility smile effect arises from the introduction of fractional Brownian motion indeed become obvious along the time-to-maturity, it pertains the curvature of the volatility curve, giving us extra freedom when it comes to modeling.

In chapter 10, the calibration aspect of the model is explored, based on the calibration methodology outlined in [CHJ09], [CT04], this is made possible given the robust nature of the simulation scheme, a multi-stage calibration scheme with stabilized parameter set is outlined. The relationship between Hurst indices and the calibrated parameters is also explored and discussed. Concluded by the comparing the implied volatility surface given by the calibrated parameters and the market prices, and discuss the strength and shortcoming of the proposed model.

The future prospect of the research on fractional Brownian motion includes exploring for the possibility of a fully explicit approximation scheme. As well as the effect on the change of measure on the Hurst index: estimating the Hurst index with econometric tools such as R/S statistics is considered as estimation under the statistical measure, while option prices based calibration recovers the risk-neutral Hurst index. A possible linkage between the two calibrated indices will greatly enrich the analytical literature on the topic.

Acknowledgments: I wish to express our gratitude to Professor Alex Novikov for sharing relevant research materials with us, and Professor Bernt Øksendal and Professor Enriquez Nathanaël for interesting discussions and remarks. And many thanks to Professor Masaaki Kijima for providing guidance and opportunities. And this research is made available by the generous support from Asian Human Resource Fund by Tokyo Metropolitan University.

A Defining fractional Brownian motion with M-operator

This is similar to the idea of constructing Brownian motion with fractional integration. Or can be written succinctly in terms of M-operator introduced by Biagini, Oksendal [BHOZ08], where we introduce briefly here, and later show that it coincide with the definition put forth by Bender [Ben03]:

Definition A.1.

$$\widehat{Mf}(y) = |y|^{1/2-H} \widehat{f}(y), \qquad y \in \mathbb{R}$$

where

$$\widehat{g}(y) \coloneqq \int_{\mathbb{R}} e^{-ixy} g(x)\, dx$$

Denotes the Fourier transform.

For $0 < H < 1$

$$Mf(x) = -\frac{d}{dx} \frac{C_H}{(H-1/2)} \int_{\mathbb{R}} (t-x) |t-x|^{H-3/2} f(t)\, dt$$

where

$$C_H = \left\{ 2\Gamma\left(H - \frac{1}{2}\right) \cos\left[\frac{\pi}{2}\left(H - \frac{1}{2}\right)\right] \right\}^{-1} \left[\Gamma(2H+1) \sin(\pi H)\right]^{\frac{1}{2}}$$

Here $\Gamma(\cdot)$ denotes the classical gamma function.

For the case we are interested in:

Definition A.2.
Particularly, for $\frac{1}{2} < H < 1$

$$Mf(x) = C_H \int_{\mathbb{R}} \frac{f(t)}{|t-x|^{3/2-H}} dt$$

And if $H = \frac{1}{2}$, then

$$Mf(x) = f(x)$$

Also

$$\|f\|_H \coloneqq \|Mf\|_{L^2(\mathbb{R})}$$

And the inner product on this space is:

$$\langle f, g \rangle_H = \langle Mf, Mg \rangle_{L^2(\mathbb{R})}$$

Define

$$M\mathbf{1}_{[0,t]}(x) \coloneqq M[0,t]\, x$$

For the indicator function$\mathbf{1}_{[a,b]}(x)$, for $a < b$

$$M[a,b](x) = \frac{\left[\Gamma(2H+1)\sin(\pi H)\right]^{1/2}}{2\Gamma(H+1/2)\cos\left[\pi/2\,(H+1/2)\right]} \left[\frac{b-x}{|b-x|^{3/2-H}} - \frac{a-x}{|a-x|^{3/2-H}} \right]$$

This was calculated by applying the direct definition of the M-operator on the indicator function.

Theorem A.1.
With Parseval's Theorem, we know

$$\begin{aligned}\int_{\mathbb{R}}\left[M\left[a,b\right]\left(x\right)\right]^{2}dx &= \frac{1}{2\pi}\int_{\mathbb{R}}\left[\widehat{M\left[a,b\right]}\left(\xi\right)\right]^{2}d\xi \\ &= \frac{1}{2\pi}\int_{\mathbb{R}}\left|\xi\right|^{1-2H}\frac{\left|e^{-ib\xi}-e^{-ia\xi}\right|^{2}}{\left|\xi\right|^{2}}d\xi \\ &= \left(b-a\right)^{2H}\end{aligned}$$

Here we have applied the fact that, the Fourier transform of the indicator function has the following expression:

$$\widehat{\mathbf{1}\left[a,b\right]}\left(\xi\right)=\frac{\left[e^{-ib\xi}-e^{-ia\xi}\right]}{-i\xi}$$

Since $M\left[s,t\right]=M\left[0,t\right]-M\left[0,s\right]$ for $s<t$, by polar-identity

$$\int_{\mathbb{R}}M\left[0,t\right]\left(x\right)M\left[0,s\right]\left(x\right)dx=\frac{1}{2}\left(\left|t\right|^{2H}+\left|s\right|^{2H}-\left|t-s\right|^{2H}\right)$$

And this coincides with the autocovariance structure from the beginning of the paper.

Theorem A.2.
Furthermore, from the paper it is shown that:

$$\begin{aligned}E\left[B^{H}\left(s\right)B^{H}\left(t\right)\right] &= \int_{\mathbb{R}}M\left[0,s\right]\left(x\right)M\left[0,t\right]\left(x\right)dx \\ &= \frac{1}{2}\left(\left|t\right|^{2H}+\left|s\right|^{2H}-\left|s-t\right|^{2H}\right)\end{aligned}$$

Finally we have the following theorem:

Theorem A.1.

$$\int_{\mathbb{R}}f\left(t\right)dB^{H}\left(t\right)=\int_{\mathbb{R}}Mf\left(t\right)dB\left(t\right),\qquad f\in L_{H}^{2}\left(\mathbb{R}\right)$$

It's easy to see:

$$B^{H}\left(t\right)=\int_{\mathbb{R}}M_{H}\left[0,t\right]\left(u\right)dB\left(u\right)$$

Here $M_{H}\left[\cdot,\cdot\right]$ is the M-transformed Indicator function on region $\left[0,t\right]$ with Hurst-index H,

Conversely, we have:

Lemma A.1.

$$B\left(t\right)=\int_{\mathbb{R}}M_{1-H}\left[0,t\right]\left(u\right)dB^{H}\left(u\right)$$

Remark: The M-operator can be succintly written in terms of fractional integration:

$$M_H f = K_H I_-^{H-1/2} f, \qquad \text{for } \frac{1}{2} < H < 1$$

where $I_-^{H-1/2}$ is a fractional integration to the order of $H - 1/2$, and $K_H \equiv \Gamma\left(H + \frac{1}{2}\right)\left(\int_0^\infty \left((1+s)^{H-1/2} - s^{H-1/2}\right) ds + \frac{1}{2H}\right)^{-1/2}$ is the normalizing constant. This definition coincide with Comte, Renault's if the process is defined only on $[0, t]$. Indeed, Bender [Ben03] shows that the M-operator, or the stochastic integration with respect to a fractional Brownian motion can be succintly concluded by the notion of fractional integration:

The M-operator can be rewritten in the notation of fractional calculus such as:

Definition A.3.

$$M_\pm^H f \equiv \begin{cases} K_H D_\pm^{-(H-1/2)} f & \text{for } 0 < H < \frac{1}{2} \\ f & \text{for } H = \frac{1}{2} \\ K_H I_\pm^{H-1/2} f & \text{for } \frac{1}{2} < H < 1 \end{cases} \tag{A.1}$$

Here $I_\pm^\alpha,\ 0 < \alpha < 1$, is the fractional integral of Weyl's type, defined as:

$$\begin{aligned} \left(I_-^\alpha f\right)(x) &:= \frac{1}{\Gamma(\alpha)} \int_x^\infty f(t)(t-x)^{\alpha-1} dt \\ \left(I_+^\alpha f\right)(x) &:= \frac{1}{\Gamma(\alpha)} \int_{-\infty}^x f(t)(t-x)^{\alpha-1} dt \end{aligned} \tag{A.2}$$

And $D_\pm^\alpha$ is the fractional derivative of Marchaud's type $(\epsilon > 0)$

$$\left(D_{\pm,\epsilon}^\alpha f\right)(x) := \frac{\alpha}{\Gamma(1-\alpha)} \int_\epsilon^\infty \frac{f(x) - f(x \mp t)}{t^{1+\alpha}} dt$$

and

$$\left(D_\pm^\alpha f\right)(x) := \lim_{\epsilon \downarrow 0+} \left(D_{\pm,\epsilon}^\alpha f\right)$$

So that,

Theorem A.3.

$$B_t^H = \int_{\mathbb{R}} \left(M_-^H \mathbf{1}_{[0,t]}\right)(s)\, dB_s \tag{A.3}$$

and

$$\int_0^t f(s)\, dB_s^H = \int_{\mathbb{R}} \left(M_-^H \left(\mathbf{1}_{[0,t]} f\right)\right)(s)\, dB_s \tag{A.4}$$

Theorem A.4. (fractional integration-by-parts)

As shown in [Ben03], under some mild assumption. There is the related integration-by-parts relationship for fractional integrations:

$$\int_{\mathbb{R}} f(s) \left(M_-^H g\right)(s)\, ds = \int_{\mathbb{R}} \left(M_+^H f\right)(s)\, g(s)\, ds \tag{A.5}$$

B Conditional Distribution of exponential-fractional-OU volatility process

B.1 Conditional Distribution

Since we impose the exponential-OU process structure, it is easy to see that the volatility has a log-normal distribution, from the probability distribution function where the long-term mean is

$$e^{\theta+0.5Var(X_T)}$$

In order to arrive at a particular long-term mean, it is necessary to calculate this value explicitly, it is quite involved for a fractional Brownian motion drive process X_T, we outline the calculation put forth by Pipiras and Taqqu [PT01]. This procedure is not necessary within our option-pricing framework, since the parameters $\sigma(0)$ and κ are calibrated against the market data instead of having a hard-set target. We included the methodology here for completion sake.

B.1.1 Fractional Riemann-Liouville Integral

In order to understand the theoretical calculation involves the fractional Brownian motion, it is necessary to introduce the notion of the fractional Riemann-Liouville integral, where the fractional derivative slightly different from the definition from the previous appendix. Following the work of Pipiras and Taqqu [PT00], [PT01], we choose the Riemann-Liouville integral, which is defined in the compact interval $[0, T]$, for some $T > 0$, a finite time horizon and in order to be consistent with the paper we will be citing, we have the following Hurst index notation: $\kappa = H - \frac{1}{2}$, and we are only interested in the case $\kappa > 0$, displaying long-range dependence. For some $f \in L^2(\mathbb{R})$, we have the Riemann-Liouville integral

Definition B.1.

$$(I^{\kappa}_{T-}f)(s) = \frac{1}{\Gamma(\kappa)}\int_s^T f(r)(r-s)^{\kappa-1}dr, \qquad 0 \le s \le T$$

This integral that always exists if $f \in L^2(\mathbb{R})$.
And it has the fractional derivative which is the counterpart of the fractional integral

$$(D^{\kappa}_{T-}g)(u) = -\frac{1}{\Gamma(1-\kappa)}\left(\frac{g(u)}{(T-u)^{\kappa}} + \kappa\int_u^T \frac{g(u)-g(s)}{(s-u)^{\kappa+1}}ds\right), \qquad 0 < u < T$$

Similar to ordinary calculus, we have the following equality: $I^{-\kappa}_{T-} = D^{\kappa}_{T-}$

Theorem B.1. (fractional Brownian motion integrand space)
The following space of possible integrand has been introduced for $\kappa \in (0, \frac{1}{2})$:

$$\Lambda_T^\kappa := \left\{ f : [0,T] \to \mathbb{R} \left| \int_0^T \left[s^{-\kappa} I_{T-}^\kappa \left((\cdot)^\kappa f(\cdot) \right)(s) \right]^2 ds < \infty \right. \right\}$$

for $f, g \in \Lambda_T^\kappa$, define the scalar product

$$\langle f, g \rangle_{\kappa,T} := \frac{\pi\kappa(2\kappa+1)}{\Gamma(1-2\kappa)\sin(\pi\kappa)} \int_0^T s^{-2\kappa} \left[I_{T-}^\kappa \left((\cdot)^\kappa f(\cdot) \right)(s) \right] \left[I_{T-}^\kappa \left((\cdot)^\kappa g(\cdot) \right)(s) \right]$$

for $\kappa = 0$,$\langle f, g \rangle_{\kappa,T} = \langle f, g \rangle_{L^2}$, and $\langle \cdot, \cdot \rangle_{\kappa,T} = \|\cdot\|_{\kappa,T}$
With the fractional stochastic integral, we have the following isometry:

$$\left\| \int_0^T c(s) dB^\kappa(s) \right\|_{L^2}^2 = \|c(\cdot)\|_{\kappa,T}$$

We have the following lemma for conditional expectation:

Lemma B.1.

$$E\left[B^\kappa(t) \left| B^\kappa(s), v \in [0,s] \right. \right] = B^\kappa(s) + \int_0^s \Psi^\kappa(s,t,v)\, dB^\kappa(v) \tag{B.1}$$

where for $v \in (0,s)$, $\Psi(s,t,v)$ is a deterministic kernel defined as:

$$\begin{aligned} \Psi^\kappa(s,t,v) &= v^{-\kappa} \left(I_{s-}^{-\kappa} \left(I_{t-}^\kappa (\cdot)^\kappa \mathbf{I}_{[s,t]}(\cdot) \right) \right)(v) \\ &= \frac{\sin(\pi\kappa)}{\pi} v^{-\kappa} (s-v)^{-\kappa} \int_s^t \frac{z^\kappa (z-s)^\kappa}{z-v} dz \end{aligned} \tag{B.2}$$

For $v \notin (0,s)$, $\Psi^\kappa(s,t,v) = 0$.
Then for $c \in \Lambda_T^\kappa$,

$$E\left[\int_0^t c(v) dB^\kappa(v) \left| B^\kappa(v), v \in [0,s] \right. \right] = \int_0^s c(v) dB^\kappa(v) + \int_0^s \Psi_c^\kappa(s,t,v) dB^\kappa(v) \tag{B.3}$$

and

$$\begin{aligned} \Psi_c^\kappa(s,t,v) &= v^{-\kappa} \left(I_{s-}^{-\kappa} \left(I_{t-}^\kappa (\cdot)^\kappa c(\cdot) \mathbf{I}_{[s,t]}(\cdot) \right) \right)(v) \\ &= \frac{\sin(\pi\kappa)}{\pi} v^{-\kappa} (s-v)^{-\kappa} \int_s^t \frac{z^\kappa (z-s)^\kappa}{z-v} c(z)\, dz \end{aligned} \tag{B.4}$$

Again, for $v \notin (0,s)$, $\Psi_c^\kappa(s,t,v) = 0$.

For such an fractionally stochastic integral, we have the following characteristic function:

Lemma B.2.

$$\begin{aligned} E\left[e^{iu\int_0^t c(v)dB(v)}\middle|\,\mathcal{F}_s\right] &= \exp\left\{iu\left[\int_0^s c(v)dB^\kappa(v)+\int_0^s \Psi_c^\kappa(s,t,v)dB^\kappa(v)\right]\right\} \\ &\times \exp\left\{-\frac{u^2}{2}\left(\left\|c(\cdot)\,\mathbf{1}_{[s,t]}(\cdot)\right\|_{\kappa,T}^2-\left\|\Psi_c^\kappa(s,t,\cdot)\,\mathbf{1}_{[0,s]}(\cdot)\right\|_{\kappa,T}^2\right)\right\} \end{aligned}$$

So the fractionally stochastic integral $\int_0^t c(u)dB^\kappa(u)|\,\mathcal{F}_s$ is normally distributed with the following moments:

$$\begin{aligned} E\left[\int_0^t c(v)dB^\kappa(v)|\,\mathcal{F}_s\right] &= \int_0^s c(v)dB^\kappa(v)+\int_0^s \Psi_c^\kappa(s,t,v)dB^\kappa(v) \\ Var\left[\int_0^t c(v)dB^\kappa(v)|\,\mathcal{F}_s\right] &= \left\|c(\cdot)\,\mathbf{1}_{[s,t]}(\cdot)\right\|_{\kappa,T}^2-\left\|\Psi_c^\kappa(s,t,\cdot)\mathbf{1}_{[0,s]}(\cdot)\right\|_{\kappa,T}^2 \end{aligned}$$

With the OU-process driven by fBM, Fink, Kluppelberg, Zahle (2010), has proved the following:

Lemma B.3.

$$\begin{aligned} dX(t) &= (k(t)-a(t)X(t))\,dt+\sigma(t)dB^\kappa(t), \qquad X(0)\in\mathbb{R}, \qquad t\in[0,T] \\ X(t) &= X(0)e^{-\int_0^t a(s)ds}+\int_0^t e^{-\int_s^t a(u)du}k(s)ds+\int_0^t e^{-\int_s^t a(u)du}\sigma(s)dB^\kappa(s), \qquad t\in[0,T] \end{aligned}$$

Then similar to the previous characteristic function, we have the following:

Lemma B.4.

$$\begin{aligned} E\left[e^{iuX(t)}\middle|\,\mathcal{F}_s\right] &= \exp\left\{iu\left[X(s)e^{-\int_s^t a(v)dv}+\int_s^t e^{-\int_v^t a(w)dw}k(v)dv+\int_0^s \Psi_c^\kappa(s,t,v)dB^\kappa(v)\right]\right\} \\ &\times \exp\left\{-\frac{u^2}{2}\left(\left\|c(\cdot)\,\mathbf{1}_{[s,t]}(\cdot)\right\|_{\kappa,T}^2-\left\|\Psi_c^\kappa(s,t,\cdot)\,\mathbf{1}_{[0,s]}(\cdot)\right\|_{\kappa,T}^2\right)\right\} \end{aligned}$$

with $c(\cdot)=\sigma(\cdot)\,e^{-\int_\cdot^t a(w)dw}$, $X(t)|\,\mathcal{F}_s$ is normally distributed with

$$\begin{aligned} E\left[X(t)|\,\mathcal{F}_s\right] &= X(s)e^{-\int_s^t a(v)dv}+\int_s^t e^{-\int_v^t a(w)dw}k(v)dv+\int_0^s \Psi_c^\kappa(s,t,v)dB^\kappa(v) \\ Var\left[X(t)|\,\mathcal{F}_s\right] &= \left\|c(\cdot)\,\mathbf{1}_{[s,t]}(\cdot)\right\|_{\kappa,T}^2-\left\|\Psi_c^\kappa(s,t,\cdot)\mathbf{1}_{[0,s]}(\cdot)\right\|_{\kappa,T}^2 \end{aligned}$$

The difficulty of calculating this quantity lies within calculating the norm of the fractional integral, which as we have seen, has a singularity at $t\downarrow 0$. Fink, Kluppelberg, Zahle [FKZ10] has outlined a discretization scheme for $\kappa\in(0,\frac{1}{2})$, which I will included here:

Theorem B.2.

$$\left\|c(\cdot)\mathbf{1}_{[0,t]}(\cdot)\right\|_{\kappa,T}^2 = \frac{\pi\kappa(2\kappa+1)}{\Gamma(1-2\kappa)\sin(\pi\kappa)(\Gamma(\kappa))^2}\int_0^T s^{-2\kappa}\left(\int_s^T \frac{r^\kappa c(r)\mathbf{1}_{[0,t]}(r)}{(r-s)^{1-\kappa}}dr\right)^2 ds$$

The next step is to discretize the integral, decomposing the outer integral, $n \in \mathbb{N}$, and $0 = s_0 \leq s_1 \leq \cdots \leq s_n = T$.

$$\int_0^T s^{-2\kappa}\left(\int_s^T \frac{r^\kappa c(r)\mathbf{1}_{[0,t]}(r)}{(r-s)^{1-\kappa}}dr\right)^2 ds = \sum_{i=0}^{n-1}\int_{s_i}^{s_{i+1}} s^{-2\kappa}\left(\int_s^T \frac{r^\kappa c(r)\mathbf{1}_{[0,t]}(r)}{(r-s)^{1-\kappa}}dr\right)^2 ds$$

Within the $s \in [s_i, s_{i+1}]$, we can approximate by extending the lower limit:

$$\int_s^T \frac{r^\kappa c(r)\mathbf{1}_{[0,t]}(r)}{(r-s)^{1-\kappa}}dr \approxeq \int_{s_i}^T \frac{r^\kappa c(r)\mathbf{1}_{[0,t]}(r)}{(r-s_i)^{1-\kappa}}dr$$

For $i = 0, \cdots, n-1$, and partition $[s_i, s_{i+1}]$ into $s_i = u_0^i \leq u_1^i \leq \cdots \leq u_{m_i}^i = s_{i+1}$, for some $m_i \in \mathbb{N}$.

$$\begin{aligned}\int_{s_i}^T \frac{r^\kappa c(r)\mathbf{1}_{[0,t]}(r)}{(r-s_i)^{1-\kappa}}dr &= \sum_{j=0}^{m_i-1}\int_{u_j^i}^{u_{j+1}^i}\frac{r^\kappa c(r)\mathbf{1}_{[0,t]}(r)}{(r-s_i)^{1-\kappa}}dr \\ &\approxeq \frac{1}{\kappa}\sum_{j=0}^{m_i-1}\left[\left(u_{j+1}^i - s_i\right)^\kappa - \left(u_j^i - s_i\right)^\kappa\right]\frac{\left(u_j^i\right)^\kappa c(u_j^i) + \left(u_{j+1}^i\right)^\kappa c\left(u_{j+1}^i\right)}{2}\end{aligned}$$

Since we have $\Gamma(\kappa)\cdot\kappa = \Gamma(\kappa+1)$,

$$\begin{aligned}\left\|c(\cdot)\mathbf{1}_{[0,t]}(\cdot)\right\|_{\kappa,T}^2 = \quad & \frac{\pi\kappa(2\kappa+1)}{\Gamma(2-2\kappa)\sin(\pi\kappa)(2\Gamma(\kappa+1))^2}\sum_{i=0}^{n-1}\left[s_{i+1}^{1-2\kappa} - s_i^{1-2\kappa}\right] \\ \times \quad & \left[\sum_{j=0}^{m_i-1}\left[\left(u_{j+1}^i - s_i\right)^\kappa - \left(u_j^i - s_i\right)^\kappa\right]\left(u_j^i\right)^\kappa c\left(u_j^i\right) + \left(u_{j+1}^i\right)^\kappa c\left(u_{j+1}^i\right)\right]^2\end{aligned}$$

Choose $s_i = 0.01, i = 0, \cdots, 100t$ and $u_j^i = 0.01(i+j), j = 0, \cdots, 100t - i$, we have

$$\begin{aligned}&\left\|c(\cdot)\mathbf{1}_{[0,t]}(\cdot)\right\|_{\kappa,T}^2 \\ \approxeq\ & \frac{\pi\kappa(2\kappa+1)}{\Gamma(2-2\kappa)\sin(\pi\kappa)(2\Gamma(\kappa+1))^2}0.01^{1+2\kappa}\sum_{i=0}^{100t-1}\Bigg(\left[(i+1)^{1-2\kappa} - i^{1-2\kappa}\right] \\ & \times \sum_{j=0}^{100t-i-1}\left[(j+1)^\kappa - j^\kappa\right]\left[(i+j)^\kappa c(0.01(i+j)) + (i+j+1)^\kappa c(0.01(i+j+1))\right]\Bigg)\end{aligned}$$

For proof and detail we refer reader to the Pipiras and Taqqu paper [PT00], [PT01], and the discretization scheme and the proof to Fink, Kluppelberg, Zahle [FKZ10].

C Conditional Expectation for Iterative Stochastic Integrals

These are the formulas included in the paper by [Tak99], which is very useful for complicated conditional expectation, the result is proved by Mallivan Calculus. Let $W_t^i, i = 1, \cdots, 5$ be ordinary Brownian motions with correlation $d\left\langle W^i, W^j \right\rangle_t = \rho_{i,j} dt$. And $y_i(t), i = 1, \cdots, 5$ be deterministic functions of time. And $\Sigma := \int_0^T y_1^2(t)\, dt$, and the stochastic integral as defined before $J_T(y_1) = \int_0^T y_1(t)\, dW_t^1$.

Then there are following formulas, to calculate conditional expectations of various orders:

First, we look at the 2nd-order iterative stochastic integral:

$$E\left[\int_0^T y_3(t)\left(\int_0^t y_2(s)\, dW_s^2\right) dW_t^3 \middle| J_T(y_1) = x\right] = v_1\left(\frac{x^2}{\Sigma^2} - \frac{1}{\Sigma}\right) \tag{C.1}$$

where

$$v_1 = \int_0^T \rho_{1,3} y_3(t)\, y_1(t)\left(\int_0^t \rho_{1,2} y_2(s)\, y_1(s)\, ds\right) dt$$

3rd-order iterative stochastic integral:

$$E\left[\int_0^T y_4(t)\left(\int_0^t y_3(s)\left(\int_0^s y_2(u)\, dW_u^2\right) dW_s^3\right) dW_t^4 \middle| J_T(y_1) = x\right] = v_2\left(\frac{x^3}{\Sigma^3} - \frac{3x}{\Sigma^2}\right) \tag{C.2}$$

where

$$v_2 = \int_0^T \rho_{1,4} y_4(t)\, y_1(t)\left(\int_0^t \rho_{1,3} y_3(s)\, y_1(s)\left(\int_0^s \rho_{1,2} y_2(u)\, y_1(u)\, du\right) ds\right) dt$$

For the cross-product iterative stochastic integral:

$$\begin{aligned} & E\left[\left(\int_0^T y_3(t)\left(\int_0^t y_2(s)\, dW_s^2\right) dW_t^3\right)\left(\int_0^T y_5(t)\left(\int_0^t y_4(s)\, dW_s^4\right) dW_t^5\right) \middle| J_T(y_1) = x\right] \\ = \;& v_3\left(\frac{x^4}{\Sigma^4} - \frac{6x^2}{\Sigma^3} - \frac{3}{\Sigma^2}\right) + v_4\left(\frac{x^2}{\Sigma^2} - \frac{1}{\Sigma}\right) + v_5 \end{aligned} \tag{C.3}$$

where

$$
\begin{aligned}
v_3 &= \left(\int_0^T \rho_{1,3} y_3(t)\, y_1(t) \left(\int_0^t \rho_{1,2} y_2(s)\, y_1(s)\, ds\right) dt\right) \left(\int_0^T \rho_{1,5} y_5(t)\, y_1(t) \left(\int_0^t \rho_{1,4} y_4(s)\, y_1(s)\, ds\right) dt\right) \\
v_4 &= \int_0^T \rho_{1,3} y_3(t)\, y_1(t) \left(\int_0^t \rho_{1,5} y_5(t)\, y_1(s) \left(\int_0^s \rho_{2,4} y_4(u)\, y_2(u)\, du\right) ds\right) dt \\
&\quad + \int_0^T \rho_{15} y_5(t)\, y_1(t) \left(\int_0^t \rho_{1,3} y_3(t)\, y_1(s) \left(\int_0^s \rho_{2,4} y_4(u)\, y_2(u)\, du\right) ds\right) dt \\
&\quad + \int_0^T \rho_{1,3} y_3(t)\, y_1(t) \left(\int_0^t \rho_{2,5} y_5(t)\, y_2(s) \left(\int_0^s \rho_{1,4} y_1(u)\, y_2(u)\, du\right) ds\right) dt \\
&\quad + \int_0^T \rho_{1,5} y_5(t)\, y_1(t) \left(\int_0^t \rho_{3,4} y_4(t)\, y_3(s) \left(\int_0^s \rho_{1,2} y_2(u)\, y_1(u)\, du\right) ds\right) dt \\
&\quad + \int_0^T \rho_{3,5} y_5(t)\, y_3(t) \left(\int_0^t \rho_{1,2} y_2(t)\, y_1(s) \left(\int_0^s \rho_{1,4} y_4(u)\, y_1(u)\, du\right) ds\right) dt \\
v_5 &= \int_0^T \rho_{3,5} y_5(t)\, y_3(t) \left(\int_0^t \rho_{2,4} y_4(s)\, y_2(s)\, ds\right) dt
\end{aligned}
$$

We end with the following example:

$$
\begin{aligned}
& E\left(a_2(t) \middle| a_1(t) = x\right) \\
= \; & E\left(\int_0^t p_2(s) \left(\int_0^s \sigma^{(0)}(u)\, dW_u^S\right) dW_s^S + \int_0^t p_3(s) \left(\int_0^s p_4(u)\, dW_u^v\right) dW_s^S \middle| \int_0^T p_1(t)\, dW_t^1 = x\right) \\
= \; & E\left(a_{2,1}(t) + a_{2,2}(t) \middle| a_1 = x\right) \qquad \text{(C.4)}
\end{aligned}
$$

Substituting $y_1(t) = p_1(t)$, $y_2(t) = \sigma^{(0)}(t)$,$y_3(t) = p_2(t)$,
$\rho_{12} = d\left\langle W^S, W^S\right\rangle_t / dt = 1$, $\rho_{12} = d\left\langle W^S, W^S\right\rangle_t / dt = 1$, into (C.1).

Then for the first part:

$$
\begin{aligned}
E\left(a_{2,1}(t) \middle| a_1(t) = x\right) &= E\left(\int_0^t p_2(s) \left(\int_0^s \sigma^{(0)}(u)\, dW_u^S\right) dW_s^S \middle| \int_0^t p_1(s)\, dW_s^1 = x\right) \\
&= \left[\int_0^t p_1(s)\, p_2(s) \left(\int_0^s \sigma^{(0)}(u)\, p_1(u)\, du\right) ds\right] \left(\frac{x^2}{\Sigma^2} - \frac{1}{\Sigma}\right) \qquad \text{(C.5)}
\end{aligned}
$$

Substituting $y_1(t) = p_1(t)$, $y_2(t) = p_4(t)$,$y_3(t) = p_3(t)$,
$\rho_{12} = d\left\langle W^S, W^v\right\rangle_t / dt = \rho$, $\rho_{13} = d\left\langle W^S, W^S\right\rangle_t / dt = 1$, into (C.1).

$$
\begin{aligned}
E\left(a_{2,2}(t) \middle| a_1(t) = x\right) &= E\left(\int_0^t p_3(s) \left(\int_0^s p_4(u)\, dW_u^v\right) dW_s^S \middle| \int_0^t p_1(s)\, dW_s^1 = x\right) \\
&= \left[\int_0^t p_1(s)\, p_3(s) \left(\int_0^s \rho p_1(u)\, p_4(u)\, du\right) ds\right] \left(\frac{x^2}{\Sigma^2} - \frac{1}{\Sigma}\right) \qquad \text{(C.6)}
\end{aligned}
$$

Putting together,

$$\begin{aligned} & E\left(a_2(t)|\, a_1(t)=x\right) \\ = & \left[\int_0^t p_1(s)\, p_2(s)\left(\int_0^s \sigma^{(0)}(u)\, p_1(u)\, du\right) ds + \int_0^t p_1(s)\, p_3(s)\left(\int_0^s \rho p_1(u)\, p_4(u)\, du\right) ds\right]\left(\frac{x^2}{\Sigma^2}-\frac{1}{\Sigma}\right) \end{aligned} \tag{C.7}$$

Recovers the first line of equation (8.34). The rest of the terms are derived similarly, and the pdf approximation is calculated by the definition of Hermite function.

References

[ALV07] E. Alos, J.A. Leon, and J. Vives. On the short-time behavior of the implied volatility for jump-diffusion models with stochastic volatility. *Finance and Stochastics*, 11(4):571589, 2007.

[AMN01] E. Alos, O. Mazet, and D. Nualart. Stochastic calculus with respect to gaussian processes. *The Annals of Probability*, 29(2):766801, 2001.

[BBM96] R.T. Baillie, T. Bollerslev, and H.O. Mikkelsen. Fractionally integrated generalized autoregressive conditional heteroskedasticity. *J. Econometrics*, 74:330, 1996.

[BCdL98] F.J. Breidt, N Crato, and P de Lima. The detection and estimation of long memory in stochastic volatility. *J. Econometrics*, 83:325348, 1998.

[BD87] P.J. Brockwell and R.A. Davis. *Time Series: Theory and Methods*. Springer, New York, 1987.

[Ben03] C. Bender. An s-transform approach to integration with respect to a fractional brownian motion. *Bernoulli*, 9(6):955983, 2003.

[BHOZ08] F. Biagini, Y. Hu, B. Oksendal, and T. Zhang. *Stochastic Calculus for Fractional Brownian Motion and Applications*. Springer, 2008.

[BK79] G. Booth and F. Kaen. Gold and silver spot prices and market information efficiency. *Financial Review*, 14:2126, 1979.

[BKK82] G. Booth, F. Kaen, and P. Koveos. R/S analysis of foreign exchange rates under two international monetary regimes. *Journal of Monetary Economics*, 10:408415, 1982.

[BM96] T. Bollerslev and H.O. Mikkelsen. Modeling and pricing long memory in stock market volatility. *J. Econometrics*, 73:151184, 1996.

[BSV06] C. Bender, T. Sottinen, and E. Valkeila. Arbitrage with fractional brownian motion? *Theory of Stochastic Procsses*, 12(28, no.3-4), 2006.

[CCR12] F. Comte, L. Coutin, and E. Renault. Affine fractional stochastic volatility models. *Annals of Finance*, 8:337378, 2012.

[CdL94] N Crato and P de Lima. Long-range dependence in the conditional variance of stock returns. *Economics Letters*, 45:281285, 1994.

[Che03] P. Cheridito. Arbitrage in fractional brownian motion models. *Finance and Stochastics*, 7:533553, 2003.

[CHJ09] P. Christoffersen, Steven L. Heston, and K. Jacobs. The shape and term structure of the index option smirk: Why multifactor stochastic volatility models work so well. *Management Science*, 55(12):19141932, December 2009.

[Cho88] R.Y. Chou. Volatility persistence and stock valuations: Some empirical evidence using garch. *Journal of Applied Econometrics*, 3(4):279294, 1988.

[CM99] P. Carr and D.B. Madan. Option valuation using the fast fourier transform. *Journal of Computational Finance*, 2:61–73, 1999.

[Con07] R Cont. Volatility clustering in financial markets: Empirical facts and agent-based models. In *Long Memory in Economics*, page 289310. Springer, 2007.

[CR96] F. Comte and E. Renault. Long memory continuous time models. *J. Econometrics*, 73:101149, 1996.

[CR98] F. Comte and E. Renault. Long memory in continuous-time stochastic volatility models. *Mathematical Finance*, 8:291323, 1998.

[CT04] R. Cont and P. Tankov. Non-parametric calibration of jump-diffusion option pricing models. *Journal of Computational Finance*, 7(3), 2004.

[CV12] A. Chronpoulou and F.G. Viens. Estimation and pricing under long-memory stochastic volatility. *Annals of Finance*, 8(2-3):379403, 2012.

[DGE93] Z Ding, C.W.J. Granger, and R. Engle. A long memory property of stock market returns and a new model. *J. Empirical Finance*, 1:83106, 1993.

[DH87] R.A. Davis and D.S. Harte. Tests for hurst effect. *Biometrika,*, 74:95102, 1987.

[Die02] T. Dieker. *Simulation of Fractional Brownian Motion*. Master thesis, Vrije Universiteit, Amsterdam, 2002.

[DN97] C.R. Dietrich and G.M. Newsam. Fast and exact simulation of stationary gaussian processes through circulant embedding of the covariance matrix. *SIAM J. Sci. Computing*, 18:10881107, 1997.

[DPS00] D. Duffie, R. Pan, and K. Singleton. Transform analysis and asset pricing for affine jump-diffusion. *Econometrica*, 68:13431376, 2000.

[DS94] F. Delbaen and W. Schachermayer. A general version of the fundamental theorem of asset pricing. *Math. Ann.*, 300:463520, 1994.

[DU99] L. Decreusefond and A.S. Ustunel. Stochastic analysis of the fractional brownian motion. *Potential Anal.*, 10(2):177–214, 1999.

[Dup94] B. Dupire. Pricing with a smile. *Risk*, 7:1820, 1994.

[EB86] R. Engle and T. Bollerslev. Modelling the persistence of conditional variances. *Econometric Review*, 5:150, 1986.

[Ell06] R.J. Elliott. Ito formulas for fractional brownian motions. In *Mathematical Finance Conference in honor of The 60th Birthday of Dilip B. Madan*, Nobert Wiener Center, University of Maryland, 2006.

[Enr04] N. Enriquez. A simple construction of the fractional brownian motion. *Stochastic Processes and Their Applications*, 109:203223, 2004.

[FK12] H. Funahashi and M. Kijima. A chaos expansion approach for the pricing of contingent claims. *Research Paper Series No.99, Tokyo Metropolitan University*, 2012.

[FKZ10] H. Fink, C. Kluppelberg, and M. Zahle. Conditional characteristic functions of processes related to fractional brownian motion. *Working Paper, Center for Mathematical Science, Technische Universitat Munchen, Germany*, 2010.

[Fla89] P. Flandrin. On the spectrum of fractional brownian motion. *IEEE Transactions on Information Theory*, 35:197199, 1989.

[FMKT82] Y. Fujikoshi, K. Morimune, N. Kunitomo, and M. Taniguchi. Asymptotic expansions of the distributions of the estimates of coefficients in a simultaneous equation system. *Journal of Econometrics*, 18:191205, 1982.

[Fuk11] M. Fukasawa. Asymptotic analysis for stochastic volatility: Martingale expansion. *Finance and Stochastics*, 15:635654, 2011.

[Fun12] H. Funahashi. *A Chaos Expansion Approach Under Hybrid Volatility Models*. 2012.

[GF77] M. Greene and B. Fielitz. Long-term dependence in common stock returns. *Journal of Financial Economics*, 4:339349, 1977.

[Gra66] C.W.J. Granger. The typical spectral shape of an economic variable. *Econometrica*, 34:150161, 1966.

[Hes93] S.L. Heston. A closed-form solution for options with stochastic volatility with applications to bond and currency options. *The Review of Financial Studies*, 6(2):327343, 1993.

[HKR84] B. Helms, F. Kaen, and R. Rosenman. Memory in commodity futures contracts. *Journal of Futures Markets*, 4:559567, 1984.

[Hos84] J.R.M. Hosking. Modeling persistence in hydrological time series using fractional differencing. *Water Resources Research*, 20:18981908, 1984.

[HW87] J Hull and A White. The pricing of options on assets with stochastic volatilities. *Rev. Finan. Studies*, 3:281300, 1987.

[JPR94] E. Jacquier, N.G. Polson, and P.E. Rossi. Bayesian analysis of stochastic volatility models. *J. Bus. and Econ. Statistics*, 12:371417, 1994.

[Kol40] A.N. Kolmogorov. Wienersche spiralen und einige andere interessante kurvenim hilbertschen raum. *C.R. (Doklady) Acad. URSS (N.S)*, 26:115118, 1940.

[LeR89] S. LeRoy. Efficient capital markets and martingales. *Journal of Economic Literature*, 27:15831621, 1989.

[Lew00] A. Lewis. *Option Valuation under Stochastic Volatility with Mathematica*. Finance Press, Newport Beach, CA, 2000.

[Lo91] A.W. Lo. Long-term memory in stock market price. *Econometrica*, 59:12791331, 1991.

[Mah90a] S. Maheswaran. Empirical implications of arbitrage free asset markets. *Discussion Paper, Department of Economics, University of Minnesota*, 1990.

[Mah90b] S. Maheswaran. Predictable short-term variation in asset prices: Theory and evidence,. *Working Paper, Carlson School of Management, University of Minnestoa*, 1990.

[Man65] B.B. Mandelbrot. Une classe de processus homothgtiques a soi; application a la loi climatologique de h. e. hurst. *C.R. Acad. Sci. Paris*, 260:32743277, 1965.

[Mer87] R. Merton. On the current state of the stock market rationality hypothesis. In *Macroeconomics and Finance: Essays in Honor of Franco Modigliani*. 1987.

[MR99] D. Marinucci and P.M. Robinson. Alternative forms of fractional brownian motion. *J. Statistical Planning and Inference*, 80:111122, 1999.

[MVN68] B.B. Mandelbrot and J.W. Van Ness. Fractional brownian motions, fractional noises and applications. *SIAM Review*, 10:422437, 1968.

[MW69] B.B. Mandelbrot and J. Wallis. Computer experiments with fractional gaussian noises. part 1,2,3. *Water Resources Research*, 5:228267, 1969.

[NMW99] I. Norros, P. Mannersalo, and J.L. Wang. Simulation of fractional brownian motion with conditionalized random midpoint displacement. *Advances in Performance Analysis*, 2:77101, 1999.

[Nua06] D. Nualart. *The Malliavin Calculus and Related Topics*. Springer: Berlin, 2006.

[Oks00] B. Oksendal. *Stochastic Differential Equations: An Introduction with Applications*. Springer, Berlin, 2000.

[Pax97] V. Paxson. Fast, approximate synthesis of fractional gaussian noise for generating self-similar network traffic. *Computer Communication Review*, 27:518, 1997.

[PHJI02] E. Perrin, R. Harba, R. Jennane, and I. Iribarren. Fast and exact synthesis for 1-d fractional brownian motion and fractional gaussian noises. *IEEE Signal Processing Letters*, 9:382384, 2002.

[PT00] V. Pipiras and Murad S. Taqqu. Integration questions related to fractional brownian motion. *Probability Theory and Related Fields*, 118:251291, 2000.

[PT01] V. Pipiras and Murad S. Taqqu. Are classes of deterministic integrals for fractional brownian motion on an interval complete? *Bernoulli*, 7:878897, 2001.

[Rog97] L.C.G. Rogers. Arbitrage with fractional brownian motion. *Mathematical Finance,*, 7:95105, 1997.

[Roz67] Yu. A. Rozanov. *Stationary random processes*. Holden-Day, San Francisco, 1967.

[Sco87] L Scott. Option pricing when the variance changes randomly: Estimation and an application. *J. Financial and Quant. Anal.*, 22:419438, 1987.

[ST94] G. Samorodnitsky and M.S. Taqqu. *Stable Non-Gaussian Random Processes - Stochastic Models with Infinite Variance*. 1994.

[SZ99] R Schobel and J. Zhu. Stochastic volatility with an ornstein-uhlenbeck process: An extension. *Review of Finance*, 3:23–46, 1999.

[Tak99] A. Takahashi. Asymptotic expansion approach to pricing financial contingent claims. *Asia-Pacific Financial Market*, 6:115151, 1999.

[Taq75] M. Taqqu. Weak convergence to fractional brownian motion and to the rosenblatt process. *Z. Wahr. Verw. Gebiete*, 31:287302, 1975.

[WC94] A.T.A. Wood and G. Chan. Simulation of stationary gaussian processes in [0,1]d. *J. Computational and Graphical Statistics*, 3:409432, 1994.

[Yos01] N. Yoshida. Malliavin calculus and martingale expansion. *Bull. Sci. Math.*, 125:431456, 2001.